



SEEK WISDOM, ELEVATE YOUR INTELLECT AND SERVE HUMANITY!

Addis Ababa University
አዲስ አበባ ዩኒቨርሲቲ



Addis Ababa University

College of Natural and Computational Sciences

School of Earth Sciences

**Steady-State Numerical Groundwater Flow Modeling Using
Processing MODFLOW; In Case of Upper Mille River Catchment,
Upper Awash Basin, North-Eastern Ethiopia**

A Thesis submitted to
School of Earth Sciences of Addis Ababa University
In Partial Fulfilment to the Degree of Masters of Science in
Hydrogeology

By: Amanuel Godie Gigar
Advisor: Dr. Dessie Nedaw

September 2021
Addis Ababa, Ethiopia

Addis Ababa University
College of Natural Sciences
School of Earth Sciences

**Steady-State Numerical Groundwater Flow Modeling Using
Processing MODFLOW; In Case of Upper Mille River Catchment,
Upper Awash Basin, North-Eastern Ethiopia**

BY: Amanuel Godie

Advisor: Dr. Dessie Nedaw

**A Thesis Submitted to the School of Earth Sciences of Addis Ababa University
in Partial Fulfillment of the Requirements for the Degree of Master of Science in
Hydrogeology**

September, 2021

Addis Ababa, Ethiopia

Declaration

By my signature below, I declare and confirm that this thesis is my own original work. I have followed all ethical and technical principles of research in the preparation, data collection, data analysis and compilation of this thesis. Any scholarly article that is included in the thesis has been given acknowledgment through references.

Name: Amanuel Godie

Signature: -----

Date: September, 2021

This thesis has been submitted for examination with my approval as University Advisor

Name: Dr. Dessie Nedaw

Signature.....

Date.....

ADDIS ABABA UNIVERSITY
SCHOOL OF GRADUATE STUDIES
SCHOOL OF EARTH SCIENCES

**Steady-State Numerical Groundwater Flow Modeling Using
Processing MODFLOW; In Case of Upper Mille River Catchment,
Upper Awash Basin, North-Eastern Ethiopia**

By:

Amanuel Godie

Approved by the Examining Committee

Dr. Balemwal Atnafu	_____	_____
Head, School of Earth Sciences	Signature	Date
Dr. Dessie Nedaw	_____	_____
Advisor	Signature	Date
Prof. Tenalem Ayenew	_____	_____
Examiner	Signature	Date
Dr. Tilahun Azagegn	_____	_____
Examiner	Signature	Date

TABLE OF CONTENTS

<u>TABLE OF CONTENTS</u>	<u>I</u>
<u>LIST OF FIGURES</u>	<u>V</u>
<u>LIST OF PLATES</u>	<u>VII</u>
<u>LIST OF TABLES</u>	<u>VIII</u>
<u>ABSTRACT</u>	<u>IX</u>
<u>ACKNOWLEDGMENT</u>	<u>X</u>
<u>LIST OF ACRONYMS</u>	<u>XI</u>
<u>CHAPTER ONE</u>	<u>1</u>
<u>INTRODUCTION</u>	<u>1</u>
1.1 BACKGROUND OF THE STUDY	1
1.2 PROBLEM STATEMENT	3
1.3 OBJECTIVE OF THE STUDY.....	3
1.3.1 MAIN OBJECTIVE.....	3
1.3.2 SPECIFIC OBJECTIVES	3
1.4 RESEARCH QUESTIONS	4
1.5 LITERATURE REVIEW	4
1.5.1 PREVIOUS GEOLOGICAL WORKS	5
1.5.2 PREVIOUS HYDROGEOLOGICAL WORKS	5
1.5.3 PREVIOUS WORKS ON MODELING.....	7
1.6 METHODOLOGY	8
1.7 MATERIALS AND SOFTWARE USED	13
1.8 STRUCTURE/OUTLINE OF THE THESIS	14
1.9 SIGNIFICANCE OF THE STUDY.....	15
<u>CHAPTER TWO</u>	<u>16</u>
<u>STUDY AREA DESCRIPTION</u>	<u>16</u>
2.1 LOCATION AND ACCESSIBILITY.....	16
2.2 PHYSIOGRAPHY OF THE WATERSHED	17
2.3 SLOPE/ GRADIENT OF THE WATERSHED	18
2.4 DRAINAGE PATTERN OF THE WATERSHED	19

2.5 SOIL TYPE AND TEXTURE.....	20
2.6 CLIMATE ZONE OF THE WATERSHED	21
2.7 LAND USE LAND COVER (LULC)	22
<u>CHAPTER THREE</u>	<u>24</u>
<u>HYDROMETEOROLOGY AND RECHARGE ESTIMATION</u>	<u>24</u>
3.1 METEOROLOGICAL STATIONS	24
3.2 METEOROLOGICAL PARAMETERS	24
3.2.1 PRECIPITATION.....	24
3.2.2 TEMPERATURE	27
3.3 GROUNDWATER RECHARGE ESTIMATION USING WB METHOD	28
3.3.1 EVAPOTRANSPIRATION.....	28
3.3.2 SURFACE RUNOFF	33
3.3.3 GROUNDWATER RECHARGE	35
3.4 GROUNDWATER RECHARGE ESTIMATION USING SWAT MODEL	36
3.5 COMPARISON OF WB AND SWAT MODEL RESULTS.....	40
<u>CHAPTER FOUR.....</u>	<u>41</u>
<u>REGIONAL AND LOCAL GEOLOGY.....</u>	<u>41</u>
4.1 REGIONAL GEOLOGICAL SETTING.....	41
4.2 REGIONAL LITHO-STRATIGRAPHIC UNITS.....	42
4.2.1 PLATEAU BASALTIC FORMATION	43
4.2.2 PLATEAU SILICIC FORMATION	43
4.2.3 SHIELD VOLCANICS (TARMABER FORMATION).....	43
4.3 LOCAL STRATIGRAPHIC UNITS.....	44
4.3.1 LOWER/ ASHANGE BASALT	44
4.3.2 MIDDLE/AIBA BASALT	45
4.3.3 KEMISE RHYOLITE.....	46
4.3.4 UPPER/TARMABER BASALT	46
4.3.5 UNCONSOLIDATED QUATERNARY SEDIMENT DEPOSITS	46
4.4 GEOLOGICAL STRUCTURES	47
<u>CHAPTER FIVE</u>	<u>49</u>
<u>AQUIFER CHARACTERIZATION AND CONCEPTUAL MODEL DEVELOPMENT</u>	<u>49</u>

5.1 INTRODUCTION.....	49
5.2 GROUNDWATER INVENTORY POINTS	50
5.3 PHYSICO-CHEMICAL PARAMETERS	52
5.3.1 ELECTRICAL CONDUCTIVITY (EC)	53
5.3.2 TOTAL DISSOLVED SOLIDS (TDS)	54
5.3.3 pH.....	55
5.4 HYDRAULIC PROPERTIES OF AQUIFERS	55
5.4.1 HYDRAULIC CONDUCTIVITY	56
5.4.2 TRANSMISSIVITY	57
5.5 HYDROGEOLOGIC UNITS OF THE WATERSHED	58
5.5.1 HIGH PRODUCTIVE INTERGRANULAR POROSITY AQUIFERS	58
5.5.2 MEDIUM PRODUCTIVE DOUBLE POROSITY VOLCANIC AQUIFER	59
5.5.3 LOW PRODUCTIVE AQUIFER.....	61
5.6 GROUNDWATER FLOW (RECHARGE-DISCHARGE ZONES)	63
5.7 CONCEPTUAL HYDROGEOLOGICAL MODEL	65
<u>CHAPTER SIX.....</u>	68
<u>NUMERICAL GROUNDWATER FLOW MODELING.....</u>	68
6.1 INTRODUCTION.....	68
6.2 GOVERNING EQUATION OF GROUNDWATER FLOW	68
6.3 MODEL DESIGN.....	69
6.3.1 MODEL GEOMETRY	69
6.3.2 MODEL DISCRETIZATION	69
6.4 MODEL INPUT PARAMETERS	70
6.4.1 MODELING ENVIRONMENT	70
6.5 STRESSES	72
6.6 MODEL SIMULATION.....	73
6.6.1 MODEL CALIBRATION	73
6.6.2 EVALUATION OF MODEL CALIBRATION.....	74
<u>CHAPTER SEVEN</u>	76
<u>RESULT AND DISCUSSION</u>	76
7.1 INTRODUCTION.....	76
7.2 ESTIMATED RECHARGE RESULTS	76

7.3 RESULTS OF AQUIFER CHARACTERIZATION	76
7.4 STEADY-STATE SIMULATED RESULTS.....	77
7.4.1 HYDRAULIC HEADS	77
7.4.2 WATER BUDGETS	78
7.5 MODEL SENSITIVITY ANALYSIS	79
7.6 SCENARIO ANALYSIS	81
7.7 MODEL LIMITATIONS	84
<u>CHAPTER EIGHT</u>	<u>85</u>
<u>CONCLUSION AND RECOMMENDATION.....</u>	<u>85</u>
8.1 CONCLUSIONS	85
8.3 RECOMMENDATIONS	87
<u>REFERENCES</u>	<u>88</u>
<u>APPENDICES</u>	<u>ERROR! BOOKMARK NOT DEFINED.</u>

LIST OF FIGURES

Figure 1: Flowchart showing the summary of the methods and approaches followed to achieve the proposed objectives from the very beginning to the end of the research work.	12
Figure 2: Inset location map of Upper Mille river catchment	16
Figure 3: 3D Physiographic map of Upper Mille catchment using Surfer 15 software	17
Figure 4: Slope classification map of Upper Mille river catchment.....	18
Figure 5: Drainage pattern and density of Upper Mille river catchment.....	19
Figure 6: Soil texture classification map of the Upper Mille river catchment.....	20
Figure 7: Traditional climatic zone map of Upper Mille river catchment.....	21
Figure 8: Land use land cover classification map of Upper Mille river catchment.....	22
Figure 9: Constructed Thiessen polygon for each station.....	25
Figure 10: Mean monthly precipitation for each meteorological station.....	26
Figure 11: Mean monthly precipitation of Upper Mille River catchment.....	27
Figure 12: Average Mean monthly air temperature of Upper Mille river catchment.....	28
Figure 13: Average monthly Potential evapotranspiration	30
Figure 14: Mean monthly actual evapotranspiration of Upper Mille catchment.....	33
Figure 15: Shows the Proportion of the Water balance components.....	35
Figure 16: Mean monthly precipitation and runoff derived from SWAT Model	37
Figure 17: Mean monthly PET and AET derived from the SWAT Model	38
Figure 18: Average annual hydrologic components obtained from SWAT model	39
Figure 19: Geological map of upper Mille catchment (adopted from GSE, 2014)	48
Figure 20: EC distribution map of the watershed interpolated from point measurements	53
Figure 21: TDS distribution map of the watershed interpolated from point measurements.....	54
Figure 22: Hydraulic conductivity distribution map of the study area interpolated from point measurements.....	56

Figure 23: Interpolated transmissivity distribution map of Upper Mille catchment	57
Figure 24: Aquifer classification map of the study area based on the productivity nature of each comprise units	62
Figure 25: Schematic hydrogeological map which shows the possible groundwater flow direction of Upper Mille watershed.	64
Figure 26: Schematic conceptual model of groundwater occurrence and circulation in the upper Mille watershed (not scaled) exploratory well log data were used to construct the cross-section.	66
Figure 27: Schematic conceptual model of groundwater occurrence and circulation in the upper Mille watershed (not scaled) exploratory well log data were used to construct the cross-section.	67
Figure 28: Model domain discretization of Upper Mille river catchment	71
Figure 29: Scatter plot of simulated to the observed fit of water levels	74
Figure 30: simulated groundwater level contour map of the model domain	78
Figure 31 : Sensitivity analysis of the effect of selected parameters on the RMSE Value of Water level.....	81
Figure 32: Decline in simulated water level due to possible increase in the pumping rate	83
Figure 33: Decline in simulated water level due to possible increase in the pumping and decrease in the recharge rate.....	84

LIST OF PLATES

Plate 1: Highly weathered and fractured Ashange basalt exposed to the east of Wuchale (left) and near Lake Hayk (right).....	45
Plate 2: Cliff forming columnar middle /Aiba basalt near Wuchale town	45
Plate 3 : Valley fill unconsolidated sediment in the Girana valley (left) and river cut exposure near Wuchale (right)(B).....	47
Plate 4: Developed springs having a yield of 1L/s (left) and 0.5L/s (right) which emerged in the Ashange basalt to the north of Hayk towns, these springs have low TDS, EC, and temperature and they are used as drinking water for the local community.	51
Plate 5: Installed deep borehole in the left and its lithological, and geophysical logging in the right (the logging was taken from AWDSA well completion report) drilled on the unconsolidated sediments. The well has a depth of 240m and the top 140m is unconsolidated sediment and the rest is the basaltic unit.....	52
Plate 6: Lithological and geophysical logging and pumping test measurement of a borehole drilled on the thick unconsolidated sediment around Girana valley for irrigation purposes which has a yield of 84.3l/s.	59
Plate 7: Lithologic log of a borehole drilled on moderately productive basaltic aquifer with the top 35m is soil and clay to gravel sediments (source: ADSWE, 2019).	60

LIST OF TABLES

Table 1: A summary of the proportion of each land use land cover type.....	23
Table 2: Estimation of mean annual precipitation using Thiessen polygon method.....	26
Table 3: Mean monthly precipitation of Upper Mille River catchment.....	27
Table 4: Latitude correction values of 11 ⁰ N Latitude.....	30
Table 5: Step by step calculation of Actual Evapotranspiration from PET.....	32
Table 6: <i>Average Hydrologic parameters derived from SWAT model</i>	37
Table 7: Comparison of water balance components computed using WB and SWAT Model methods.....	40
Table 8: Fieldwork Inventory points and the parameters measured for each point.....	50
Table 9: Calibration evaluation of mean errors using observed and simulated heads.....	75
Table 10: Simulated and observed hydraulic heads in each observational borehole.....	77
Table 11: Model-calculated steady-state hydrologic budget for the whole model (the unit of the flows is [L ³ /t]).....	79
Table 12: RMSE head changes with different recharge and hydraulic conductivity from the calibrated values.....	80
Table 13: Decline in water level simulated by increasing from the current pumping rate.....	82

ABSTRACT

Different approaches have been used to investigate the hydrogeology of a complex fractured volcanic and unconsolidated Quaternary sediment aquifer system in the Upper Mille catchment (part of the lower Awash basin) located at the western escarpment of Afar rift. The water balance components of the watershed have been estimated using Water Balance (WB) and SWAT modeling techniques. The mean annual precipitation, actual evapotranspiration, surface runoff, and groundwater recharge of the watershed has been quantified as 1132mm, 775mm, 251mm, and 105mm respectively by the WB method whereas, using the SWAT model these components are estimated as 1083mm, 558mm, 335mm, and 150mm respectively with an interflow of 39mm. The groundwater system and the spatial variability of the different aquifers have been studied using conventional hydrogeological investigation, and numerical groundwater flow modeling techniques. The watershed has been classified into different hydrogeologic units based on the productivity of aquifer units using the data obtained from lithologic logs of deep boreholes, pumping test results, stratigraphic settings, and topographic position of each unit. Based on this, the lithologic units were classified into three hydrogeologic units; high productive intergranular aquifer, medium productive fractured aquifer, and low productive aquifer having different conductivity, transmissivity, and discharge amount as observed from drilled boreholes. Schematic hydrogeological cross-sections, TDS and EC distribution maps, and groundwater head distribution contour maps were produced using lithologic logs of drilled deep boreholes, field measured inventory water points, and water level measurement respectively. Based on converging evidence from geological, hydrogeological, and topographic settings a conceptual model that approximates the groundwater system of the Upper Mille watershed was developed. The conceptual model was converted into a numerical groundwater flow model by applying a steady-state groundwater flow model governing equation using Processing MODFLOW packages. The model was simulated and model calibration carried out by manual trial and error adjustment of the input parameters until the values of the observed and simulated head results were within the acceptable error. Head distribution and water budgets of the watershed was quantified. The calibrated model simulates a mean annual groundwater recharge of **89.1mm/year**. The total inflow and outflow of the system is almost equal (**$3.73 \times 10^7 \text{m}^3/\text{day}$**). The results of the sensitivity analysis indicates that the model is highly sensitive for a change in hydraulic conductivity and recharge rate. Two types of scenario analysis were done. The first scenario was by increasing the amount of groundwater extraction by 50, 100, and 200% from the current pumping rate. The simulation results in an average decline of water level by **12.2**, **19.1**, and **23m** respectively. The second scenario was analyzed firstly by decreasing the recharge by 50% while keeping the current rate of pumping and then simultaneously decreasing the current recharge by 50% and increasing the groundwater abstraction by 100%. In these cases, the model shows an average decline in simulated hydraulic head by **7m** and **17.4m** from the current water level.

Keywords: Water balance, Recharge, Hydrogeological unit, Conceptual model, Numerical model, Calibration, Scenario analysis, Sensitivity analysis

ACKNOWLEDGMENT

This thesis work could not be accomplished without the support and contribution of different institutions and individuals from the beginning to the end of my research work.

First off, I would like to thank Addis Ababa University, School of Earth Sciences for offering the opportunity to pursue my Master's program as well as the provision of funding for this thesis research along with logistical resources needed to conduct the fieldwork.

Secondly, my deepest gratitude goes to my instructor as well as my main advisor Dr. Dessie Nedaw for his constructive comments, follow-ups, and encouragement throughout the lifetime of this thesis work. I would also show my appreciation to Addis Ababa water work enterprises, National Meteorological agency, Amhara water work design and supervision enterprise, Wollo zonal water offices, and local communities living in the study area for giving data needed for this work.

Lastly, I wish to extend my special thanks to my friends and brothers, especially Mr. Belay Molla, Mr. Gebeyaw Ayele, Mr. Amanuel Habtamu and Mr. Granit Xhaka, for their much-needed assistance during fieldwork and throughout the research. The assistance provided by my family; Mom (Ayingda Enyew), Dad, and brothers are greatly appreciated.

LIST OF ACRONYMS

ACPWL	Accumulated Potential Water Loss
AET	Actual Evapotranspiration
AWC	Available Water Capacity
BH	Boreholes
DEM	Digital Elevation Model
EARS	East African Rift System
EC	Electrical Conductivity
FAO	Food and Agriculture Organization
GPS	Global Positioning System
GW	Groundwater
HRU	Hydrologic Response Unit
LULC	Land use Land Cover
MER	Main Ethiopian Rift
NMA	National Meteorological Agency
P	Precipitation
PET	Potential Evapotranspiration
SM	Soil Moisture
SP	Springs
SWAT	Soil and Water Assessment Tool
SWL	Static Water Level
T	Temperature
TDS	Total Dissolved Solids
WB	Water Balance
PMWIN	Processing MODFLOW for Windows
ITCZ	Inter-Tropical Convergence Zone
CFB	Continental flood basalt
A.s.l	Above sea level
B.s.l	below sea level
WAM	Western Afar Margin

CHAPTER ONE

INTRODUCTION

1.1 Background of the Study

Ethiopia is thought to have abundant groundwater resources that can be useful for domestic, industrial, and agricultural purposes. The availability of high rainfall, favorable environmental features including the geology, topography, and climatic conditions could be factors for the occurrence of voluminous groundwater resources in the country. Ethiopian aquifers are categorized into three broad groups; sedimentary, volcanic, and metamorphic aquifers (Wakgari Furi, 2010). From these aquifer types, the volcanic aquifer is the dominant aquifer type that covers most of the Ethiopian landmass than others with highly variable composition and stratigraphic setup associated with the earth dynamics and interventions (Andarge Yitbarek, 2009).

Generally, the geology, hydrogeology, and the geomorphology of Ethiopia is the result of complex orogenic evolution which includes the following major events with their time frame: Terrain accretion and collision in the Precambrian; Peneplanation, Glaciations, and Gondwana breakup in Paleozoic; cyclic marine transgression and regression events leading to accumulation of Multilayered sedimentary rocks in the Mesozoic; huge continental flood basalt eruption and formation of the rift valley in Cenozoic; sedimentation, and deep incision of river valleys and pluvial interpluvial sediment accumulation in the Quaternary period (Seifu Kebede, 2013). These mega-events have left distinct imprints on the landscape, hydrology, and groundwater occurrence in Ethiopia.

Even though Ethiopia is known for its huge groundwater resource, scarcity of fresh water is a serious challenge now facing many parts of the world including our country Ethiopia. Water scarcity is expected to increase in the future because of the increasing demands associated with population growth and economic development (Maliva, 2004). Climate change may also contribute to local water scarcity through changes in precipitation amounts, patterns, and increased evapotranspiration. Fresh groundwater is a critical resource because of its often-good quality, year-round availability, and location near areas of demand. In many places, fresh groundwater resources are being either depleted or contaminated (or both) as a result of over-pumping and other anthropogenic activities.

About 97% of the earth's water lies in the form of seas and oceans, containing salt which is not suitable for direct consumption like drinking, cooking, industrial and irrigational purposes. Only

3% of the water available on earth is freshwater (A. Balasubramanian, 2015). More than 2% exists as ice caps and glaciers, and about 1% is spread in the form of rivers, lakes, groundwater, and water vapor. From the freshwater alone, almost 66.7% is locked up in the form of ice caps and glaciers. About 30.1% is found below the surface as groundwater. The surface water, which is directly available on the land surface is only 0.3%, the rest 0.9% is found in the form of water vapor and soil water. The available surface water (0.3%) is shared by lakes, swamps, and running water like rivers. As indicated above, the amount of available freshwater is less, as a result, proper reserve quantification of this precious resource needs a model to fully understand its occurrence, dynamics, and characteristics. Better management of groundwater resources is required to obtain the maximum value from these assets and to ensure that their use is sustainable.

Numerical groundwater modeling has become the fundamental tool for evaluating groundwater resources. The development of a variety of robust, efficient, and flexible model codes and user-friendly graphical user interfaces (GUIs), along with the exponential growth of computational power, has resulted in numerical modeling becoming an essential element in most groundwater investigations. Groundwater models are used to develop an understanding of historical and current conditions which helps to predict the response of aquifers to future stresses, which could be groundwater pumping and change in the amount of groundwater recharge associated with climate change and human interventions. The model result can also be applied for the operation of groundwater remediation, developing aquifer recharge systems, and to understand the changes in natural recharge amount caused by climate change (Maliva, 2004).

The occurrence, distribution, movement, and chemistry of water are very different depending on the nature of surface and subsurface materials and the existing geological structures. Qualitative and quantitative aquifer characterization and developing more or less accurate conceptual models that can at least approximate the hydrogeological characteristics of an area is very essential for knowing the groundwater potential of the catchment.

Field-based quantification of groundwater budget components should be part of the conceptual model developed to provide an initial understanding of the major inflow and outflow portions of the model domain. The conceptual model should at least describe and approximate the hydraulic properties (porosity, hydraulic conductivity, transmissivity) of rock units, boundary conditions (no flow, constant head, and head-dependent), amount and distribution of recharge and discharge, groundwater flow system, aquifers extent (thickness and distribution), etc. After developing the conceptual model of the groundwater system an appropriate mathematical code is selected based on the objective and the availability of data, budget, time, etc. Mathematical representation of

hydrogeologic processes necessarily requires simplifying assumptions. Those assumptions are embodied in the governing equation while transforming the conceptual model into mathematical groundwater flow governing equations.

1.2 Problem Statement

In the upper Mille catchment, many wells are drilled currently for groundwater-based irrigation and water for drinking purposes. There are some previously worked researches related to hydrogeology which focused on; quantifying the amount of recharge, characterizing the aquifer system (aquifer types, and hydraulic parameters distribution), investigating surface water groundwater interaction, and characterizing the hydrochemistry of the aquifer in the area. But, knowing only the occurrence and the chemistry of groundwater can't be a guarantee for the sustainable use and management of this underground natural resource. In the area, there are many towns like Hayk, Boru, Wuchale, Wurigessa, and Mersa which need groundwater for different purposes. As discussed before, even if there are some hydrogeological works in the area; the mechanism of groundwater flow, the response of the aquifer for future stress, and the groundwater head distribution on different scenarios is not yet determined. Moreover, knowing the rate of extraction is very useful for the sustainable use of groundwater. To better understand the groundwater system (aquifer properties, groundwater flow, to predict the future groundwater head under different pumping scenarios, and to recommend on the groundwater resource development plans) of the upper Mille river catchment, steady-state numerical groundwater flow modeling is very essential. The present study fills the gaps that have been discussed so far and it can also be used as a preliminary database for future detailed hydrogeological work within the present watershed and nearby catchments.

1.3 Objective of the Study

1.3.1 Main objective

The main objective of this study is to develop a steady-state numerical groundwater flow model of the study area using Processing MODFLOW.

1.3.2 Specific objectives

Here are some of the specific objectives which have been given special emphasis by this research work:

- ⊕ Estimating the Groundwater recharge by different techniques (WB and SWAT model),

- ⊕ Classifying the aquifers into different hydrogeological units based on their hydraulic properties and productivity,
- ⊕ Developing a conceptual model which best approximates the hydrogeology of the area,
- ⊕ Design a groundwater flow model to have a look at the impact of a change in hydrogeological parameters on the groundwater system.
- ⊕ To well understand the effect of pumping (current and predicted) on regional or local groundwater levels of the catchment.

1.4 Research questions

Some research questions which lead to formulating a proposal to do the study in the area are the prime-motor of the research. These research questions are used as a guide to focus on the proposed objectives. By considering the time, budget, availability of data, and objective of the research, the following questions have been formulated;

- ⊕ What is the groundwater recharge amount and distribution within the study area?
- ⊕ How much is the rate of abstraction of groundwater due to pumping in the study area?
- ⊕ Which lithologic units have good groundwater potential?
- ⊕ How is the groundwater head contour of the study area respond to a change in groundwater recharge and a change in the rate of groundwater abstraction for different Well operation scenarios?

⇒ All these questions are formulated before starting the actual research work and used to develop a scientific hypothesis and keep the researcher (me) on the right track. In the end, all the above-listed questions are answered in a different section of the research.

1.5 Literature Review

Many geological and hydrogeological types of research have been conducted by different by giving special emphasis on; geology, geochemistry, tectonics associated with rifting, surface, and groundwater with different approaches and objectives. Some of the reviews that have been used for the present study are categorized based on the intent of the study, such as a review on geology, hydrogeology, and modeling. This list is intended to provide background information that helps to develop a better understanding of the groundwater system (recharge estimation, aquifer characterization, and steady-state numerical groundwater flow simulation) of the upper Mille river

catchment. This literature review list is not meant to be all-inclusive. Each category is appropriately cited and referenced based on AAU referencing style as presented here below.

1.5.1 Previous geological works

The regional geology and the geology of the neighbor catchments have been studied by many researchers. Recently, the geology of the western afar margin is studied by [Zwaan, F., et al. \(2020\)](#) which focused on the structural analysis of the western afar margin in which the upper Mille river basin is found. Accordingly, the study concluded that the N-S-oriented WAM forms a major transitional zone between the Ethiopian Plateau and Afar rift system. The area is characterized by NNW-SSE normal fault, small-scale antithetic faults, and an associated series en-echelon marginal grabens later on filled with young sediments which used as a major aquifer system in the area.

According to [Mesfin Sahele \(2001\)](#) most lithological units which are found on the border of the MER are; colluvium and river channel deposits, alluvial deposits, scoriaceous and basaltic lava flow, and fractured basalt, welded tuff, and rhyolite. The dominant rock units in the NW Ethiopian plateau are basalt and rhyolite on which the rhyolites either overlie the flood basalt sequence or are found interbedded with the upper parts of the flood basalt succession ([Dereje Ayalew and Gezahegn Yirgu, 2003](#)). Two main phases of quaternary volcanism and rifting are identified here based on stratigraphic and tectonic relationships ([Bekele Abebe et al., 2007](#)).

1.5.2 Previous hydrogeological works

Hydrogeological works which focused on groundwater chemistry, aquifer characterization, groundwater assessment, surface water groundwater interaction, and related works are categorized and reviewed under this category. Some of the literature reviews are within and nearby catchments whereas, others are not but which are much related and quite important for the present study (Aquifer characterization and steady-state numerical groundwater flow modeling in case of upper Mille river basin).

The most recent hydrogeological research work in the study area was conducted by [Eden Dessalegn \(2020\)](#) which is entitled “Groundwater Assessment of Upper Mille Basin”. By the study, the groundwater recharge was calculated by using Base-flow separation, chloride mass balance, and SWAT model techniques. Based on this study the amount of mean annual precipitation is 1157.6mm and the groundwater recharge of the watershed is 135.9 mm, 115.66 mm, and 140.48 mm respectively. The aquifer is characterized and grouped into hydrologic units. High values of hydraulic conductivity and transmissivity are observed in the alluvial and colluvial

sediments. Whereas, low values of hydraulic conductivity and transmissivity are observed in the swampy and rhyolitic rock units. The main productive aquifer of the area is the unconsolidated quaternary sediments. The hydrochemistry data of the watershed indicates that; the recharge areas are rich in Ca-Mg-HCO₃ or Mg-Ca-HCO₃ water type, northern and central part of the valley is rich in Ca-Mg-Na-HCO₃ or Mg-Ca -NaHCO₃ water type, and Na-Ca-HCO₃ Water-type towards the eastern corridor of the river catchment. The present study estimates the water balance components of the area using the water balance method which is yet applied in the study area and using the SWAT model to compare the results obtained from the two methods. And the recharge is used later as an input for the steady-state numerical groundwater flow modeling.

Some part of Upper Mille watershed was studied by **Molla Demile (2000)** which gives emphasizes on the hydrology, hydrogeology, and hydrochemistry of Hayk-Hardibo lakes system. According to this study, two major hydrostratigraphic units are identified. These units are quaternary unconsolidated sediments and fractured volcanic rocks, both having a good permeability and transmissivity. Even if the volcanic units have good permeability and transmissivity they are considered as poor aquifers due to their morphological setting but good recharge zones, recharging the Quaternary unconsolidated sediments that occupy low lying flat areas in the studied catchment. Generally, the volcanic rocks lie within the recharge zone while the Quaternary sediments lie in the discharge zone (**Mesfin Sahele, 2001**).

In the case of Ethiopian rift volcanic aquifers, the groundwater flow, recharge, and geochemical evolutions in the volcanic and associated aquifers of the region are very complex. The single most important factor that controls the groundwater flow continuity between the high rainfall region in the plateau and the rift floor aquifers is the geological architecture of the interface zone (**Seifu Kebede et al. 2008**).

There are also some previously worked researches which mainly focused on the hydrochemistry of the groundwater using different approaches to investigate the usefulness of the water for domestic, industrial, and agriculture purposes. The water quality is mainly controlled by the occurrence of basic and acidic volcanic rocks, major tectonic discontinuity, soil type, and the topographic setup. In addition to classification for drinking, irrigation, and industrial purposes, the analysis of the chemistry of groundwater is useful for prediction and understanding of the movement and direction of groundwater flow, recharge discharge estimation, and climatic influence. The usefulness of groundwater for various purposes can be established based on the type and concentration of the dissolved solutes. Based on the hydro-chemical analysis the

dominant water type in the present study area is bicarbonate with both transitional and basic types. Generally, the groundwater and surface water of the area is suitable for irrigation and drinking purposes (GSE, 2017).

Integrated geological, geophysical, and hydrodynamic, hydrogeochemical, and environmental isotopic studies together with a simple regional groundwater flow model help to conceptualize aquifer distribution, groundwater dynamics, and the relationship between aquifer systems (Tilahun Azagegn, 2014).

A detailed and multi approached study was conducted in the awash basin by Andarge Yitbarek, (2009). In the study hydrochemistry, and isotope hydrogeology methods are applied and confirmed that these methods are very essential for the understanding of groundwater systems in every aspect.

1.5.3 Previous works on modeling

Modeling is relatively a new science, especially in Ethiopia. Due to the lack of data on groundwater and surface water, numerical groundwater flow modeling is yet to be done in the study area. Nowadays, Numerical Modeling is exercised by many researchers in different parts of Ethiopia. In the following literature's many of the modeling works are done out of the present study area but aiming to achieve a similar objective with this study.

According to W, Anderson, and Woessener (1992), models are conceptual descriptions or approximations that describe physical systems using mathematical equations; they are not exact descriptions of physical systems or processes. By mathematically representing a simplified version of a hydrogeological system, reasonable alternative scenarios can be predicted, tested, and compared. The applicability or usefulness of a model depends on how closely the mathematical equations approximate the physical system being modeled (W, Anderson, and Woessener, 1992). To evaluate the applicability or usefulness of a model, it is necessary to have a thorough understanding of the physical system and the assumptions embedded in the derivation of the mathematical equations. The mathematical model contains the same information as the conceptual one but is expressed as a set of equations that are amenable to analytical and numerical solutions (Drawdown, 1996).

Recently, part of the lower Awash basin was studied by Mulatu Tarekegn (2020). The study is entitled "Steady State Groundwater Flow Modelling of the Sunuta Catchment (Western Afar Region)". The study gives a special emphasis on the effect of groundwater pumping for Irrigation. This study was conducted adjacent to the present study area. The water balance components of the

catchment are calculated using WetSpss modeling which is again used as an input for the numerical flow modeling of the catchment. The recharge of the catchment-based on the WetSpss model is estimated as 61.1mm/year. Based on the sensitivity analysis of the model, the groundwater head of the catchment is highly sensitive to a change in horizontal hydraulic conductivity and groundwater recharge rate. The model simulates a mean annual groundwater recharge of 50.20mm/year which is close to the estimated recharge using the WetSpss model. This shows that modeling is very applicable for the study area which is adjacent to the present study area. Based on this the present study tries to characterize the general groundwater flow condition and head distribution of the catchment.

Getachew Asmare (2005) conduct a model-based groundwater system analysis for the Hayk-Hardibo catchment (part of the present study) to understand the interaction between the surface and groundwater of the Hayk-Hardibo Catchment. The values obtained from the steady-state numerical model suggest the volumetric water budget terms of the groundwater flow components for the Hayk-Hardibo catchments. The simulated values of the model are as follows: Groundwater inflow is $6.5393855E+04m^3/day$ and groundwater outflow $65389m^3/d$ which means that a substantial amount of groundwater leaves catchment.

The groundwater dynamics of volcanic and sedimentary rock were characterized by many researchers in different basins of Ethiopia. Some of the hydrogeological researches particularly on groundwater modeling which used as a background for the present study are; ([Behailu Birhanu et al., 2018](#); [Tenalem Ayenew, 2001](#); [Tenalem Ayenew & Tilahun Azagegn, 2008](#); [Tilahun Azagegn, 2014](#); [Berehanu et al., 2017](#); [Girmay et al., 2015](#)).

1.6 Methodology

To achieve the previously stated main and specific objectives, different approaches and methodologies with the aid of different types of equipment have been followed to conduct this study starting from pre-fieldwork secondary data collection to the completion of this research work. These methods and approaches are adapted in three different phases, pre-field (Phase-I) work, fieldwork (Phase-II), and post-field (Phase-III) work. In each phase, different materials and activities have been practiced. The detailed research work procedures are described as follows.

⊕ Pre-fieldwork (Phase-I)

Pre-field works are activities that are done before going to the field. The major activities are previous works assessment and data collection like hydrometeorological data, well completion

reports, pumping test data, and hydrogeological loges were collected from different institutions and organizations (Ministry of Water Resources, private company data sources, Ethiopian Geological Survey) which is then organized to make it available for the research. Then, following the appraisal of the proposal all the reliable secondary data were arranged to prepare a database and base map of the study area. After identifying the gaps to be filled and data that need field verification, field preparation was carried out including preparation of the field equipment like, GPS, deep meter, topographic map, geological maps, EC-meter, and other materials that are helpful for the actual fieldwork.

⊕ **Fieldwork (Phase-II)**

Fieldwork is the second phase which is mainly done in the field. The major field activities are collecting secondary data from different sources and primary data from the study area. The primary data includes measuring groundwater levels, taking readings of borehole locations and elevation using GPS, water quality survey (pH, Temperature, Electrical conductivity), field verification of the study area, and determination of physical boundaries. The field observation was focused on the description of the geology, lithology, geomorphologic setting, surface water divide, location of recharge, and discharge areas, qualitative and quantitative characterizing of surface water bodies, taking photos of the representative geological exposures, water inventory points, and geological structures. Secondary data such as borehole logs, pumping test data, hydrogeology feasibility reports, and well completion reports were collected from the water offices which exist in the area.

⊕ **Post fieldwork (Phase-III)**

Post-field activities are done after the fieldwork which is mainly on data processing, analyzing, and interpretation of primary and secondary data, which were collected before and during the fieldwork. In this stage, the geological, hydrogeological, structural data are assembled into usable formats. The aquifer is characterized by interpreting the processed primary and secondary data and then a conceptual model was developed. This includes a description of the groundwater flow system associated with surface water bodies, as well as hydro-stratigraphic units and system boundaries. Water balance components were calculated using different methods. To characterize the major aquifer systems: pumping test data of boreholes, hydrogeological logs, and geological and structural data were interpreted. Groundwater contour maps were produced from field water Level measurements of boreholes and dug wells. Here, below is a detailed description of how

sampling is designed, how the water balance components were quantified, how the conceptual model developed, how the numerical model applied, and how scenario selection and analysis were done.

Primary and secondary data were collected before and during the fieldwork. Important geological and hydrogeological data were gathered from literature, water offices, and individuals before going to the field. These data are assembled into meaningful formats and used as preliminary information to know the hydrogeology of the Upper Mille river catchment. During the fieldwork primary, geological and hydrogeological data were collected from surface lithological exposures and inventory water points. Borehole data (static water level, depth, yield, conductivity, transmissivity, lithologic section, EC, TDS, pH, etc.) are collected from regional water offices (water work design, water supply offices) to the kebele level. Physical boundary conditions were investigated. Springs, boreholes, lakes, and rivers were systematically addressed and inventoried. From those inventory points, necessary data were measured and recorded which later compiled and changed into meaningful information which used to understand the hydrogeology of the upper Mille catchment.

The location, physiography, drainage pattern, soil, slope, climate zone, and LULC map of the catchment were produced by ArcGIS, Surfer, and global Mapper using satellite images, FAO soil classification, etc.

Meteorological parameters (rainfall, temperature) were systematically arranged to tabulate the water balance components (precipitation, evapotranspiration, surface runoff, groundwater recharge) of the catchment using the meteorological data obtained from the National Meteorological Agency (NMA), FAO soil database, and Sentinel-2 LULC data. The ultimate goal of tabulating the water balance component of the area is to know the amount of mean annual groundwater recharge added to the subsurface water. The mean annual groundwater recharge of the catchment was calculated using the Water Balance (WB) and Soil Water Assessment Tool (SWAT) model techniques. Later on, the estimated recharge was used as an input parameter for the steady-state numerical modeling.

The geological map of the area was adopted from GSE 2014. By processing, analyzing, and integrating primary and secondary data obtained from literature, and field inventory points using appropriate software's hydraulic conductivity (K), transmissivity (T), EC and TDS distribution, groundwater level contour, hydrogeologic cross-section maps were produced. By embodying all these, lithological maps were transformed into hydrogeological units, and then aquifer

classification and schematic hydrogeological map of the catchment were produced. All these were used to develop an appropriate conceptual model which approximates the hydrogeological conditions of the Upper Mille catchment.

After conceptual model development, the mathematical model consisting of a governing equation and boundary conditions was selected. A steady-state numerical flow model (Processing MODFLOW-2005) were used to translate the already developed conceptual model into the mathematical model code which is governed by groundwater model flow equations. Following this, the model was designed to translate the conceptual model into a numerical groundwater flow model by designing the grid/mesh, setting boundary conditions, assigning values of aquifer parameters, and hydrologic stresses, and the model were simulated. Then arguably calibrating the model by changing the hydraulic properties (K value), and the amount of recharge to establish the validity of the conceptual and numerical models. The model calibration was evaluated using RMSE statistical approaches. The model domain water budget components were simulated. Sensitivity analyses were done. In the end, different scenario analyses were conducted to forecast the response of the system to future stress (pumping and recharge rate) events. The scenario was selected based on the possibility of an increasing rate of groundwater abstraction and decreasing recharge due to expected increasing demand and climatic change respectively in the future. The increasing demand for groundwater for drinking and irrigation will put pressure to drill additional boreholes which will result in the extraction of much water relative to the current abstraction rate from the subsurface. In this study, the scenarios were analyzed by decreasing the recharge and increasing the current pumping rate. Doing this, the hydraulic head distribution of the model domain was observed in the discussion section of the study.

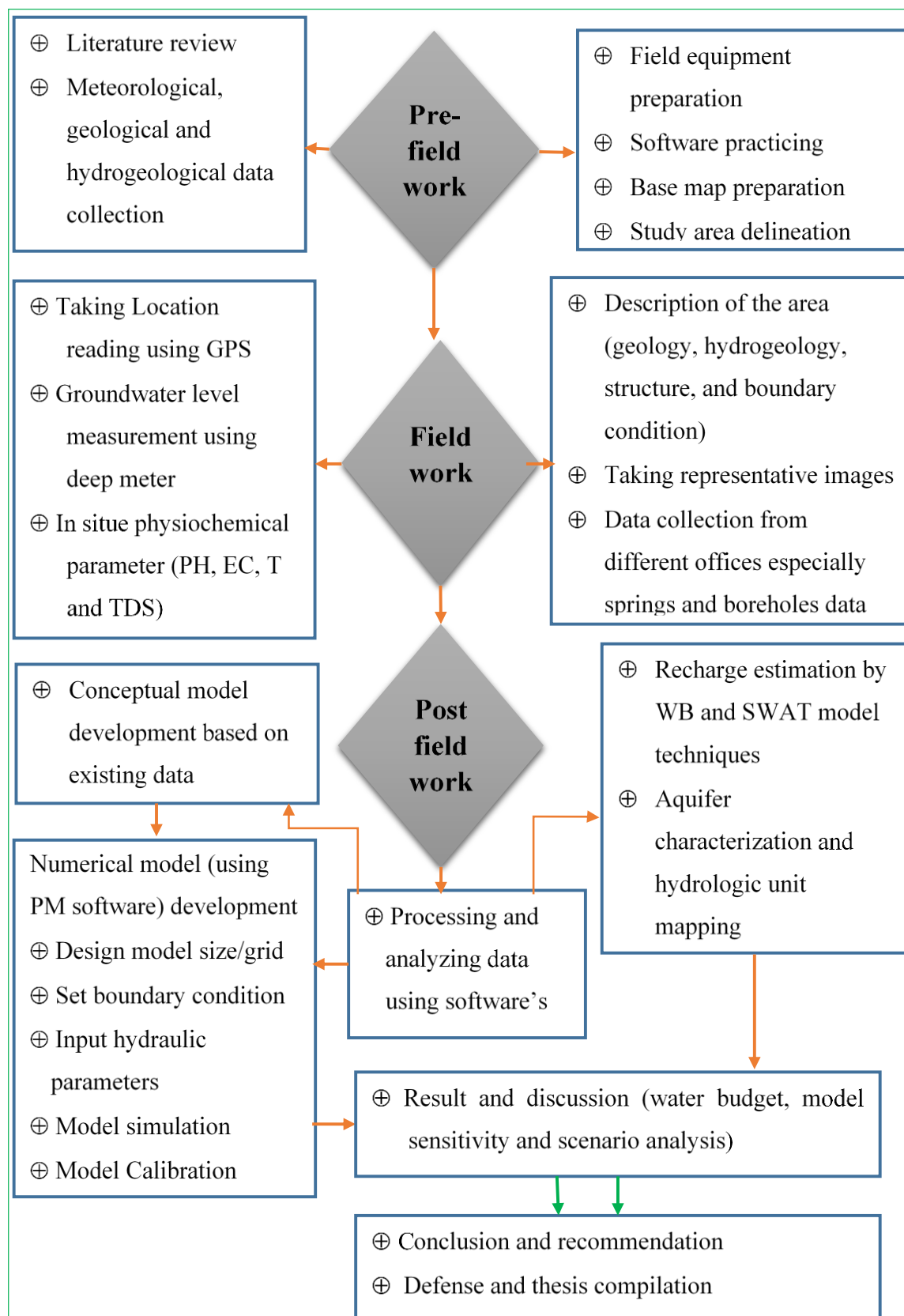


Figure 1: Flowchart showing the summary of the methods and approaches followed to achieve the proposed objectives from the very beginning to the end of the research work.

1.7 Materials and Software Used

Different materials and software were used to process, analyze, and manipulate different formats of data.

A. Materials

The common most used materials during this research work are listed as follows.

- ⊕ **GPS:** - used to locate and search the location of points of interest including wells, exposures, and boundaries of the area, etc.
- ⊕ **Digital camera:** - used for capturing images of exposures, water points, well fields, and anything important for the research work.
- ⊕ **Deep meter:** - used for measuring the static water level of shallow and deep boreholes
- ⊕ **Meter:** - It is used for measuring lithological exposures, the size of structural discontinuities, and the width of rivers in the selected sites.
- ⊕ **Maps:** - Different maps (topographic, geological, and hydrogeological) are used during the fieldwork to know the area well and to select the best Travers direction that needs more interest.
- ⊕ **Stationary materials:** - These are used for recording what I have seen in the field before compiling into softcopy format. These materials include a handbook, pencils, markers, rulers, etc.
- ⊕ **Personal computer:** - It is used to process the whole research work and to run the software.

B. Software's

- ⊕ **ARGIS 10.1 tools:** - To delineate and produce several maps such as location map, soil map, hydraulic conductivity map, water level contour maps, geological map, hydrogeological map, computation of different characteristics of the basin.
- ⊕ **AutoCAD-2007-** It is used to construct a hydrogeological cross-section along the selected lines.
- ⊕ **Sulfur-12:** - Used to produce a 3D physiographic map of the catchment from the DEM.
- ⊕ **Global Mapper:** - To change the data into a suitable format for processing MODFLOW

- ⊕ **Processing MODFLOW-2005:** - It was used for the groundwater modeling simulation with different scenarios.
- ⊕ **SciDavis:** - Used to plot different kinds of graphs

1.8 Structure/Outline of the Thesis

This research work is organized into eight different chapters and many subchapters within each chapter.

CHAPTER ONE: Deals with the general introduction which contains the background, statement of the problem, objective (main and specifics), research questions, literature review, methodology and materials used, and significances of the study. All these are presented in separated subchapters.

CHAPTER TWO: Gives the general physical descriptions of the upper Mille river catchment which includes; physiography, climate, soil texture, slope, land use land cover, drainage pattern, surface water body (streams/rivers, springs, lakes, and wetlands).

CHAPTER THREE: This chapter focused on the hydro-meteorological characteristics of the study area. This includes meteorological station description, meteorological parameters quantification (precipitation, temperature, etc.), and determination of areal depth precipitation using Thiessen polygon method, evaporation, runoff, and recharge estimation using different techniques (WB and SWAT model).

CHAPTER FOUR: Presents the regional and study area lithological and structural descriptions. This chapter includes litho-hydrostratigraphic relationships in the upper Mille basin as observed from exploratory drilling, field mapping, and complemented data collected from several sources.

CHAPTER FIVE: Deals with aquifer characterization and classification of the units into different hydrologic groups based on the geology, geomorphology, structure, and hydraulic parameters. In this chapter lithostratigraphic units presented in chapter four are transformed into hydrological units.

CHAPTER SIX: In this chapter, the conceptual model developed in chapter five was transformed into numerical modeling using groundwater flow equations. The chapter includes model design,

setting input parameters and boundary conditions, and finally run the numerical model until the simulated and observed target point matched.

CHAPTER SEVEN: This is the main chapter which presents the results and basic discussions made from each section of the research. It also contains the basic discussions (sensitivity and scenario analysis) based on the results obtained from the model simulation.

CHAPTER EIGHT: This is the last chapter in which the conclusions and the recommendations were presented. And at the end, the references used during this research work are presented.

1.9 Significance of the Study

Often groundwater abstractions are carried out without the basic understanding of the groundwater recharge, the lateral and vertical extent of aquifers, and the available groundwater reserve. The most important issues to be addressed here by this research are the mechanism of groundwater flow, occurrence, and assessing the response of the system to different abstraction and recharge rates. In this regard, groundwater flow models play an important role in hydrogeological studies. The results of this study can be also very important for private and governmental drilling companies, consultant's offices, and local water bureaus to make good and sound decisions regarding sustainable and wise management of the catchment groundwater resources. Furthermore, this research can be used as a baseline or as a background for other individuals or organizations who want to conduct a further and detailed groundwater-related research study in the area. After the completion of this research work such problems related to lack of study about the hydrogeology of the area will be at least partially filled.

CHAPTER TWO

STUDY AREA DESCRIPTION

2.1 Location and Accessibility

The Upper Mille river catchment is found in the western margin of the Afar rift within the escarpment zone of the northwestern Ethiopian highlands. The area is part of the lower Awash River basin (Figure-2). It is found 440km far from Addis Ababa in the northeast and 40km in the northeast from Dessie town. The absolute location of the river catchment is confined in zone 37P between 0557969-0595777 Easting and 1236452-1300230 Northing. The total enclosed area of the watershed is about 1360Sq.km. The area is accessible through roads on the way from Dessie to Woldiya main asphalt road. But some part of the study area is inaccessible due to very steep topographic nature in which there is no any kind of roads. There are many towns within like; Sulule, Hayk, Wuchale, Wurigessa, and Mersa which makes the area accessible.

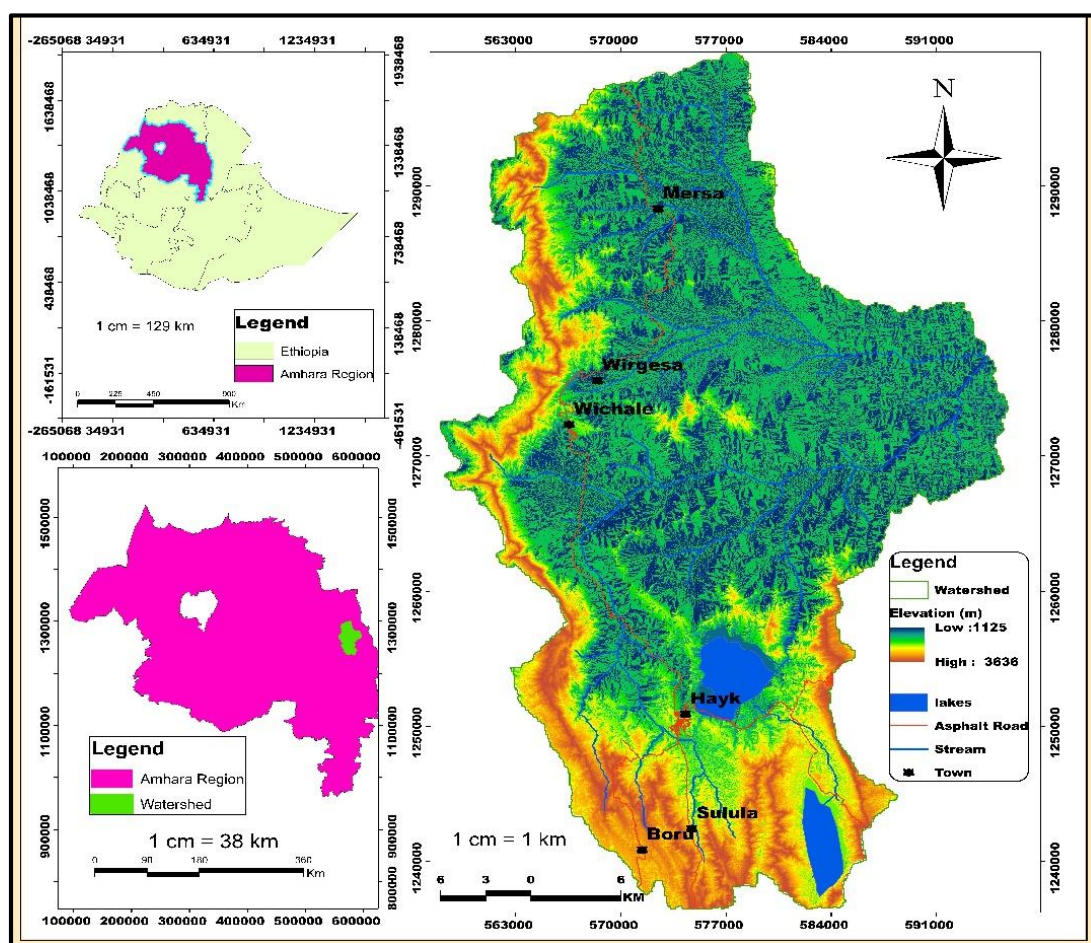


Figure 2: Inset location map of Upper Mille river catchment

2.2 Physiography of the Watershed

The physiography of the study area is very complex ranging from mountainous areas to near-flat low laying topography (Figure-3). The watershed is dominated by a chain of volcanic mountains on all sides forming the watershed divide. It is bounded in the west by NNE-SSW trending rift escarpment. Small volcanic ridges are also common. The physiography of the watershed is also characterized by the presence of deep river gorges, grabens, and lakes (Hardibo and Hayk). The current landforms and topography of the area are the result of the long-term deformation and associated volcanism. The variability of the landform is related to the geological setting (rifting, faulting, and the associated volcanism and grabens filling quaternary and recent sediments) of the area. The elevation of the study area ranges from 3640m (western part) to 1120m (eastern part) a.s.l. The nature of the physiography controls the climate, amount of runoff, degree of infiltration and percolation, surface water divide, land use land cover, etc. due to this during any hydrogeological works, it's very important to consider and evaluate the distribution of surface landforms.

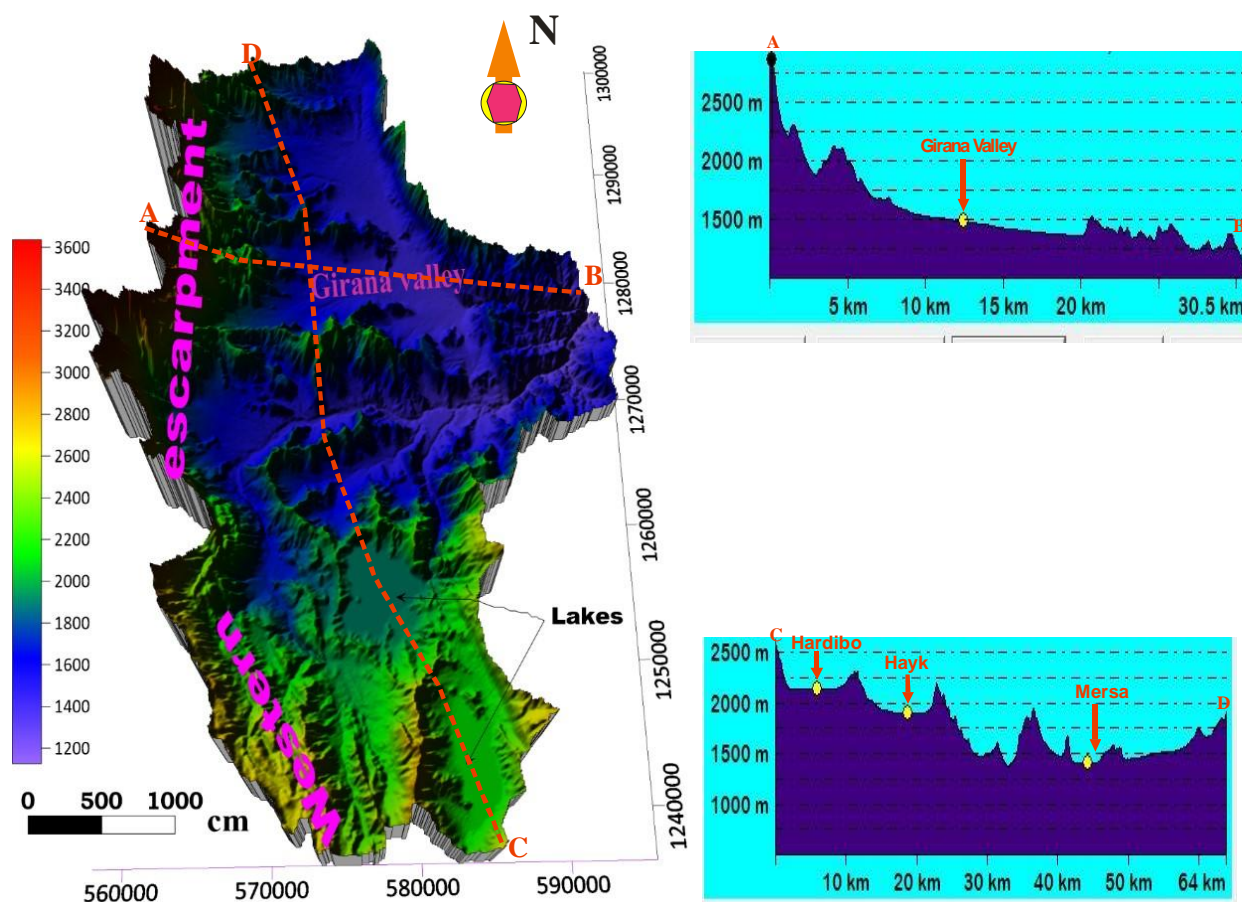


Figure 3: 3D Physiographic map of Upper Mille catchment

2.3 Slope/ Gradient of the Watershed

The slope of the watershed is not uniform. It ranges from level landforms to very steep-sided cliffs. The highest slope values are found in the sides of river gorges, western rift escarpment, and small volcanic mountains. Whereas, the middle part of the area (mapped as unconsolidated quaternary sediments) is relatively flat. The gradient of the study area watershed is classified into five classes: 0-5, 5-15, 15-25, 25-35, 35-76.8 degrees, which represent from nearly horizontal to very steep slope areas. As observed from the slope classification map (Figure-4) most of the area falls in the range from 15-25 degrees. The slope of an area controls the amount of runoff, percolation, soil thickness, vegetation cover, and density of the watershed which in turn determines the percentage of recharge from the total precipitation.

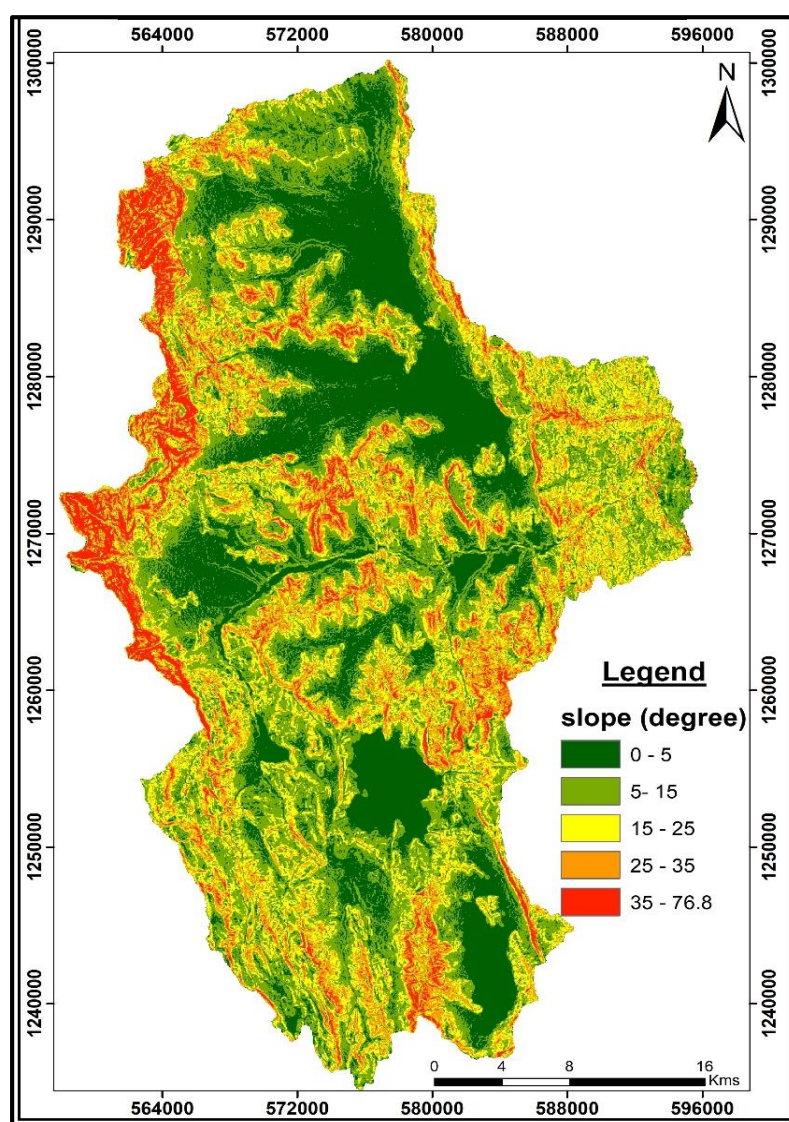


Figure 4: Slope classification map of Upper Mille river catchment

2.4 Drainage Pattern of the Watershed

The pattern and the density of the stream indicate the hydraulic characteristics of the watershed. In the area, streams have variable discharge and flow directions. Some streams flow all over the year whereas, others are dry during the dry months. Streams start from the northern, southern, and western parts of the area and drain first to southeast, north-central, respectively. Finally, all the streams join and drain to the east towards the watershed outlet. The two major streams which flow all over the year are Paso Mille and Megenagna rivers. The drainage pattern of the river networks is generally dendritic (Figure-5). The area is known for its developed and undeveloped springs which are used for different purposes. In the watershed, there are two well-known natural lakes named Lake Hayk and Lake Hardibo which cover an area of 21 and 16Sq.km respectively. Swampy/Wetlands are also common mainly near the rivers, and surrounding the two lakes.

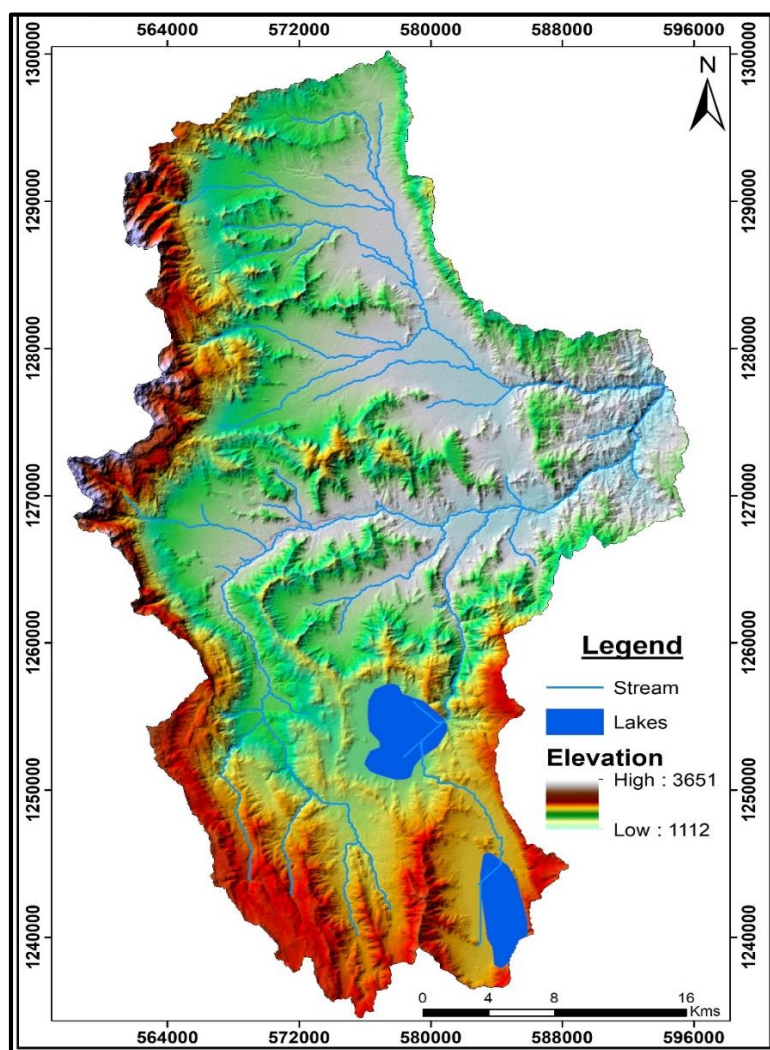


Figure 5: Drainage pattern and density of Upper Mille river catchment

2.5 Soil Type and Texture

The type, texture, and depth of soil in the area are different. The texture and the type of soil are controlled by nature and the type of subsurface formations which in turn affects the groundwater potential of an area. The soil groups of the Upper Mille watershed are classified into four major classes (Figure-6) according to the FAO soil group classification. As a result, four soil classes are distinctly mapped which are: Eutric Cambisols (CMe), Eutric Leptosols (LPe), Eutric Vertisols (VRe), and Lithic Leptosols (LPq). Eutric Cambisol soils have fine topsoil texture, 30%, 28%, and 42 % Sand, Silt, and Clay proportion, respectively and are classified as clays based on USDA texture classification. Eutric Leptosols have a medium topsoil texture, 50%, 20%, and 30% proportion of Sand, Silt, and Clay respectively, and are classified as sandy loams. Eutric Vertisols have fine topsoil texture, 21%, 25%, and 54% proportion of Sand, Silt, and Clay respectively, and are classified as Clays. Lithic Leptosols have a medium topsoil texture, 43%, 29%, and 28% proportion of Sand, Silt, and Clay respectively, and are classified as sandy loams (FAO, 2009).

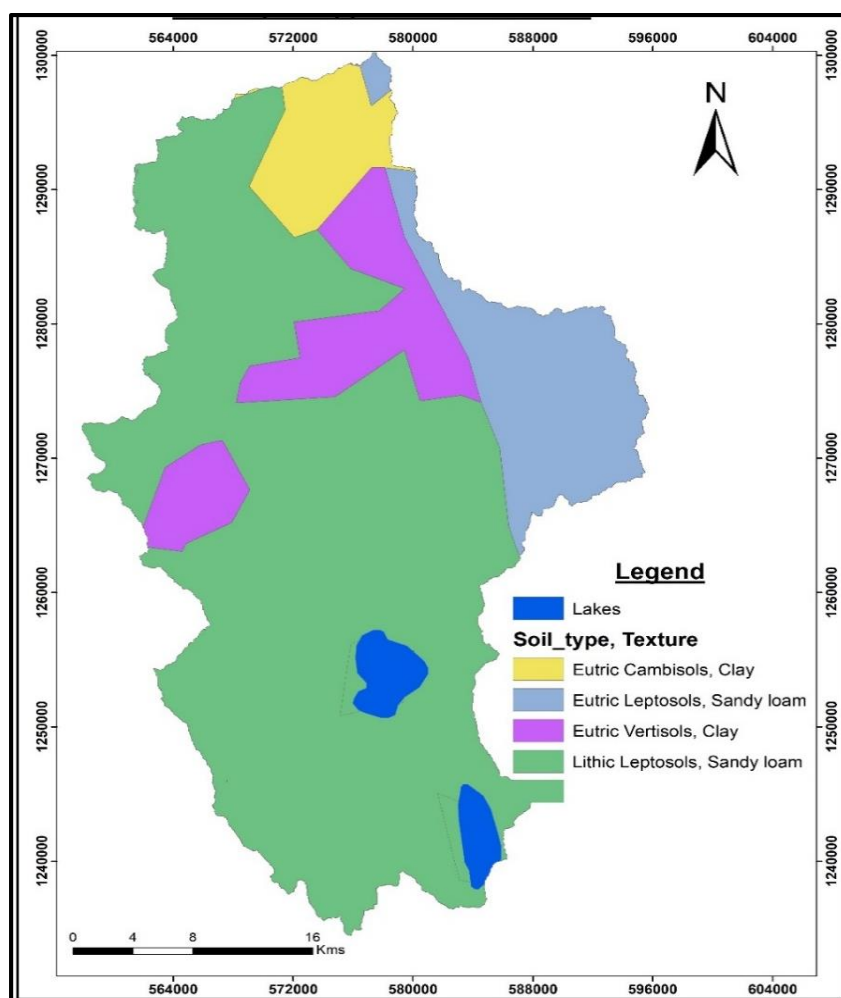


Figure 6: Soil texture classification map of the Upper Mille river catchment

2.6 Climate Zone of the Watershed

The climate of Ethiopia is mainly controlled by the seasonal migration of the Inter-tropical Convergence Zone (ITCZ) following the position of the sun relative to the earth and the associated atmospheric circulation. It is also highly influenced by the complex topography of the country. In Ethiopia, there are five traditional climate classes: Wurch (>3000m), Dega (an altitude range of 2500-3000m), Woina Dega (warm climate with altitude ranges of 1500-2500m), Kola (hot and arid type climate elevation <1500m.), and Bereha (very hot and hyper-arid climate) (NMSA, 2001). According to this classification, the upper Mille watershed lies within four different climate regions (Figure-7); Wurch, Dega, Woina Dega, and Kola. Most of the area lies within the Woina Dega climate region, whereas Wurch and Dega climate types are constrained to the western side and Kola to the downstream (eastern) areas of the watershed, respectively. Generally, temperature increases from west to east in reverse with elevation.

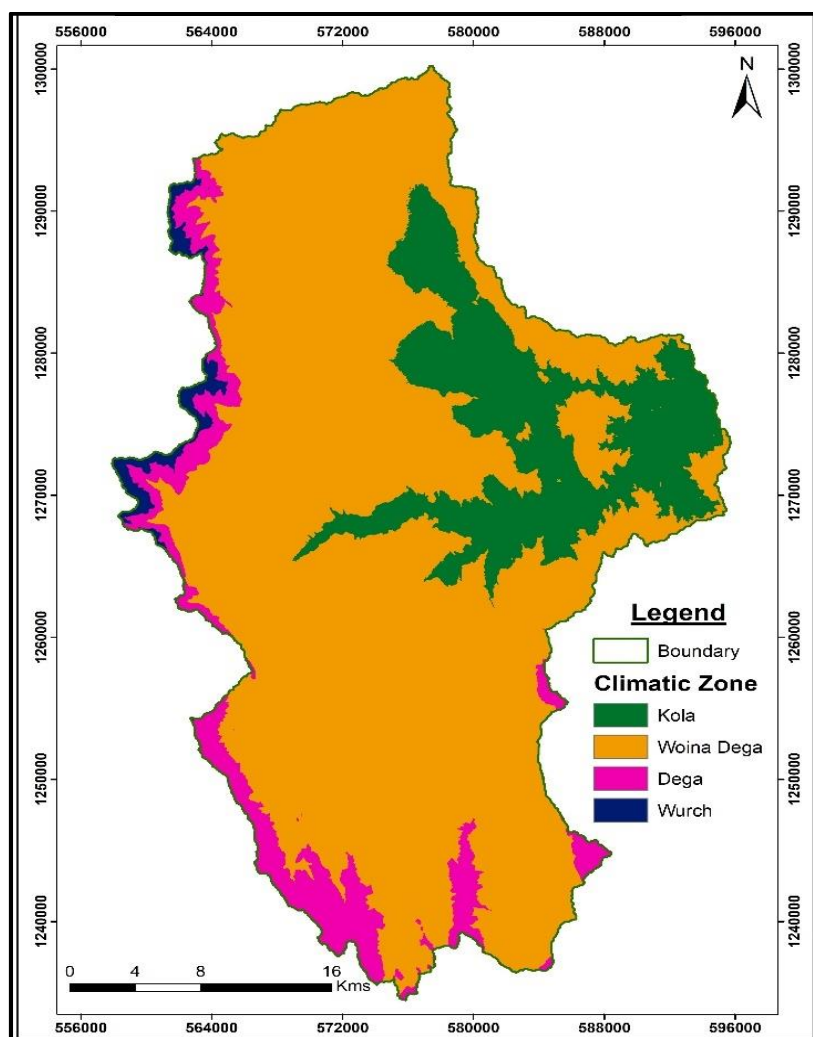


Figure 7: Traditional climatic zone map of Upper Mille river catchment

2.7 Land use Land cover (LULC)

The LULC of an area is one of the most important determinant factors affecting the water resource potential of an area. The water balance component of the watershed is highly sensitive to LULC. It is an input for the SWAT model in which it affects the amount and area of groundwater recharge, and runoff generation, etc. The LULC data of the area was found from a 20m resolution Sentinel-2 LULC map of Ethiopia. Based on the LULC map, the watershed is covered by eight land cover classes (Figure-8): Cropland, Shrub cover areas, Grassland, Tree cover areas, Aquatic or regularly flooded vegetation, Built-up areas, Bare areas, and Open water bodies.

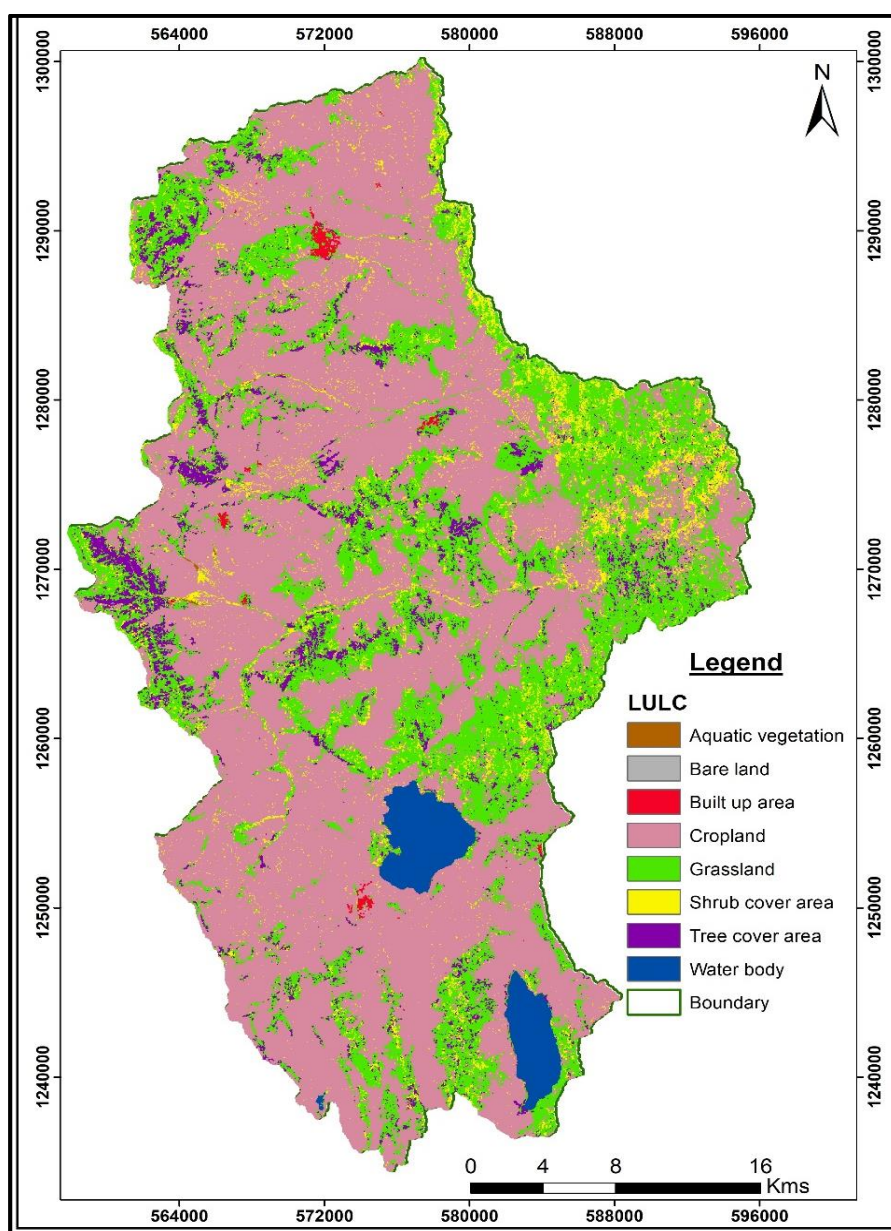


Figure 8: Land use land cover classification map of Upper Mille river catchment

Table 1: A summary of the proportion of each land use land cover type

No	Land use Land cover types	Area (Sq.km)	%
1	Cropland areas	834.3	61
2	Grassland areas	347	26
3	Shrubs cover areas	75.2	6
4	Tree cover areas	65	5
5	Open Water	34.4	2.5
6	Aquatic/ flooded	0.92	0.8
7	Built up areas	3.82	0.3
8	Bare land areas	0.04	0.003

The area is dominantly covered by croplands (61%) which account for more than half percent of the total area. The bare land area accounts for only 0.003% of the total study area, which is the minimum of all land use land cover classes. The major crops grown are; wheat, maize, tee, beans, millet, and peas. The main vegetation types are different acacia species, Bissana (corotoe), and trees.

CHAPTER THREE

HYDROMETEOROLOGY AND RECHARGE ESTIMATION

3.1 Meteorological Stations

Meteorological stations are used to record meteorological parameters like precipitation, temperature, wind speed, relative humidity, and sunshine hours. Meteorological stations within the Upper Mille watershed and nearby areas are mainly above 2nd and 3rd order. As a result, it is very difficult to get recorded data of all meteorological parameters from a single station. For this reason, missing meteorological parameter data in some of the stations were filled from New-LocClim 1.10. For this study, seven meteorological stations are used. For each parameter daily data from the National Meteorological Agency (NMA) for 19 successive years (2000-2018) are utilized. Stations within and nearby areas are, Bokeksa, Hayk, Mersa, Sirinka, Urgessa, Werebabo, and Wuchale.

3.2 Meteorological parameters

Meteorological parameters utilized for this study are precipitation and temperature. These parameters were used to quantify the water balance component of the watershed. Effective quantification of these parameters is the core point for groundwater and surface water investigation. In these subtopics, some of the parameters are quantified and presented using graphs, tables, and diagrams.

3.2.1 Precipitation

Precipitation is the only source of water for surface water bodies and groundwater aquifer systems. Precipitation is the main input (inflow) component used in the calculation of groundwater recharge estimation. To quantify the amount of mean annual precipitation in an area different method can be used like arithmetic means, Thiessen polygon, and isohyetal methods. Thiessen polygon method is applied for this particular study. To analyze the precipitation condition of the watershed, 19 years (2000-2018) daily data from seven stations were taken from NMA. Thiessen polygon maps were constructed using seven stations found in the vicinity of the watershed. The area of each polygon was known from the constructed polygons and then precipitation of each station was calculated for that area. The weighted area was calculated by dividing each Thiessen polygon area by the total area and this weighted area was multiplied by the precipitation value of each corresponding polygon. Finally,

each weighted precipitation was summed up to estimate the total average annual precipitation of the area.

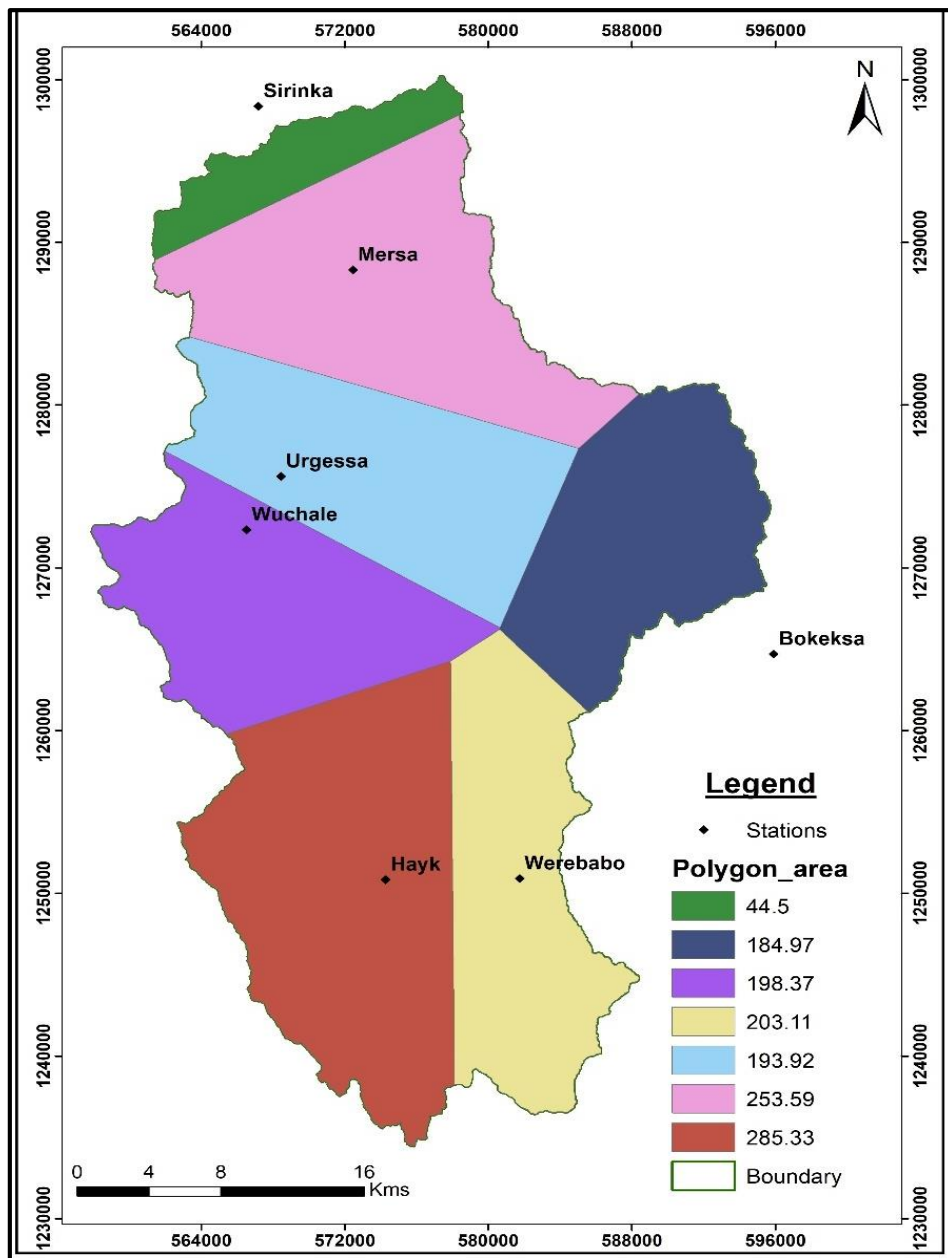


Figure 9: Constructed Thiessen polygon for each station

Table 2: Estimation of mean annual precipitation using Thiessen polygon method

Station	Prec (Pi)	Area (Ai)	Area (At)	Ai/At	Pi*(Ai/At)
Bokeksa	1090.379	184.97	1363.8	0.13563	147.8881
Hayk	1193.879	285.33	1363.8	0.20922	249.7834
Mersa	988.2316	253.59	1363.8	0.18595	183.7617
Sirinka	1065.59	44.508	1363.8	0.03264	34.78086
Urgessa	1155.837	193.92	1363.8	0.14219	164.3485
Werebabo	1172.947	203.11	1363.8	0.14893	174.687
Wuchale	1219.25	198.37	1363.8	0.14545	177.3399
Total					1132.589

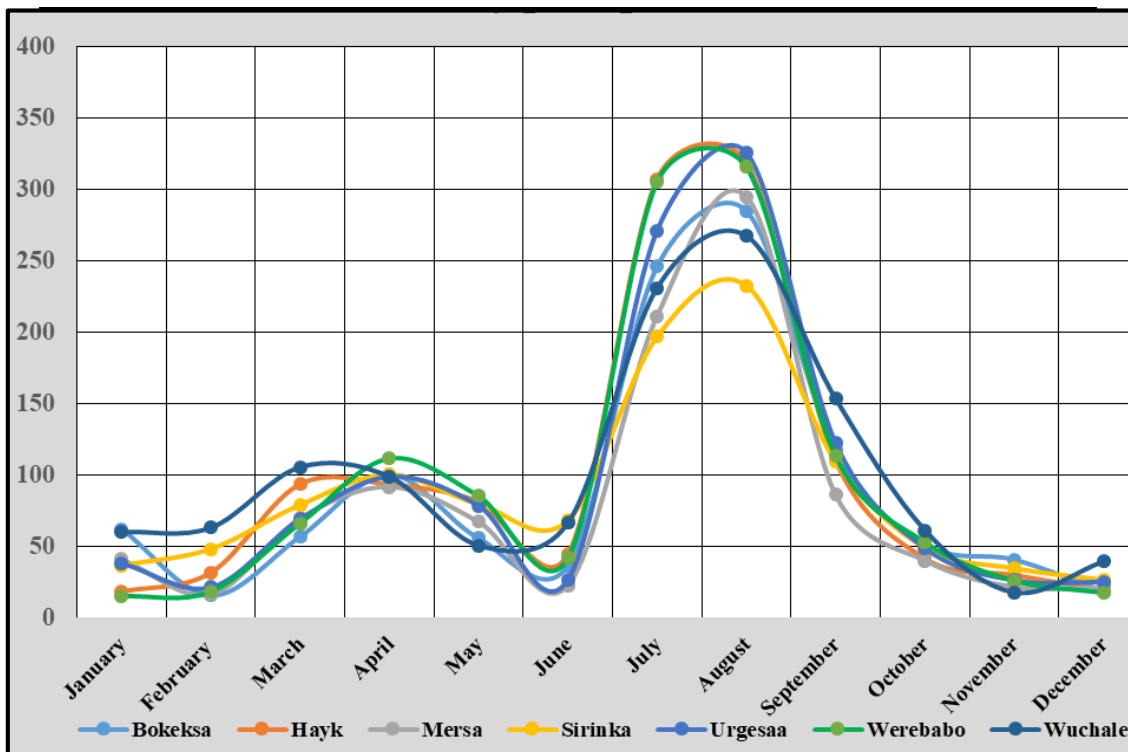


Figure 10: Mean monthly precipitation for each meteorological station

As observed (Figure-10), the average monthly precipitation for each station is minimum from October to mid-June whereas, maximum precipitation is observed from mid-June to mid-September. A small rainy season (Belg rainfall) is observed in March and April. Peak rainfall occurs in July and August whereas, the least rainfall is recorded in November, December, January, and February.

Table 3: Mean monthly precipitation of Upper Mille River catchment

Month	Jan	Feb	Mar	Apr	May	Jun	Jul	Aug	Sept	Oct	Nov	Dec
Mean	39.2	31.1	77.5	99.6	71.7	44.3	253	291.6	116.2	49.6	28.5	24.4

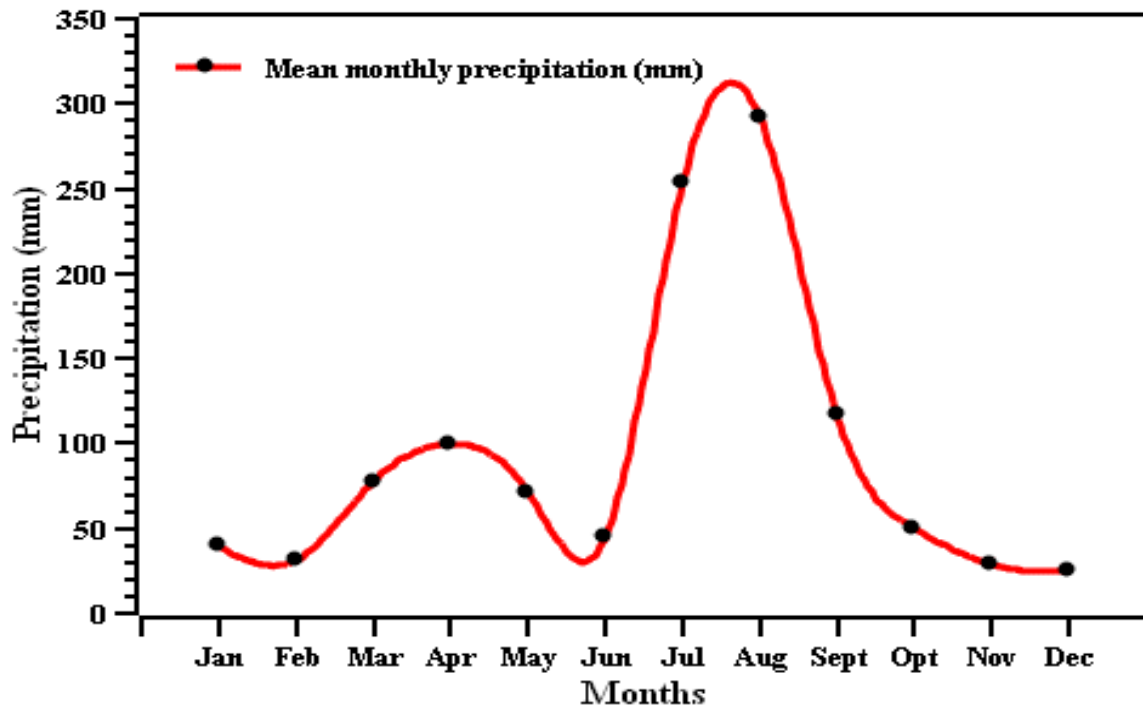


Figure 11: Mean monthly precipitation of Upper Mille River catchment

3.2.2 Temperature

Temperature is one of the controlling factors for the climate of an area which in turn affects the type of vegetation, amount of evaporation, and transpiration. Knowing the amount of mean monthly/yearly temperature is essential to determine the water balance components of an area. As indicated (Figure-12) below the mean air temperature of the area is not uniform rather it increased and decreased with time.

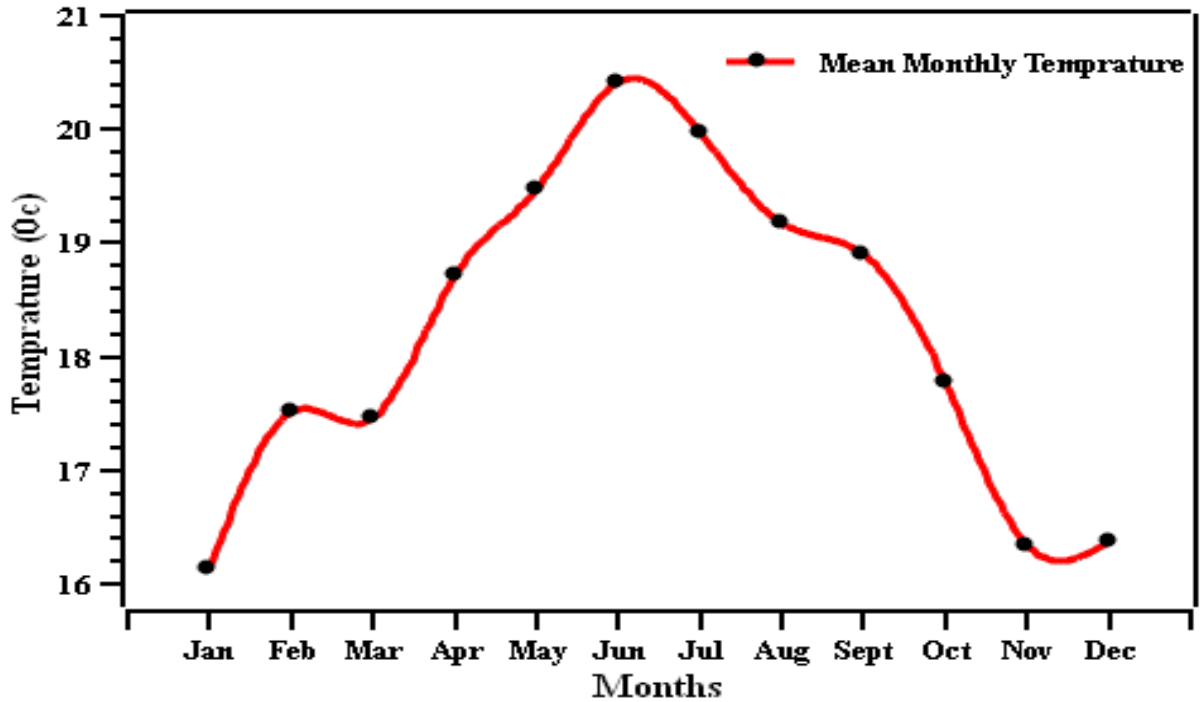


Figure 12: Average Mean monthly air temperature of Upper Mille river catchment

- ✚ The mean monthly temperature of the area attains its lowest value in November (16.34⁰C) and increases until June (20.41⁰C). June is the hottest month in the area. The area has a mean annual temperature of 18.20⁰C.

3.3 Groundwater Recharge Estimation Using WB Method

3.3.1 Evapotranspiration

Evapotranspiration is one of the outflow water balance components used in recharge estimation. The term evapotranspiration (ET) is commonly used to describe two processes of water loss from land surface to atmosphere, evaporation, and transpiration. Evaporation is the process where liquid water is converted to water vapor (vaporization) and removed from sources such as the soil surface, wet vegetation, pavement, water bodies, etc. Transpiration is the vaporization of water/liquid from plants mainly through their stomata due to the presence of solar radiation from the sun which creates a temperature difference.

A. Potential Evapotranspiration

Potential evapotranspiration refers to the amount of the possible maximum water loss through the process of evaporation and transpiration under unlimited moisture conditions. Potential evapotranspiration is calculated using the Thornthwaite method. This method uses air temperature as an index of energy available for evapotranspiration, assuming that air temperature is co-related with the integrated effect of net radiation and other controls of evapotranspiration. The available energy is shared in fixed proportion between heating the atmosphere and evapotranspiration. Potential evapotranspiration is computed using the following formula.

$$Et = 1.6b \left[\frac{10T_a}{I} \right]^a$$

Where Et - Potential evapotranspiration in cm/month T_a - Mean monthly air temperature in ($^{\circ}C$),
 b - latitude correction, I - annual heat index;

Using 19 years mean monthly air temperature, the annual heat index is calculated as;

$$I = \sum_{i=1}^{12} \left[\frac{T_{ai}}{5} \right] 1.5$$

⇒ By substituting the mean monthly air temperature given in the table into the above equation, the value of the annual heat index is found to be 83.6 (I.e., $I = 83.6$). Then the value of the exponent a can be calculated from the annual heat index using the following formula;

$$a = 0.49 + 0.0179I - 0.0000771I^2 + 0.000000675I^3$$

Then substituting for I , $a = 1.84$

The latitude of the study area is approximated to be 11° N. Hence, the latitude correction (b) for the calculation of potential evapotranspiration is given in table-4.

Table 4: Latitude correction values of 11°N Latitude

Month	Jan	Feb	Mar	Apr	May	Jun	Jul	Aug	Sep	Oct	Nov	Dec
b	0.97	0.98	1	1.03	1.05	1.06	1.05	1.04	1.02	0.99	0.97	0.96

⇒ Using the above parameters, potential evapotranspiration is calculated by substituting these values into the Thornthwaite formula. The values are presented in the graph below.

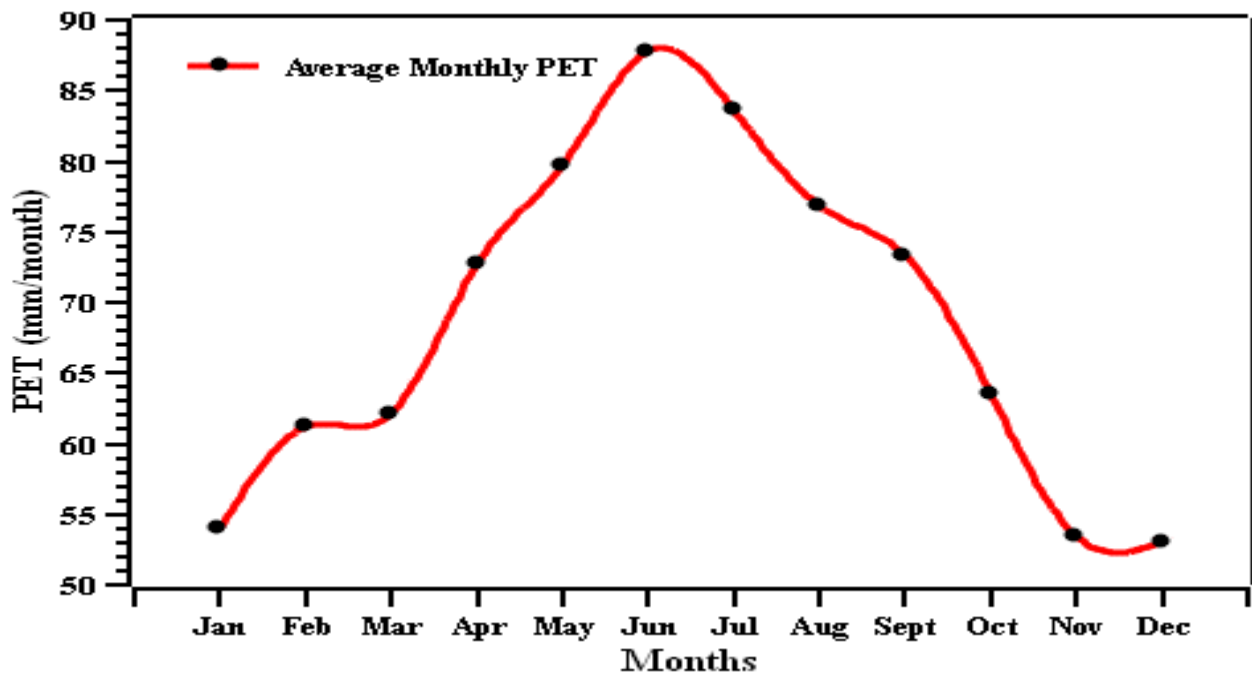


Figure 13: Average monthly Potential evapotranspiration

✚ The mean annual PET of the Upper Mille watershed is calculated to be **821.15mm/year**. From the above graph (Figure-13) it's observed that maximum PET has occurred in June (87.8mm/month) and July (83.5mm/month) since, there is unlimited soil moisture and maximum temperature whereas, minimum PET is observed in November, December, and January with a PET value of 53.3, 52.9 and 54.04 mm/month respectively in which the temperature and rainfall are low. This indicates that the amount of PET is highly related to the temperature of the study area.

B. Actual Evapotranspiration

Actual evapotranspiration is the amount of water that is evaporated in reality. Simply, it is the amount that occurs under the available moisture situation. The most popular method of computing actual evapotranspiration is through the calculation of potential evapotranspiration.

Actual evapotranspiration is calculated from potential evapotranspiration by the following procedures (Kolka & Wolf, 1998):

Step 1: PET- potential evapotranspiration calculated with the Thornthwaite equation.

Step 2: P-PET- precipitation less the potential Evapotranspiration

Step 3: Accumulated Potential Water Loss (ACPWL) - accumulated potential water loss, which is the amount of soil water lost when PET exceeds P; i.e., there is less precipitation than potential evapotranspiration. In the calculation of AET, ACPWL is not a factor until P-PET becomes negative. To determine the ACPWL for a particular month, the previous month's ACPWL and the current month's P-PET are summed. In the original program, ACPWL becomes 0 after a month in which $PET < P$.

Step 4: Soil moisture- soil storage is the maximum soil storage at field capacity (ACPWL =0). When below field capacity (ACPWL < 0), soil moisture is a function of both maximum soil storage and ACPWL.

Step 5: Delta (change in soil moisture) - the difference between soil storage in successive months when it is less than maximum. When DELTA is negative, then $AET < PET$ i.e., soil moisture is limiting evapotranspiration. When delta is positive, then $AET = PET$.

Step 6: Actual Evapotranspiration (AET) - actual evapotranspiration is the sum of available precipitation for the month \pm the change in soil moisture. When Delta is positive, $AET = PET$. When delta is negative, $AET = \text{Precipitation for the month} + \text{the absolute value of delta}$.

Table 5: Step by step calculation of Actual Evapotranspiration from PET

	Jan	Feb	Mar	Apr	May	Jun	Jul	Aug	Sep	Oct	Nov	Dec	Annual
P	39.2	31.1	77.5	99.6	71.6	44.3	253	291.6	116.2	49.6	28.5	24.4	1132.6
PET	54	61	62.1	72.7	79.7	87.8	83.6	76.8	73.3	63.5	53.4	53	821.15
P-PET	-14.8	-29.9	15.4	26.9	-8.1	-43.5	169.4	214.8	42.9	-13.9	-24.9	-28.6	
AccPot													
WL	-82.2	-112.1	-96.7	-69.8	-77.9	-121.4				-13.9	-38.8	-67.4	
AWC	200	200	200	200	200	200	200	200	200	200	200	200	
[APWL]	82.2	112.1	96.7	69.8	77.9	121.4	0	0	0	13.9	38.8	67.4	
SM													
Retained	132.6	114.2	123.3	141	135.5	109	200	200	200	186.8	164.7	142.8	
ΔSM	-10.2	-18.4	9.1	17.7	-5.5	-26.5	91	0	0	-13.2	-22.1	-21.9	
AET	49.4	49.5	62.1	72.7	77.1	70.8	83.6	76.8	73.3	62.8	50.6	46.3	775 mm

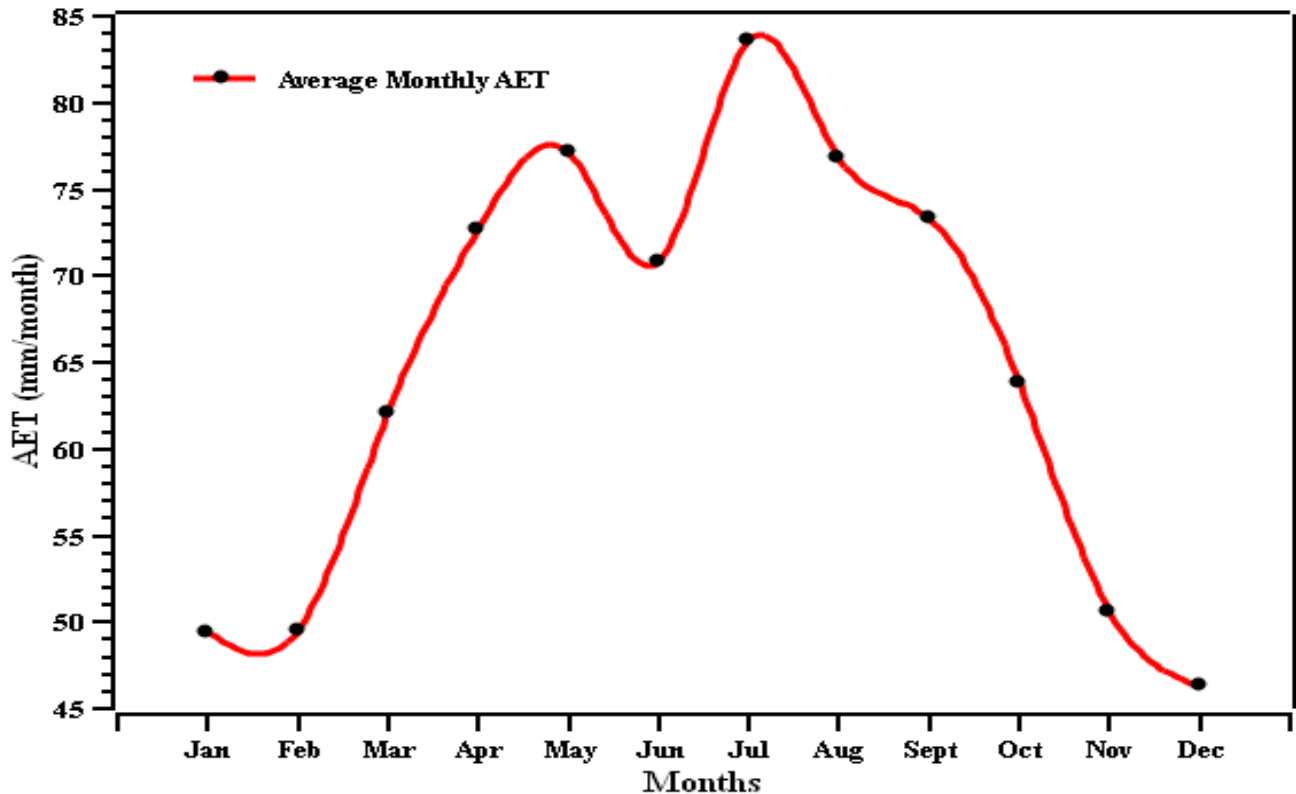


Figure 14: Mean monthly actual evapotranspiration of Upper Mille catchment

- ✚ From the above graph, the highest average monthly actual evapotranspiration under the available soil moisture condition occurs in July.
- ✚ The lowest average monthly actual evapotranspiration occurs in December and January since there is a soil moisture deficit.

3.3.2 Surface Runoff

Runoff is one of the most important hydrologic variables used in most water resource applications. The occurrence and amounts of rainfall are dependent on the characteristics of rainfall events, i.e. the intensity, duration, and distribution. Apart from these rainfall characteristics, there are several catchment-specific factors, which have a direct effect on the occurrence and volume of runoff. This includes soil type, vegetation cover, slope, and catchment type (KUMAR & GK, 2017).

Estimation of direct runoff is done using the curve number method. The Soil Conservation Service Curve Number (SCS-CN) provides an empirical relationship for estimating initial abstraction and runoff as a function of soil type and land use (KUMAR & GK, 2017). Curve Number (CN) is an

index developed by the Natural Resource Conservation Service (NRCS), to represent the potential for stormwater runoff within a drainage area. The CN for a drainage basin is estimated using a combination of land use, soil, and Antecedent soil Moisture Condition (AMC). There are four hydrologic soil groups: A, B, C, and D. Group A has the highest infiltration rates and group D has the lowest infiltration rates. Surface runoff is calculated using 19-year daily precipitation data using the following formula:

$$Q = \frac{(P - 0.2S)^2}{(P + 0.8S)}$$

$$S = \frac{100}{CN} - 10$$

- Where; S- is potential maximum retention after runoff begins; CN- is Curve Number as suggested by the American Soil Conservation Service (SCS); Q- Volume of runoff in inches; P- Rainfall depth in inches;
- The Curve Number (CN) value for the study area is approximated to be **87.5** (i.e., CN = **87.5**), and using this value potential maximum retention (S) will be;

$$S = (1000/87.5) - 10 = 1.43$$

Then, 19-year daily precipitation data which is the sum of the weighted precipitation (in inches) from seven stations which are greater than $0.2 \times S$ ($P_i > 0.2 \times S$ or $P_i > 0.286$) are taken and by substituting these values in the above runoff formula, the daily runoff (Q) values are calculated. The average of these 19-year daily values gives the total runoff for a given period. When the value of daily precipitation is less than $0.2 \times S$, the value of surface runoff (Q) is considered to be zero.

$$Q = \left[\sum (P_i - 0.2 \times S)^2 / P + 0.8 \times S \right] / n = 251.1 \text{ mm} \quad \text{where, } n \text{ is number of years which is } 19;$$

- The value of runoff showed that from the mean annual precipitation (1132mm) **22%** of it follows surface paths as a runoff.

3.3.3 Groundwater Recharge

The amount of water that percolates through the soil zone and crosses the groundwater table to fill the aquifer system is called Groundwater recharge. This is the most important parameter required in the successful development of groundwater resources, as it is the rate (or amount per unit time) that determines the amount of groundwater that can safely be abstracted from a particular aquifer (Department of Agricultural & Plantation Engineering, 2004). Groundwater recharge is likely to vary in space even over short distances as variations in soil and vegetation parameters can significantly affect the rates of recharge (Cook et al., 1989). Therefore, taking account of spatial variability in estimating recharge is very important if reasonably accurate replenishment rates to the water table are to be estimated (Department of Agricultural & Plantation Engineering, 2004). Groundwater recharge of the study area is calculated using the water balance method as follows:

$$\text{Groundwater recharge} = \text{Precipitation} - (\text{Actual evapotranspiration} + \text{Surface runoff})$$

⇒ by substituting the values of precipitation, Actual evapotranspiration, and Surface runoff the value of the groundwater recharge will be:

$$\text{Groundwater recharge (R)} = 1132.6\text{mm} - (775\text{mm} + 251.1)\text{mm} = \underline{106.5\text{mm}}$$

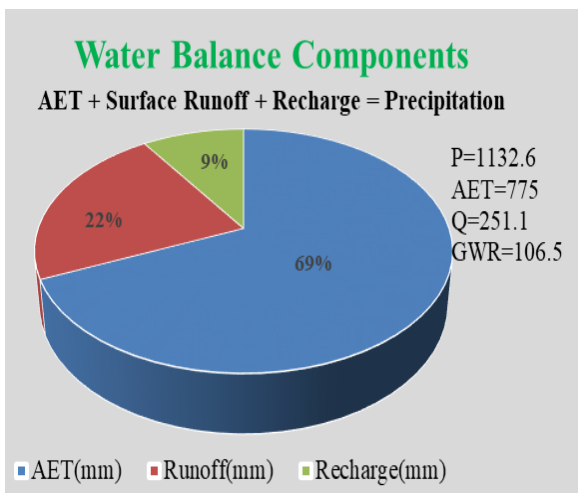


Figure 15: Shows the Proportion of the Water balance components

- ✚ From the total precipitation (1132mm) only 106.5mm (9%) of the precipitation percolates through the subsurface and joins the groundwater.
- ✚ AET and surface runoff account for 69%, and 22% of the total precipitation respectively.

3.4 Groundwater Recharge Estimation Using SWAT Model

The SWAT model is a semi-distributed, time-continuous watershed simulator operating on a daily time step (Arnold et al., 2012). SWAT model takes DEM, LULC, soil data, slope, weather data and streamflow data as input. The watershed is divided into sub-watersheds and the sub-watersheds further into Hydrologic Response Units (HRUs). The semi-distributed SWAT model is based on HRUs which are formed from overlapping maps for soil, LULC, and slope.

The principle is that each HRU is composed of specific land use, slope, and soil classes and they have similar hydrologic characteristics. The size of the sub-basin in the watershed will affect the assumption of homogeneity. Hence, the definition of a watershed, sub-basin boundaries, and streams is decided based on a Threshold area to define streams (Megersa et al, 2019). A properly projected DEM of 30m resolution was loaded to the Arc SWAT interface. Then, the DEM was masked and stream networks were created using the loaded DEM. The outlet point was selected from the streams, where the two main rivers Megenagna and Paso Mille Rivers meet. Finally, the sub-watersheds and the Boundary of the watershed were delineated based on the outlet point defined before. For defining the HRUs, slope, soil, and LULC map were loaded using the Land use/soil/slope definition menu. The soil map and LULC map were reclassified using appropriate look-up tables, and the slope map was reclassified into 5 classes of different slope value ranges. The HRUs were defined by taking multiple HRUs within each sub-watershed. To increase the number of HRUs (for better accuracy), a threshold of 0% for land use, soil, and slope was assigned. Finally, the weather input file was written using the daily weather dataset.

The watershed has an area of 1360 Km² and is divided into 160 sub-watersheds based on each stream within the watershed, which are further divided into 3329 HRUs. Finally, the model run daily from 1/1/2000-31/12/2018, and the results were printed out on a monthly scale. After running the SWAT model, the water balance component of the watershed was calculated and presented as, graphs, tables, and figures.

Table 6: Average Hydrologic parameters derived from SWAT model

Hydrologic Parameter	Jan	Feb	Mar	Apr	May	Jun	Jul	Aug	Sep	Oct	Nov	Dec	Annual
PET	54.9	57.97	105.48	123.89	140.15	138.79	154.99	149.8	131.38	109.95	82.59	66.36	1316.2
AET	18.57	20.91	36.76	41.2	53.54	83.97	100.85	86.35	42.03	31.79	23.47	18.37	557.81
Surface Runoff	8.5	16.13	33.2	16.25	24.68	51.55	55.28	45.45	40.29	29.65	4.95	9.44	335.37
Inter Flow	1.07	1.48	2.98	2.27	2.23	3.76	6.07	6.05	5.37	4.13	2.13	1.2	38.74
Total													1083.2

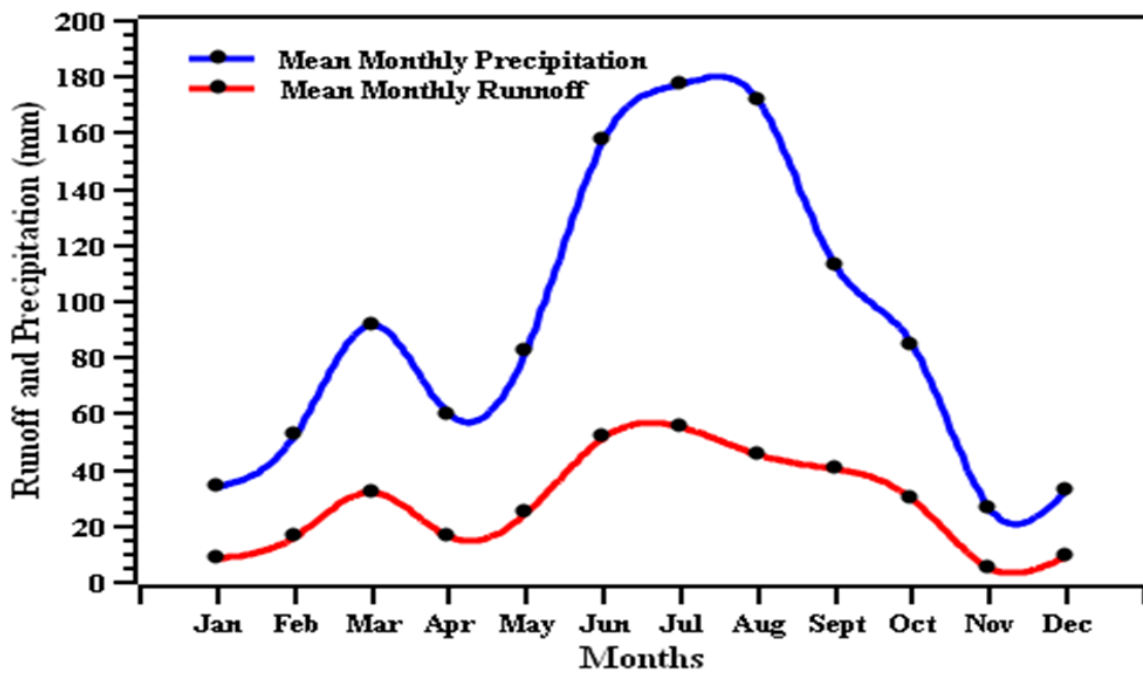


Figure 16: Mean monthly precipitation and runoff derived from SWAT Model

- ✚ **Precipitation:** - as observed in the figure (Figure-16) high mean monthly precipitation occurs from June to September whereas minimum precipitation occurs from November to mid-February. There is also short seasonal rainfall in February this is named traditionally **Belg** rainfall. The highest value of precipitation was observed in July (177.3mm), on the other hand, the lowest value of precipitation was observed in November (26.03mm). Based on the SWAT model results the mean annual precipitation of the watershed is **1083.2mm**.

✚ **Runoff:** - is some portion of the precipitation the mean monthly value of runoff shows a similar trend with mean monthly precipitation. Similarly with precipitation high amount of runoff is observed in the summer season between June and September. The highest and the lowest mean monthly runoff is observed in July (55.28mm) and November (4.95mm) respectively. The annual runoff (335.35mm) accounts for **31%** of the annual precipitation (1083mm).

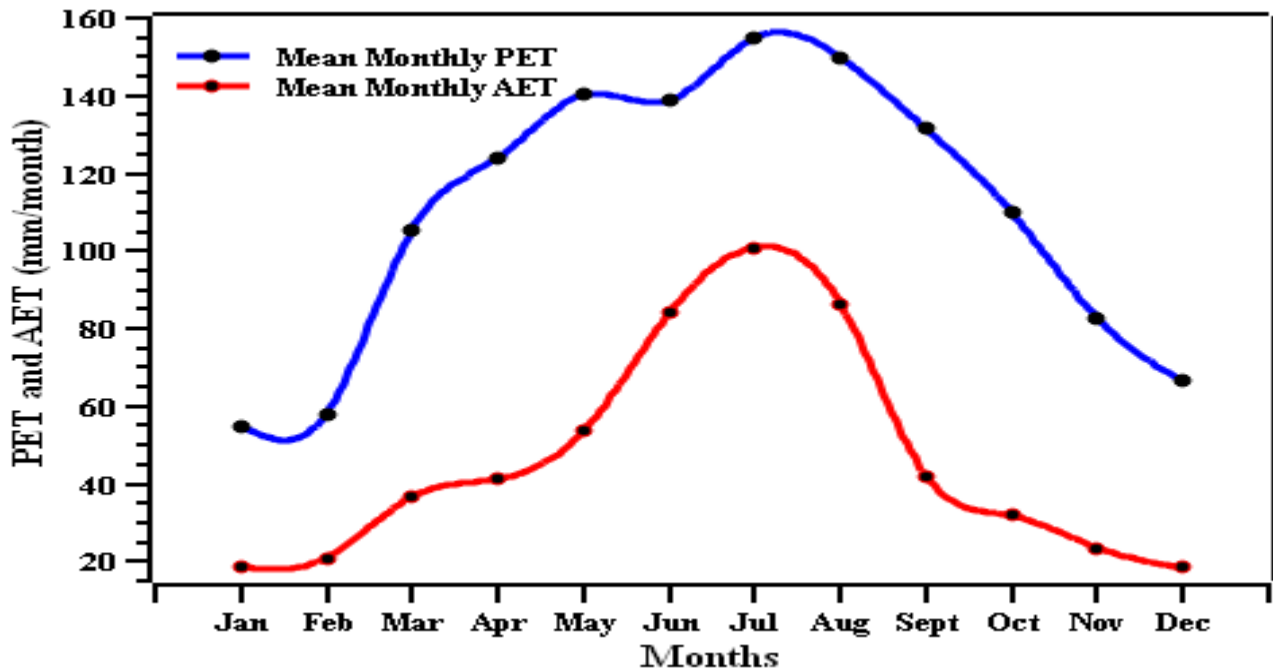


Figure 17: Mean monthly PET and AET derived from the SWAT Model

PET and AET: - The graph (Figure-17) show a continuous monthly increase in PET and AET from February to August and a decrease until December. August is the month with the highest rate of PET and AET because it is the month with the highest monthly precipitation and its AET is close to the PET because of increasing soil moisture conditions.

✚ One of the SWAT model outputs is the mean annual water balance components in the form of figures. The average annual value of WB components is shown in the figure below along with the paths followed by each component.

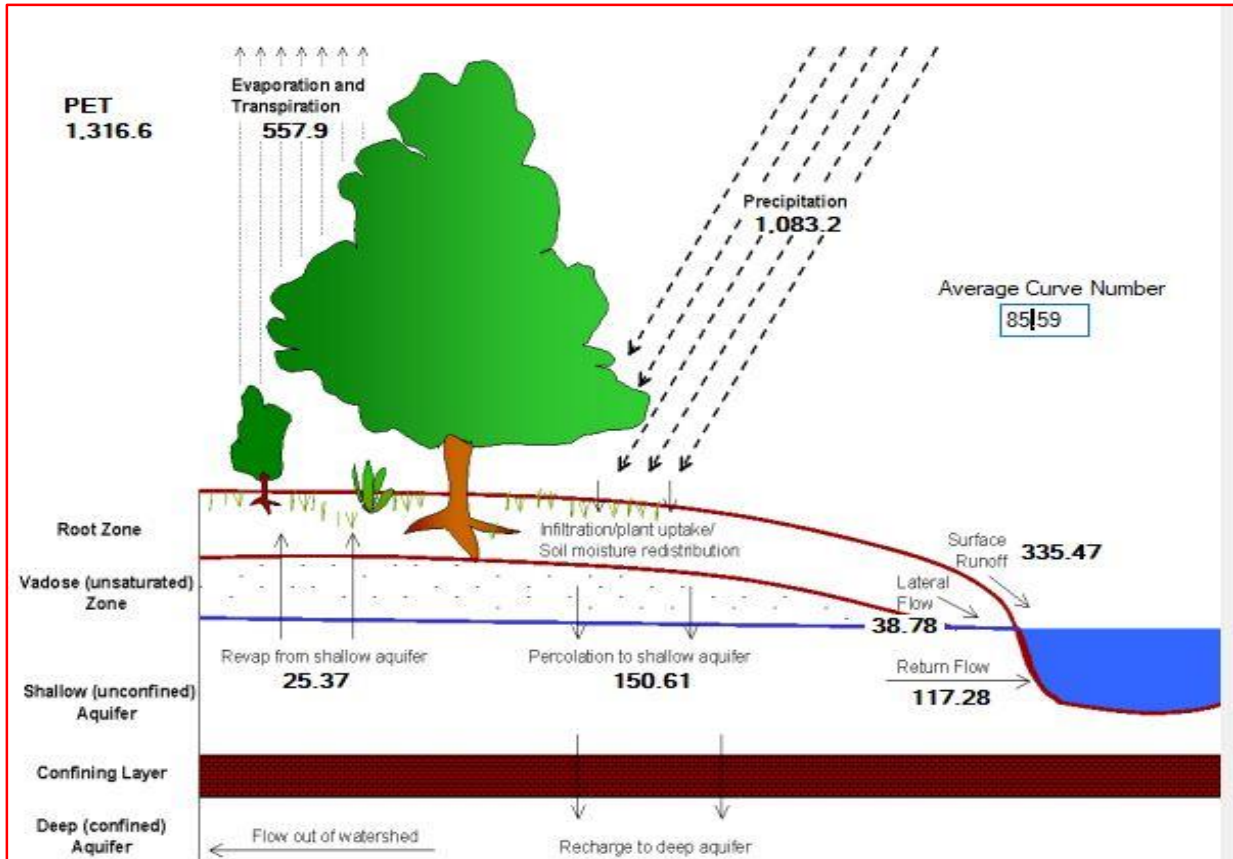


Figure 18: Average annual hydrologic components obtained from SWAT model

- ✚ As shown in the figure above, the mean annual precipitation, PET, AET, surface Runoff, and lateral flow of the watershed are 1083.2, 1316.6, 557.9, 335.47, and 38.78mm respectively.
- ✚ The mean annual recharge of the area based on this model is **150.6mm**, which is the ultimate objective of the SWAT model for this study.
- ✚ Based on the SWAT model only **13.8%** of the mean annual precipitation percolated into the groundwater system as a recharge.

⇒The output of the SWAT model is not calibrated due to the lack of recorded river discharge data in the area.

3.5 Comparison of WB and SWAT Model Results

The annual groundwater recharge estimation of the watershed has been computed using the two methods and the results have been explained above.

Table 7: Comparison of water balance components computed using WB and SWAT Model methods

Methods	WB components					
	Prec.	PET	AET	Runoff	Inter flow	GW recharge
Water balance	1132	821.15	775	251.1	0.00	106.5mm
% of Prec.		72.5%	68.5%	22.2%	0%	9.4%
SWAT Model	1083.2	-	557.9	335.47	38.78	150mm
% of Prec	-	-	51.5%	31%	3.6%	13.8%

- ✚ The values of water balance components computed using the two methods are not that much different.
- ✚ The groundwater recharge estimated using WB (106.5mm) method and SWAT Model (150mm) accounts for **9.4** and **13.8%** of the total precipitation. And the result seems acceptable since the area is very sloppy and dominantly covered by clay soil which minimizes the amount of percolation into the groundwater.

CHAPTER FOUR

REGIONAL AND LOCAL GEOLOGY

4.1 Regional Geological Setting

The East African rift system is one of the examples of continental flood basalt provinces that comprises two main segments, namely the Kenyan or Gregory Rift and the Main Ethiopian Rift (MER). Both rifts are situated on the Ethiopian to the north and Kenyan Plateaus to the south, respectively (Feyissa Dejene, 2018). The initiation of continental flood basalt (CFB) magmatism is spatially and temporally related to continental break-up, which results in the formation of oceanic crust, at least within the past 200 Ma. However, the relationships between the timing of CFB formation and rifting leading to ocean-floor formation are complex it varies in time and space (Dereje Ayalew et al., 2006). This is not unusual, in that plumes may interact with the continental lithosphere independent of plate-driving forces. Although the details of plume melting remain controversial, there is an agreement that lithospheric thinning or pre-existing thin zones are needed to produce the huge volumes of melt seen in CFB provinces (Bekele Abebe et al., 2007).

In Ethiopia, Oligocene-Miocene felsic volcanic strata (rhyolites and minor trachytes) capping the flood basalt sequences are well exposed along the western margin of the southernmost sector of the southern Red Sea and the northernmost Main Ethiopian Rift (MER). The rhyolites are preferentially localized on or near the border fault, indicating that rifting preceded or at least was coeval with the felsic volcanism in both the southern Red Sea rift and the northernmost part of the Main Ethiopian Rift (Wolfenden et al., 2004). This shows a clear relationship between the emplacement of large volumes of rhyolite and the formation of the large offset border fault systems. The timespan for silicic volcanism shows southward younging along the border fault and the silicic volcanism migrates from the wider border faults towards narrow (10 km-wide) magmatic segments within the rift (Wolfenden et al., 2004). The overall observations show multiple episodes of rift-ward migration of the locus of magmatism and faulting through time.

Along the western rift margin of the Afar depression, the flood volcanic sequences overlie marine sedimentary strata deposited on a passive continental margin in Mesozoic time (Hunegnaw et al., 1998). The volcanic packages are up to 2000 m thick and comprise basaltic lava flows overlain

by rhyolites such as ignimbrites, air-fall tufts, and lavas with interbedded basalts. The flood volcanic stratigraphy commonly shows a repetitious basalt-rhyolite succession. Silicic volcanic commonly constitute up to 50% of the preserved volcanic thickness and lie towards the top of the flood volcanic sequences (Kieffer et al., 2004). The rhyolitic centers comprise massive glassy effusive volcanic rocks and phenocryst-rich crystalline intrusions and form irregular to dome-shaped flows. The first silicic ignimbrite in the western margin of the Afar depression erupted at 30.2 Ma and bimodal basalt-rhyolite volcanism continued in parts of the broad flood basalt province until 10Ma (Kieffer et al., 2004; Wolfenden et al., 2004). The ages of the silicic volcanic rocks outside the faulted rift valley range from About 30 Ma in the north of the province to 10.8 Ma at Mount Guna (Kieffer et al., 2004; Chernet et al., 1998). Silicic volcanism occurred early during the main basaltic episode and continued to erupt with quaternary volcanism occurring in the rift valleys and central plateau (P. Mohr & Zanettin, 1988; Paul Mohr, 1987).

4.2 Regional Litho-Stratigraphic Units

In Ethiopia, Early Cenozoic volcanic rocks cover ~32% of the total surface area of the country whereas, Late Cenozoic volcanic rocks cover about ~12%. Cenozoic magmatism has built a thick succession of volcanic rocks, typically 500-1500m thick over an area about 1,000 km wide presently comprising the Northwestern, Southeastern and Southwestern uplifted plateaus and the Ethiopian and Afar rifts (Kieffer et al., 2004). A minor volume of basalt eruptions has also occurred on the plateau areas during the quaternary time.

The traps in Ethiopia presently cover an area of about 600,000 km², forming the high plateaus and resting either on flat-lying Mesozoic sedimentary rocks or on the Precambrian basement (Zwaan et al., 2020). The northwestern Ethiopian traps consist of a series of Oligo-Miocene fissure-fed basalts and subordinate felsic rocks (ash and coarse fragmental materials) that are capped by Miocene shields volcanoes (Bekele Abebe et al., 2007; Kieffer et al., 2004). The felsic rocks are interbedded with the flood basalts, particularly at upper stratigraphic levels, and consist of sequences of rhyolitic and trachytic lavas and pyroclastic rocks. Based on the works of different researchers the following lithological succession units are identified; plateau basalt, plateau silicic, and shield volcanic, from the oldest to the youngest lithologic unit respectively.

4.2.1 Plateau basaltic formation

In the northwestern traps, the volcanic pile consists of a basaltic succession overlain by a major rhyolitic formation (GSE, 2017). The basaltic pile is made up of a lower sequence (commonly known as Ashange basalts) characterized by thin lava flows, (< 10 m) forming relatively smooth or less steep topography (Tadios Chernet et al., 1998). The upper basaltic sequence (commonly referred to as Aiba basalts) is composed of thicker flows (10-50 m) that characteristically form cliffs. These rock unit successions are found overlain by the Alaji formation, which is a thick series of volcanic Acidic compositions.

4.2.2 Plateau silicic formation

Basalts and ignimbrites produce typical plateau topography, which is often extensively eroded and dissected by deep gorges. The minimum volume estimated for the silicic volcanic of the northwestern plateau is in the order of 60,000 km³ which is 20% of the total flood volcanic (Bekele Abebe et al., 2007; Tesfaye Korme et al., 1997). The thickness of the plateau ignimbrites is extremely variable, ranging from 500 m in the north (Wegel Tena area) to ~700 m in the southwest (Jima area), and as low as 30 m in the Debre Birhan area (central plateau), close to the rift margin. Individual flow units vary in thickness from ~3 m to 15 m. Several north-south trending micro-granitic dykes crop out in the plateau, especially in the Woldiya area. Three regionally distinct Oligocene rhyolite units are recognized: the Lima Limo rhyolites in the northwest plateau forming several beds capping low-Ti basalt floods, the Wegel Tena rhyolites in the east corresponding to very thick ignimbrites overlaying high-Ti flood basalts, and the Jima rhyolites located in the southwestern plateau overlaying high-Ti flood basalts. Miocene rhyolites are situated in the Molale-Debre Birhan area close to the rift margin and overlay Miocene low-Ti flood basalts (Dereje Ayalew & Gezahegn Yirgu, 2003; Wolfenden et al., 2004).

4.2.3 Shield Volcanics (Tarmaber Formation)

Shield volcanoes are a conspicuous feature of the Ethiopian plateau that distinguishes this plateau from other well-known examples such as the Deccan and Karoo. The basal diameters of the shields range from 50 to 100 km and the highest point in Ethiopia, the 4533 m high peak of Ras Dashan, is the present summit of the eroded Simien shield. This peak extends almost 2000m above the top of the flood basalts, which lies at about 2700m in the northern part of the plateau. If an additional 500

m is added to allow for eroded material, a total height of about 3 km is estimated for this volcano (Pik et al., 1999). Although smaller in diameter, the summits of many of the other shield volcanoes also exceed 4000m. The mafic volcanism that led to the construction of the basaltic plateau was characterized by a "gradational mode of eruptive style from platform building fissure eruptions towards rare shield-building eruptions". Associated with this change was a transition from a tholeiitic character in the flood basalts to a moderately highly alkaline character in the shield volcanic (Tadios Chernet et al., 1998; Dejen Hailemariam, 2018; Kieffer et al., 2004; P. Mohr & Zanettin, 1988; Wolfenden et al., 2004).

4.3 Local Stratigraphic Units

One of the main governing factors for the hydraulic characteristics of groundwater is the rock unit which is found in the area. Rock units in the study area can be generally grouped into two rock types namely older volcanic and unconsolidated quaternary sediments (P. Mohr & Zanettin, 1988; Williams, 2016). In the study area, the volcanic rocks are formed mainly during the Cenozoic flood volcanism and cover most of the steeply sloped mountains and rift escarpments. While most of the valleys and grabens are filled with thick unconsolidated young sediment deposits. The volcanic rocks in the area are lower basalt (Ashange), middle basalt (Aiba), Kemise rhyolite (Alaji) and upper basalt (Tarmaber) from the oldest (Ashange basalt) to youngest (Tarmaber basalt) respectively (Miruts Hagos, et al., 2016).

4.3.1 Lower/ Ashange basalt

Ashange basalt is the lowermost and the oldest from the volcanic stratigraphic succession in the area. Lower basalt is exposed in many parts of the study area along river beds, road cuts, a chain of mountains, and some quarry sites. From field observation, it is also characterized by thinner lava flow, smooth surface, highly weathered, dark to brownish color, tectonically disturbed having many joints and small-scaled faults, and easy to break. From the regional volcanic trap basalt successions, this rock unit is best correlated with Ashange trap basalt which is formed during the Eocene-Oligocene period (Varet, 2018). With the presence of primary columnar joints and secondary fractures, Ashange basalt acts as an aquifer with prominent permeability.



Plate 1: Highly weathered and fractured Ashange basalt exposed to the east of Wuchale (left) and near Lake Hayk (right).

4.3.2 Middle/Aiba basalt

Middle basalt is found by unconformably overlaying lower (Ashange) basalt and underlying below the rhyolitic volcanic rock succession. As the name indicates this rock unit is basaltic in composition. The unit is characterized by dark brownish color, relatively thicker lava flow, cliff-forming, less weathered relative to the lower basalt. The most common geological structures observed on the middle basalt within the study area are columnar joints, fractures including small-scale faults, and joints that show the disturbance of the area. This basaltic unit is exposed in a small part of the watershed mainly along the western rift margins and to the south of Hayk town. Due to its primary jointing structures and latter modified secondary geological structures, springs are very common. From the regional trap volcanic succession, Middle basalt is correlated with Aiba basalt ([Tadiwos Chernet et al., 1998](#)).



Plate 2: Cliff forming columnar middle /Aiba basalt near Wuchale town

4.3.3 Kemise rhyolite

This unit is found in between middle basalt (bottom) and upper basalt (top). Rhyolites are silicic in composition. Even though rhyolite is the dominant rock type within this silicic formation, ignimbrites are also common in many parts of the area associated with the dominant rhyolitic rock type. In the area, rhyolitic rock succession is mainly found in the eastern part of the watershed. The succession is generally characterized by its, white, pink, and gray color, very steep slope hill forming nature, resistance to weathering, forming thick dome-like structure. Primary and secondary porosity is not common in these rock units, which makes it a poor productive aquifer. This rock unit is best correlated with the Alaji rhyolitic succession of the regional trap series formed during the Oligo-Miocene (Dereje Ayalew and Gezahegn Yirgu, 2003; Rogers, 2006).

4.3.4 Upper/Tarmaber basalt

Upper basalt is the topmost and the youngest rock unit from the volcanic successions. Which is unconformably overlies the rhyolitic rock unit. This unit is basaltic in composition with different textures. Upper basalt is characterized by its dark color, thick succession lava flow, highly fractured and relatively weathered, columnar jointing formed during the formation of the rock unit. The columnar joints are well developed and act as a conduit for groundwater circulation. But, due to its topographic location, it is used as a good recharge zone feeding low-lying volcanic and unconsolidated aquifers. Upper basalt is exposed only on the western corridor of the escarpment zone. From the regional volcanic trap basalt successions, this rock unit is correlated with Tarmaber trap basalt which is formed during the Oligo-Miocene time (Dejen Hailemariam, 2018).

4.3.5 Unconsolidated quaternary sediment deposits

Unconsolidated deposits in the watershed include; alluvial, colluvial, aluvio-colluvial, and intermountain alluvial sediment deposits (Rooney, 2020). These deposits cover a large part of the watershed. Which is exposed in the river beds, graben-filled low-lying flat areas, and at the base of mountains and hills. Unconsolidated deposits are the youngest units from other rock types present in the area. Texturally these units are very variable from fine-grained relatively cemented to coarse-grained friable grains depending on the source and distance of transportation before being deposited in the basin. The unconsolidated nature of these deposits gives high groundwater conductivity and transmissivity. These rocks are the most productive aquifer in the watershed due to their high

permeability and specific storage capacity. Girana valley is filled with such types of deposits in which many production boreholes are drilled for irrigation and domestic uses



Plate 3 : Valley fill unconsolidated sediment in the Girana valley (left) and river cut exposure near Wuchale (right)(B)

4.4 Geological Structures

Geological structures are the main controlling factors for the groundwater potential of an area (Abraham Mechal, 2015). Geological structures can be classified into primary and secondary based on the time of their formation with the rock formation. The mechanical behaviors of the rocks are depending on the degree and type of these structures. Geological structures control the dynamics of groundwater. In the Upper Mille river catchment, secondary geological structures are very common. Small and Large-scale faults, joints, dykes, and lineaments are observed during the fieldwork. The orientation of these geological structures is variable. Since the watershed is found within the western margin of afar rift, normal faults oriented in the same way as the marginal fault (NNE-SSW) and differently oriented faults are very common (Bekele Abebe et al., 2007; P. Mohr & Zanettin, 1988; Paul Mohr, 1987; Zwaan et al., 2020). The joint spacing and aperture are different from one outcrop to another. Dykes which cross the rock section are observed in a different part of the study area. Some of the major fault systems are extracted from previous geological and hydrogeological works and

presented in the geological map (Figure-19). The presence of faults, joints, lineaments, and dykes shows the complexity of the groundwater system in the catchment.

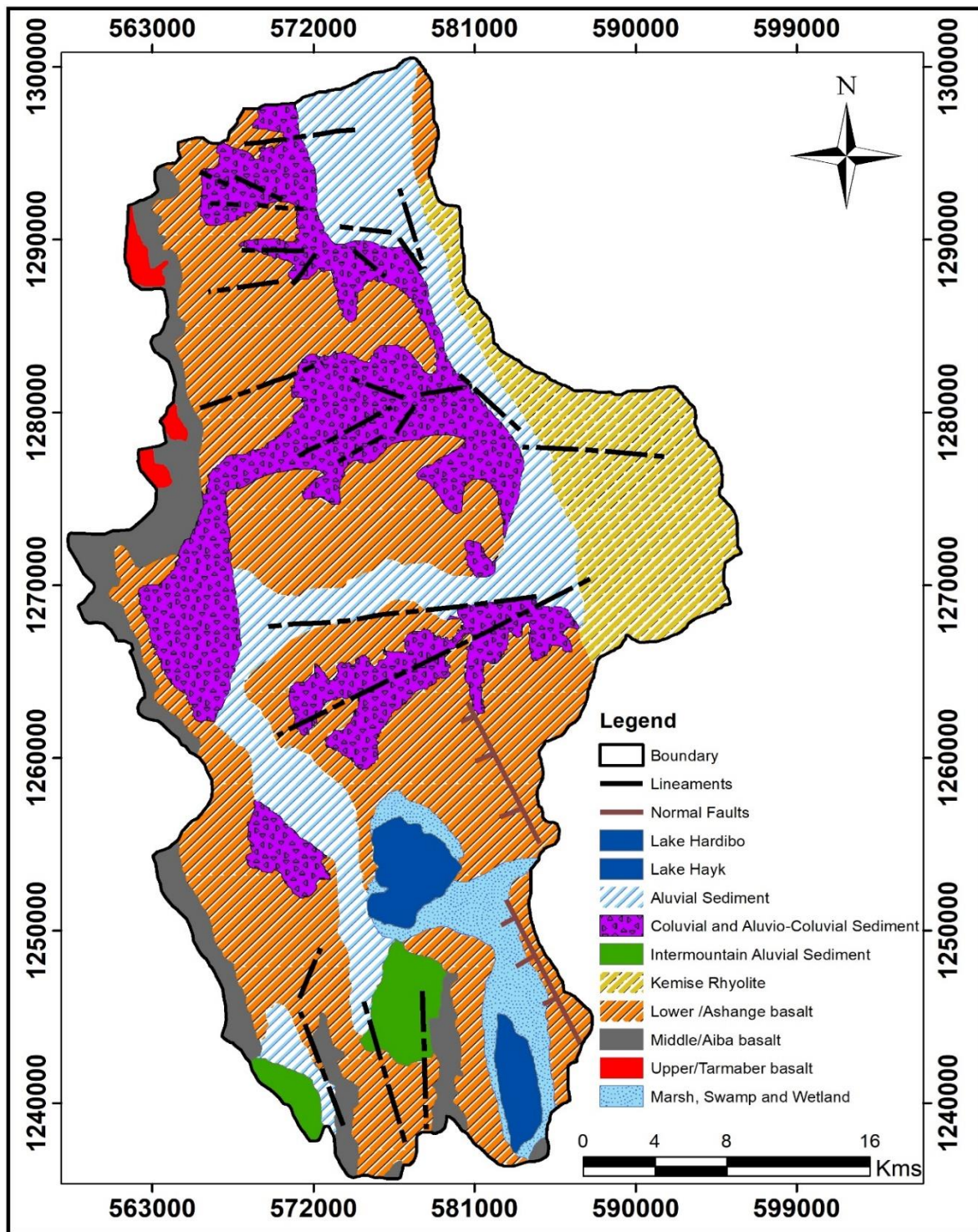


Figure 19: Geological map of upper Mille catchment (adopted from GSE, 2014)

CHAPTER FIVE

AQUIFER CHARACTERIZATION AND CONCEPTUAL MODEL DEVELOPMENT

5.1 Introduction

An aquifer is a geological formation or a group of geological formations that contains porosity to store and transmit a significant amount of water to wells and springs. The hydraulic properties of an aquifer are controlled by the texture of sediments and the fabrics of rocks that comprise the watershed (Maliva, 2004). Aquifers are hydraulically characterized and quantified by the ability to transmit, conduct and store water within the aquifer system. In addition to lithology, the distribution and the occurrence of an aquifer are highly affected by the presence and the absence of fractures such as, faults, joints, and lineaments which in turn controls the groundwater potential and the groundwater flow dynamics of the watershed. The development and efficient management of groundwater resources requires a good understanding of the hydrogeological properties of the rocks that form the major aquifer systems (Darrell. I, 1999). Understanding the hydrogeological parameters such as piezometric head, transmissivity, hydraulic conductivity, storage coefficient, aquifer thickness, etc. is very important in hydrogeological investigations.

The geology and the structure of the study area are very complex since it is located in the western margin of the Afar rift. As a result, the hydrogeology of the area is very complex and heterogonous in terms of transmissivity, conductivity, storativity, and groundwater flow dynamics. Aquifers in the Upper Mille basin are divided broadly into two categories based on the nature of porosity; aquifer which contains primary porosity and aquifer which contains double porosity. The first comprises unconsolidated alluvial, colluvium, and intermountain Quaternary sediments in which the porosities were formed during the deposition of sediments. The second category of aquifer includes those volcanic rocks which contain primary porosities like columnar jointing, bedding plane, and vesicles formed during the time of their formation, and later on, through time, these volcanic rocks have been subjected to weathering and fracturing related to tectonics giving rise to secondary porosities. The hydraulic properties of each unit are treated separately by using inventory points.

5.2 Groundwater Inventory Points

During the fieldwork, different groundwater-surface water points are inventoried to characterize the hydraulic properties of the aquifer system. Field parameter measurements inventorying is performed by taking the location of water points using GPS. PH, EC, TDS, and temperature were measured and recorded from deep boreholes, shallow hand-dug wells, springs, lakes, and rivers. Based on the hydrogeological data obtained from those inventory points in conjunction with literature reviews, hydraulic properties are investigated and the aquifer is characterized.

Table 8: Fieldwork Inventory points and the parameters measured for each point.

Inventory types	Number of points	Measured parameters
Springs	60	T, pH, TDS, yield(l/s), and elevation
Hand dug wells	6	T, SWL, pH, yield and TDS
Deep Boreholes	30	T, SWL, pH, yield and TDS
Lakes	2	T, pH, and TDS, elevation

A. Springs

In the watershed, there are many springs in different lithostratigraphic units having different discharge, pH, TDS, and temperatures. Most springs are concentrated in the bottom of ridges, hills, and along the escarpment of the marginal faults. Yield, Elevation, EC, TDS, and temperature were measured during the fieldwork. Accordingly, low EC, TDS, and temperature were observed in most of the springs which might indicate that they have a shallow groundwater circulation and active groundwater recharge. Most of the high yield springs emerge from basaltic aquifers whereas. Most of the springs are not developed and they are in poor sanitary condition however, some are well developed and protected. They are used for domestic supply and irrigation purposes. The discharge of the springs ranges from 0.1-2l/s.



Plate 4: Developed springs having a yield of 1L/s (left) and 0.5L/s (right) which emerged in the Ashange basalt to the north of Hayk towns, these springs have low TDS, EC, and temperature and they are used as drinking water for the local community.

B. Boreholes

Most of the boreholes are drilled in graben filling thick unconsolidated quaternary sediments and in the lower/ Ashange basalts due to the good productivity nature of those units. Most of the boreholes don't have an observation pipe for water level measurement, which makes it difficult to measure the groundwater level of boreholes. As a result, much data was gained from well completion reports. In the area, the static water level ranges from artesian to 60 m B.s.l. The yield of boreholes is also very variable depending on depth, aquifer type, and topographic settings. In some boreholes, discharge reached up to 80l/s, especially those deep drilled boreholes within the high productive aquifer zone whereas, less than 5l/s for shallow wells. Large variation in the discharge of boreholes is due to the heterogeneity of lithology in which the borehole is drilled, depth of fracturing and weathering, topographic setting, and other operational factors. Low TDS, pH, EC, and temperature are recorded on the western side with an increasing trend to the outlet of the Upper Mille River (eastern corridor) catchment.

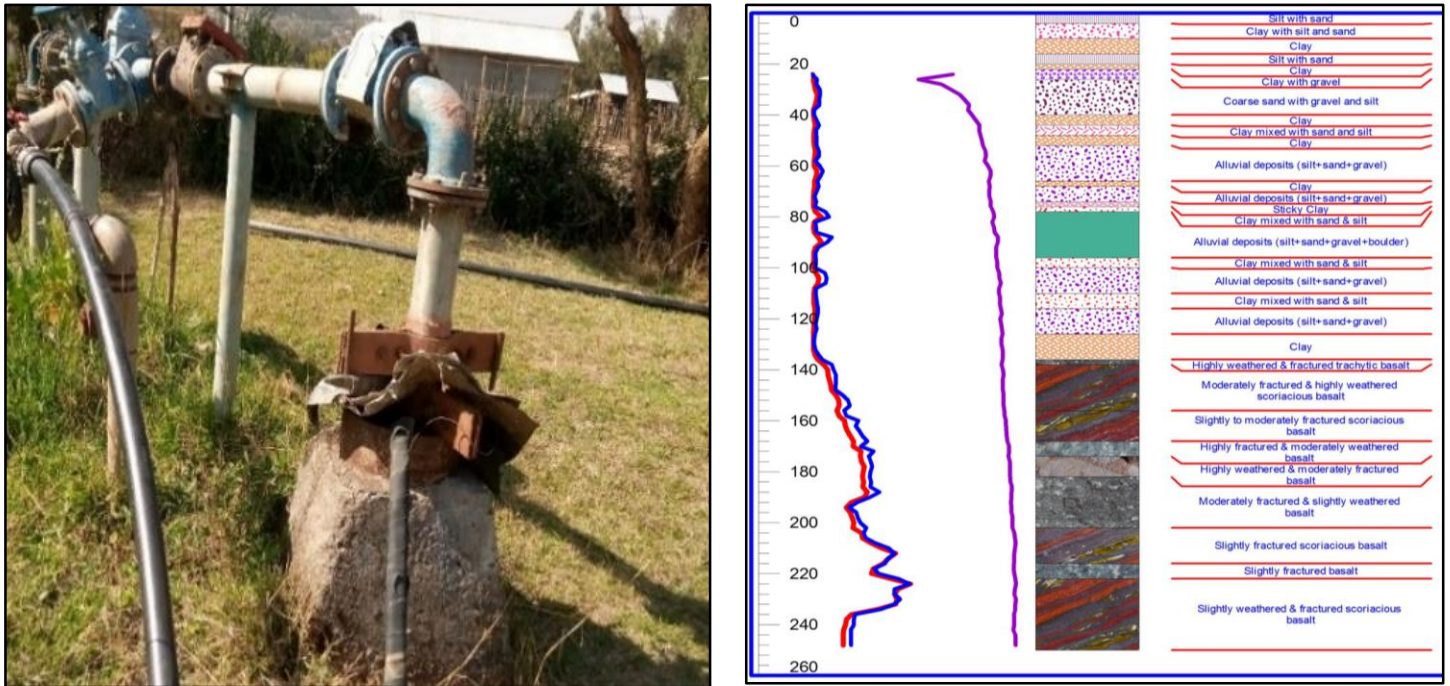


Plate 5: Installed deep borehole in the left and its lithological, and geophysical logging in the right (the logging was taken from AWDSA well completion report) drilled on the unconsolidated sediments. The well has a depth of 240m and the top 140m is unconsolidated sediment and the rest is the basaltic unit.

C. Hand-Dug wells

Most of the hand-dug wells get the water from shallow aquifers. The majority of the dug wells are drilled in the nearby towns and villages which are used as a drinking water source for the community. The highly weathered top regolith part of basalt is the major water-bearing layer for dug wells. In the area, dug wells have a depth of between 5-35m and they are in a good condition with installed hand pumps; however, some are simply open and work using a mechanical pulley system. The static water level of the dug wells' ranges from 1-25 m B.s.l. The discharge ranges from 0.5l/s to 5l/s.

5.3 Physico-Chemical Parameters

Physico-chemical parameters are very important for aquifer characterization and groundwater quality analysis (Andarge Yitbarek, 2009; Fetter, 2001). Parameters that have been given special emphasis for this research work include; EC, TDS, and PH of the watershed. Those parameters are measured on the inventory points (boreholes, springs, lakes, and rivers). The value of these parameters is used to know the general groundwater flow direction and the depth of groundwater circulation. Each of those parameters is discussed separately in the following subtopics.

5.3.1 Electrical Conductivity (EC)

EC is the measure of the electrical conductivity of water solution. Even though pure water can conduct electricity, the amount of electricity that can pass through the water solution depends on the amount and the type of dissolved ionic constituents present in the water (Delleur et al., 1999). The higher the EC, the more solute salts and ions are present in the water and Vis-versa. By measuring EC it's possible to predict the recharge-discharge zone, groundwater flow direction, and flow length of groundwater. From point measurements, a spatially distributed map is produced (Figure-20). The EC value of the watershed ranges from 310-1200 μs .

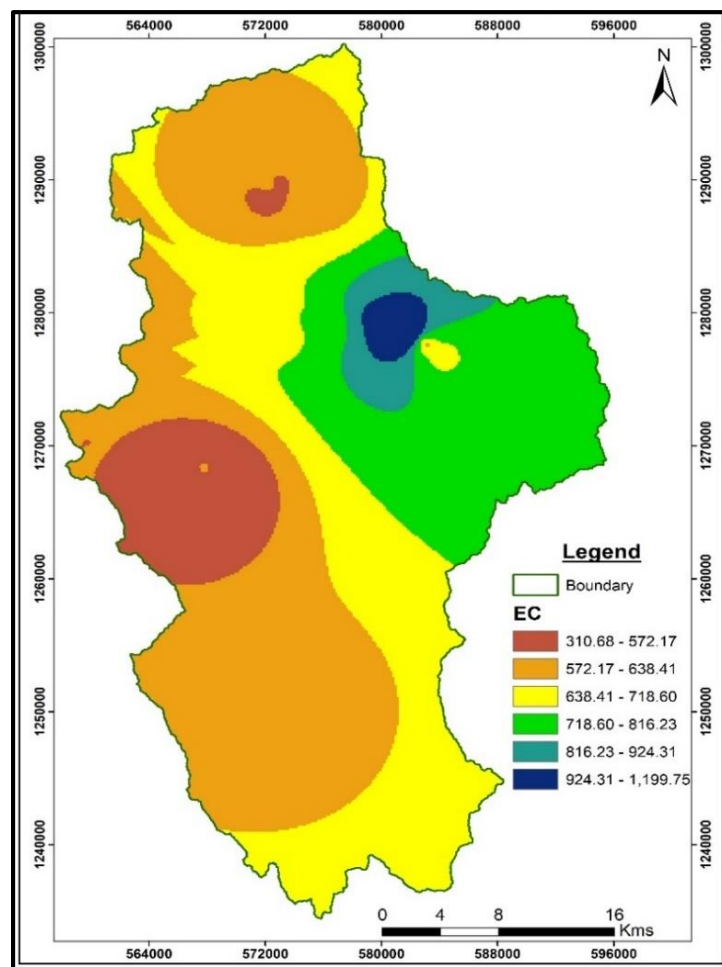


Figure 20: EC distribution map of the watershed interpolated from point measurements

From the EC distribution map of the watershed, EC values generally show a regular trend, in which the electrical conductivity of the water is lower in the recharge area and then it continued to increase to the discharge zone following the groundwater flow direction.

5.3.2 Total Dissolved solids (TDS)

TDS is the measure of the total dissolved solids present in the water. TDS point measurements were taken from water point inventories during the fieldwork and the TDS distribution map of the study area is produced by interpolation of the point measurements. The more the TDS value the longer the time of contact with the subsurface rock units and vice-versa (Wang, 2020). From the maps (Figure-21) below, it can be generalized that the higher values of TDS coincided with the outlet of the watershed while the lower values of TDS are observed in the upstream direction of the watershed. Based on this it's possible to identify the recharge and the discharge zone as well as the groundwater flow direction. The value of TDS in the watershed ranges from 200-1145mg/l.

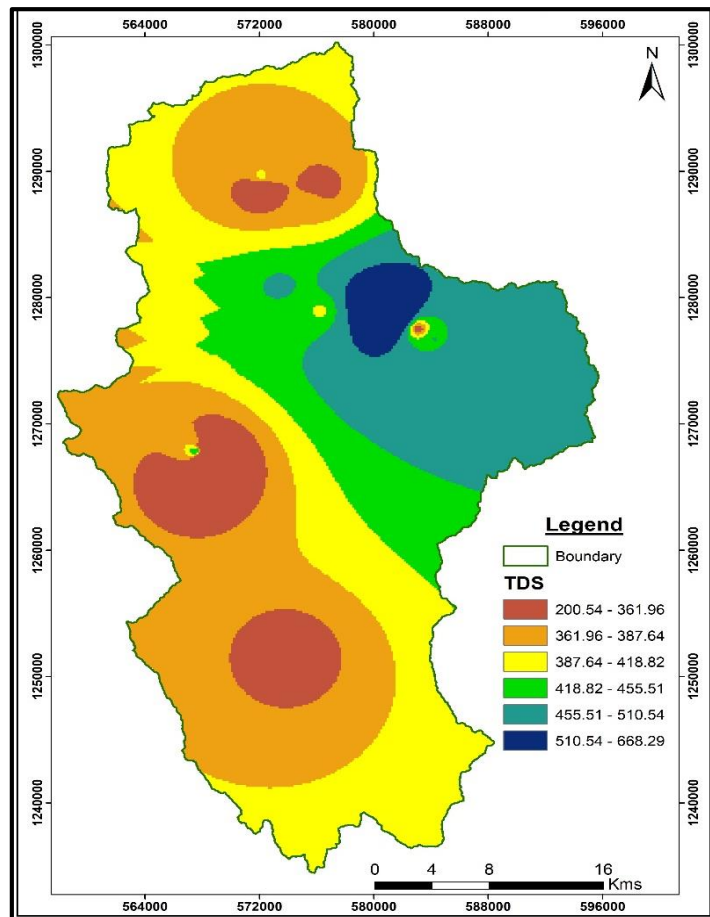


Figure 21: TDS distribution map of the watershed interpolated from point measurements

⇒ As observed from the figure above, the EC distribution map shows a similar pattern with the TDS distribution map of the watershed.

5.3.3 pH

The pH is a numerical scale that ranges from 0-14. It determines the acidity and basicity of the water solutions. The PH of pure water is 7. Solution with PH values less than 7 are acidic and solutions with PH values more than 7 are basic. pH also indicates the recharge and the discharge area of the watershed. The value of pH affects the usefulness of the water. Most of the point measurement values of the watershed converge within the range of 6.5 to 8.5. Less pH is measured on the highlands of the watershed which indicates the recharge area, whereas, high pH was observed on the outlet of the watershed which is probably the discharge area.

⇒ Generally, the value of TDS, EC, pH, and temperature are higher in deep boreholes than shallow hand-dug wells and springs. Moreover, an increasing trend was observed along the flow path.

5.4 Hydraulic Properties of Aquifers

The hydraulic properties of an aquifer such as hydraulic conductivity, transmissivity, porosity, specific storage and storage coefficient, etc. are determined using borehole pumping tests. The hydrogeology of the watershed depends on geology, geological structure, surface morphology, slope, land use land cover, and the interaction of humans with nature (Singhal & Gupta, 2010). So, the hydraulic properties of aquifers in the area are the manifestation of such controlling factors. In the watershed, the range of the values of conductivity and transmissivity is very large. The wide range of transmissivity and conductivity values is attributed to the heterogeneity of unconsolidated sediments and volcanic aquifers in the study area.

For this particular study, lateral distribution and nature of the aquifer, hydraulic properties of the aquifer are used in the conceptual model development. To characterize and classify the aquifer system into different hydrogeological groups; existing pumping test data, geologic and hydrogeologic maps, soil map, lithology obtained from borehole logs, aquifer thickness, transmissivity, hydraulic conductivity, water table depth, geological structures, and surface water features, etc. are used. Because of limited data, the spatial distribution and magnitude of hydraulic properties of the aquifer are not well-known particularly the vertical variability. The drilled wells are not also well distributed over the study area.

5.4.1 Hydraulic conductivity

Hydraulic conductivity is a measure of how easily water can pass through soils or rocks. It is defined as a constant proportionality relating the specific discharge of a porous medium under a unit hydraulic gradient of Darcy's law: high values of hydraulic conductivity indicate a permeable material through which water can pass easily; low values of hydraulic conductivity indicate that the material is less permeable (C.W. Fetter, 2000). The Hydraulic conductivity of the aquifer system generally depends on many factors such as rock type, primary and secondary structures, degree of weathering, stratigraphic setting, etc. A wide range of hydraulic conductivity values was observed in the Upper Mille aquifer system. The hydraulic conductivity ranges from 0.06-17m/day. The highest hydraulic conductivity value is observed on the unconsolidated quaternary sediments whereas, the medium conductivity values are observed on the basaltic formation. The horizontal hydraulic conductivity and permeability zones (Figure-22) have been defined based on linear interpolation (Kriging, IDW) of the available pumping test data analysis.

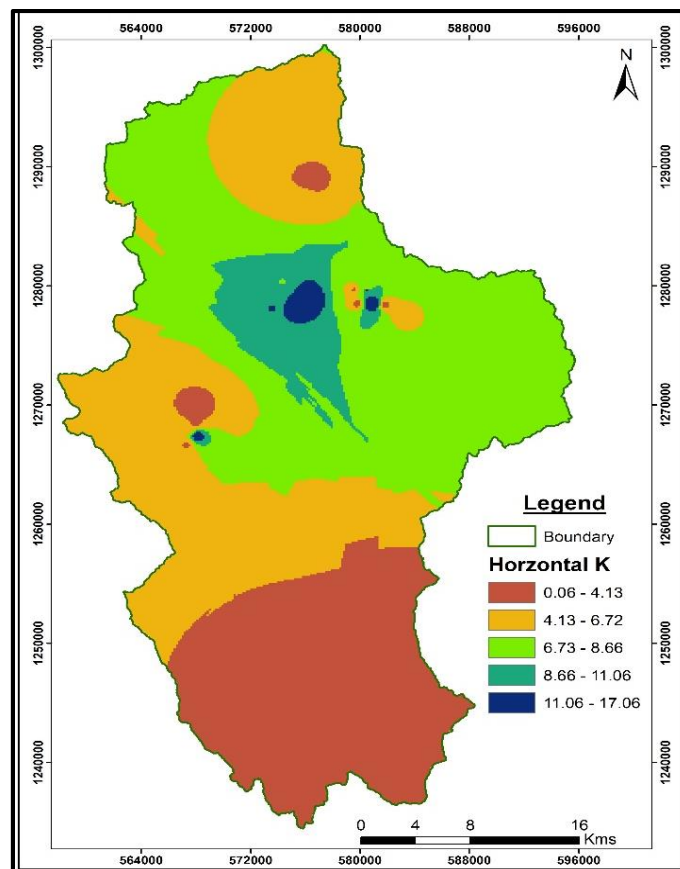


Figure 22: Hydraulic conductivity distribution map of the study area interpolated from point measurements.

5.4.2 Transmissivity

A useful concept in many hydrogeological and groundwater-related studies is the transmissivity of the subsurface formation. Transmissivity is a measure of the amount of water that can be transmitted horizontally through a unit width by the full saturation thickness of the aquifer under a unit hydraulic gradient (C.W. Fetter 2000). The transmissivity value of aquifers in the Upper Mille watershed is very variable. As shown below (Figure-23), the spatially distributed transmissivity map was constructed by interpolating point values taken from boreholes data. Different rock units have different transmissivity value depending on hydraulic conductivity and aquifer thickness. The transmissivity value of the watershed ranges from 2.44-1406m²/day.

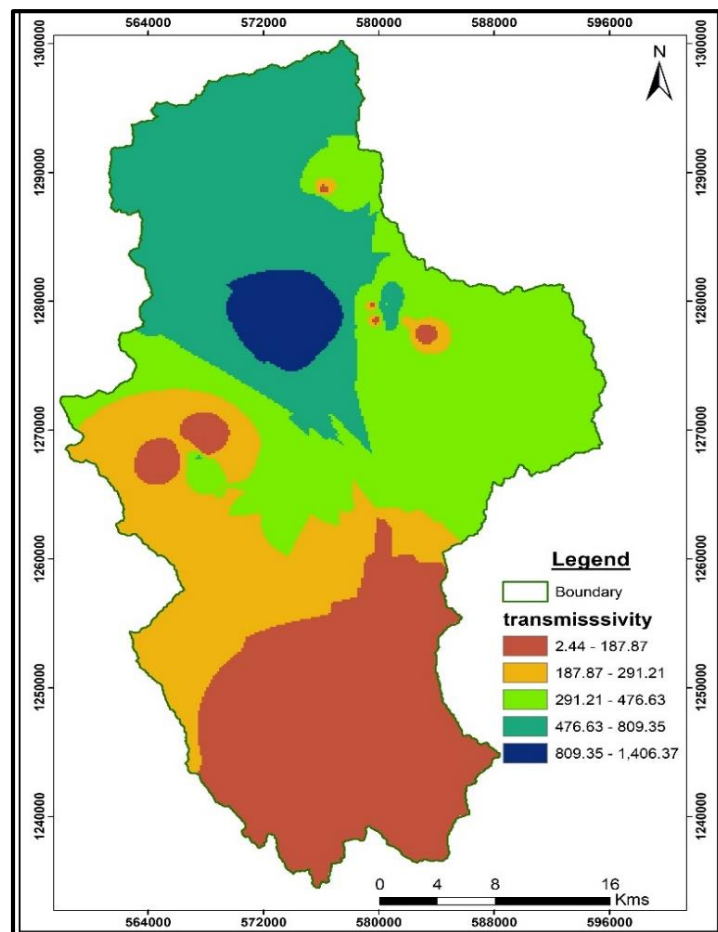


Figure 23: Interpolated transmissivity distribution map of Upper Mille catchment

⇒ The hydraulic conductivity and transmissivity maps show a similar pattern in which unconsolidated sediments have higher transmissivity and conductivity values.

5.5 Hydrogeologic Units of the Watershed

By integrating the hydrogeological properties such as infiltration capacity of surficial materials, the permeability of the rocks outcropping in the watershed, degree of weathering and fracturing, topographic and morphologic position, and hydrologic features, the lithostratigraphic units discussed in section 4.3 are transformed into hydrogeological units. To characterize in such a way, data from field observation, borehole lithological logs, pumping test results, and measured physicochemical parameters are used. Based on field hydrogeological data interpretation and mapping, lithostratigraphic units showing similar hydrogeological characteristics are grouped. Based on this, the aquifer types in the area are classified and mapped into three hydrogeological units; high productive intergranular porosity aquifer, medium productive double porosity aquifer, and slightly weathered and fractured low productive aquifer.

5.5.1 High productive intergranular porosity aquifers

In the Upper Mille watershed, high productive intergranular porosity aquifer is composed of mainly unconsolidated lithological units of alluvial, fluvial, and intermountain Quaternary sediments which have high hydraulic conductivity, transmissivity, and specific yield. The hydraulic conductivity and transmissivity of these aquifers are variable, depending on the sorting of the aquifer material and the percent of sand, silt, and clay, but generally high. Aquifers hosted in the alluvial sediments of marginal grabens comprise boulders, gravels, sands, and sandy to clayey soil of light black and reddish color sediments. Geological logs of the boreholes and the geophysical surveying results showed that the thickness of the sediment varies from place to place. The sediments are only a few tens of meters in some parts whereas, they are as thick as the intermountain grabens of Girana areas. In these regions, the thickness of the unconsolidated sediments reaches up to 300 m.

The high productivity of those units is due to the presence of large effective primary porosities formed during the deposition of those sediments. High productive aquifer lithologic units are mainly thick valley and graben fill sediments, which occupy the flat part of the study area on which major rivers are draining through. Girana valley is a typical type of valley-filled unconsolidated aquifer. Many deep boreholes and shallow hand-dug wells are drilled in this aquifer unit mainly for irrigation and domestic uses. The static water level exists near the ground surface this shows that the aquifer system

is not over-pumped. Based on spring discharge data, deep drilled boreholes, and pumping test results the hydraulic conductivity (K) and transmissivity (T) of this aquifer is very high.

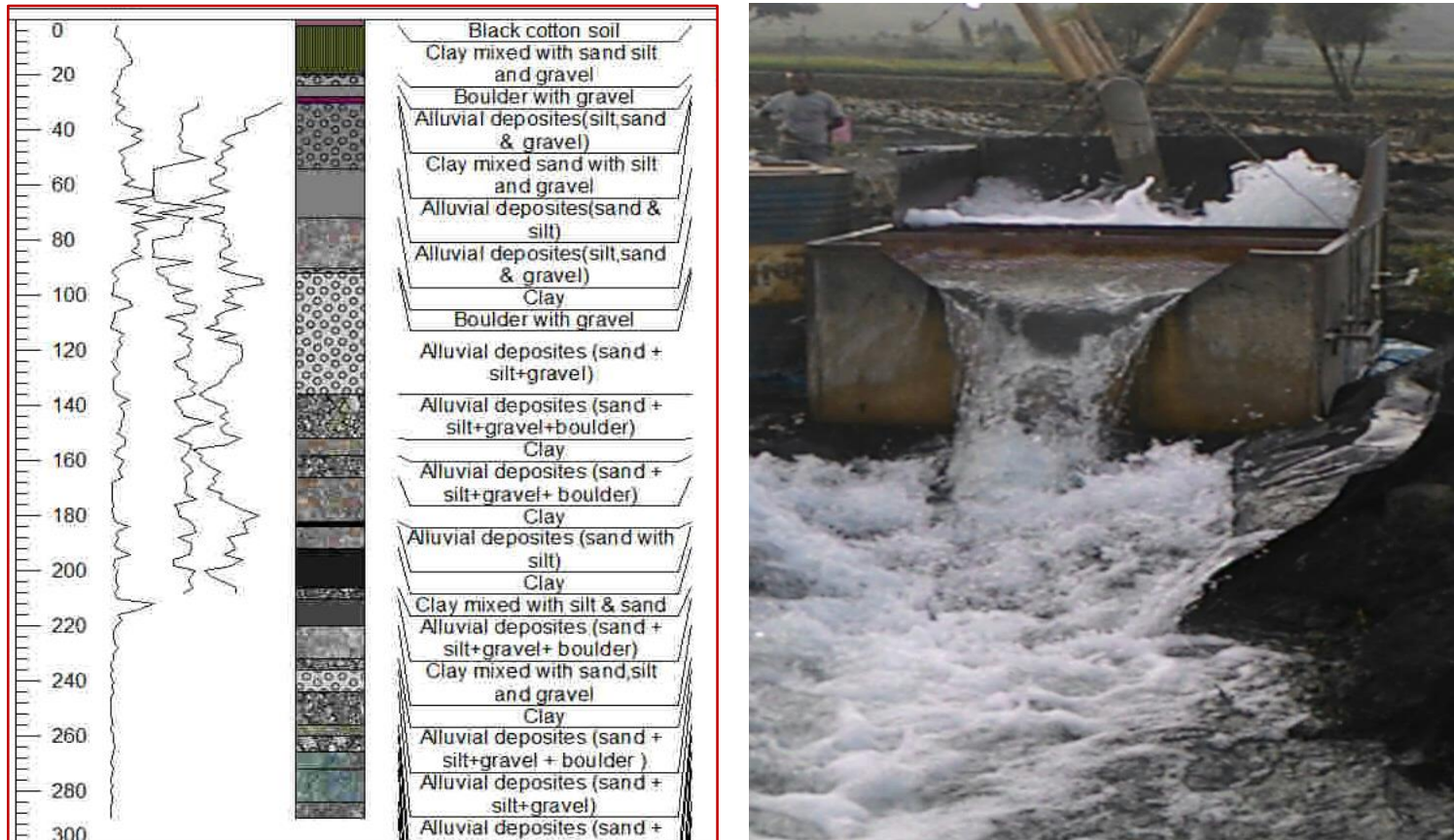


Plate 6: Lithological and geophysical logging and pumping test measurement of a borehole drilled on the thick unconsolidated sediment around Girana valley for irrigation purposes which has a yield of 84.3l/s.

5.5.2 Medium productive double porosity volcanic aquifer

The storage and movement of groundwater in the volcanic rocks largely depends on the type of porosity and permeability formed during and after the rock formation. Which contains both primary and secondary porosity associated with later deformation of rock units. Based on; borehole and spring discharge, conductivity, and transmissivity value obtained from different drilling companies and water offices lower /Ashange basalt is a medium productive double porosity volcanic aquifer. Ashange basalt is thick, deeply weathered, and fractured aquifer. Like other volcanic rocks, in the area, the main water-bearing controlling factor is fracturing. The occurrences of weathered and

fractured zones increase the porosity and the permeability of the rock and enhance the groundwater circulation and occurrence. The various opening which imparts porosity (primary and secondary) and permeability of this basaltic aquifer in the study area are; breccia zones between flows, cavities between lava flow, shrinkage cracks parallel to the flow surface called columnar joints, gas vesicles, lava tubes, fractures, and lineaments. This unit is highly affected by major NE-SW faults resulting in intense fracturing and hence high permeability (Bekele Abebe et al., 2007).

During the fieldwork, many springs and boreholes are observed which proved the wide variation in yield due to topographic setting, degree of fracturing, and weathering. Information from borehole logs, pumping test data, as well as the yield of springs showed that the Ashange basalt is the main regional aquifer of the watershed extending from south (Sulule) to north (Mersa), and the right of Wuchale along the western boundary of the watershed.

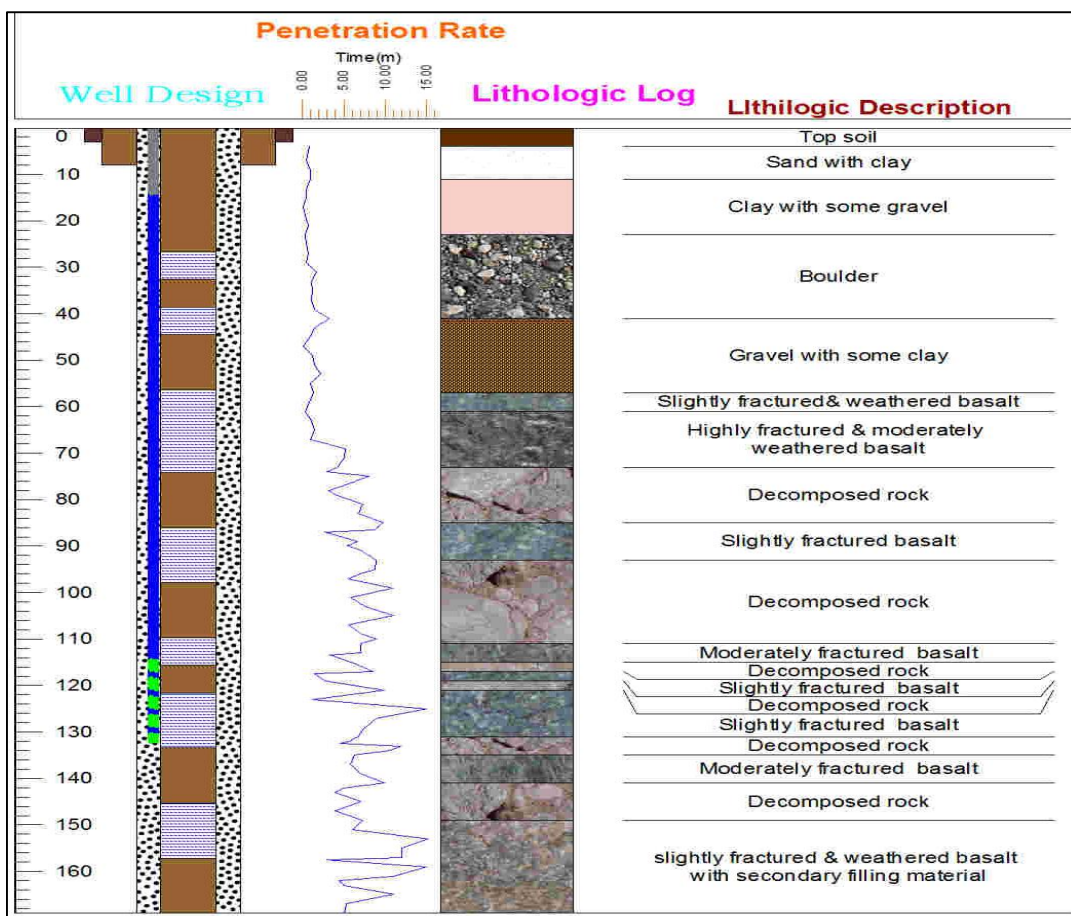


Plate 7: Lithologic log of a borehole drilled on moderately productive basaltic aquifer with the top 35m is soil and clay to gravel sediments (source: ADSWE, 2019).

5.5.3 Low productive aquifer

The groundwater potential of an aquifer is not only a matter of rock units, rather geological structures and topographic settings play a great role in controlling the quality of an aquifer in terms of productivity. In the Upper Mille watershed, some of the lithostratigraphic units are not productive due to the lack of effective primary and secondary porosity which in turn limits the permeability and the conductivity of the aquifer system. Tarmaber basalt, Aiba basalt, Kemise rhyolite, and swampy areas are grouped under low-productive aquifers. The former two units are due to the topographic setting they used as groundwater recharge zone, especially along the rift escarpment. Kemise rhyolite is due to the lack of effective primary and secondary porosity. Whereas, the swampy and wetland areas are due to the presence of a high percentage of clay and silt which lacks effective porosity. As discussed in the local geology part of the study area, Kemise rhyolite is found in the central-western part of the watershed forming highly rugged chains of mountains and volcanic domes. The permeability and transmissivity of these units are highly dependent on the secondary fracturing; however, the pore spaces are not developed enough to transmit and store the groundwater. During the field study, it was difficult to find areas of groundwater manifestation, and no boreholes were inventoried. Generally, the volcanic rock that forms steep and elevated mountainous terrain has a very limited discharge.

- ✚ High productive intergranular porosity aquifer covered about 460km² which is 35% of the total catchment area.
- ✚ Medium productive double porosity aquifer covers about 550 km² which accounts for 40% of the total watershed area.
- ✚ The low productive unit's covers a total area of 350km² which is 25% of the watershed. As indicated in the figure below this unit founds in the eastern part of the study area.

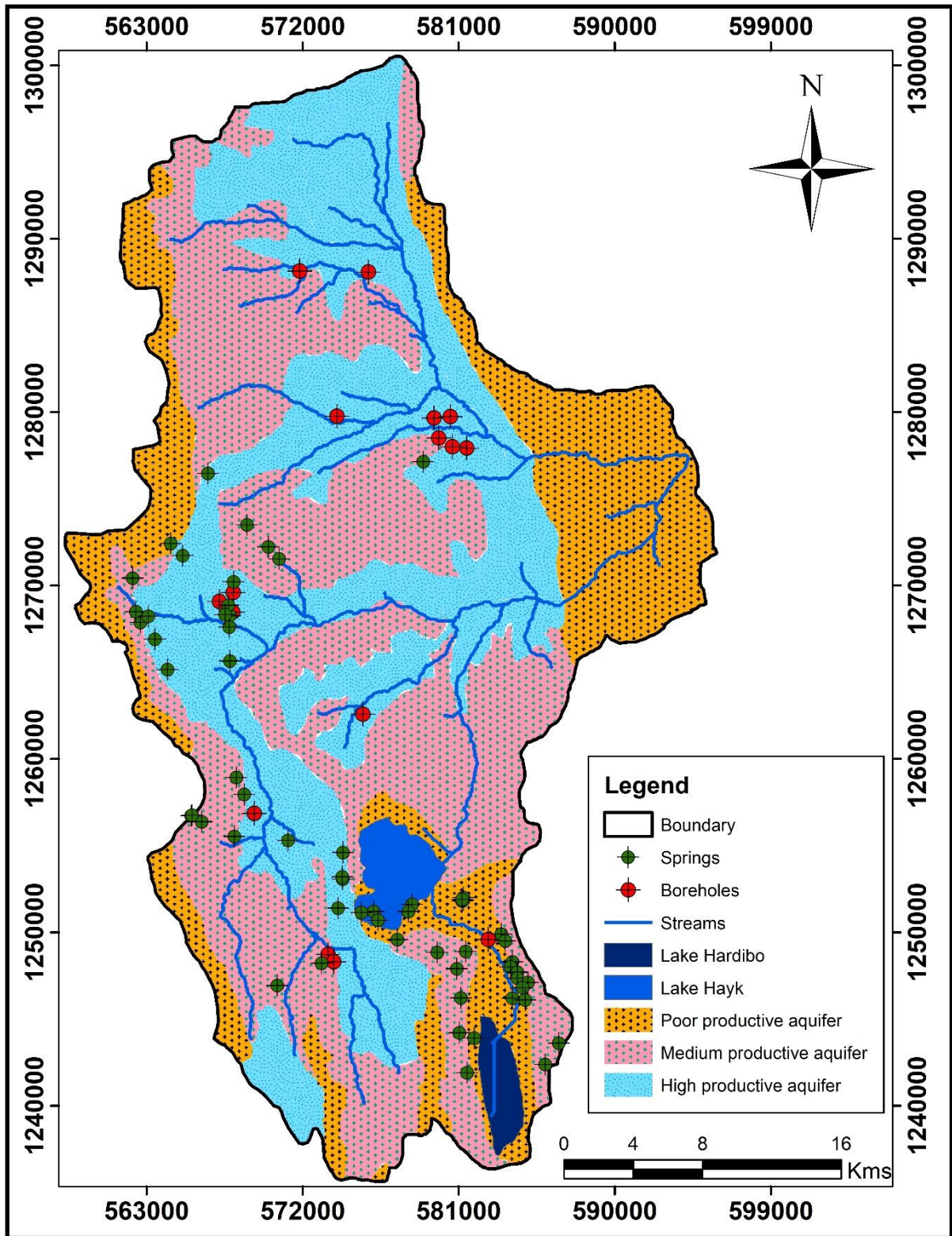


Figure 24: Aquifer classification map of the study area based on the productivity nature of each comprise units

5.6 Groundwater Flow (Recharge-Discharge zones)

The Groundwater flow is significantly influenced by geomorphology, topography, geological structures (faults, joints, and lineaments), the existence of impermeable layers, and the hydraulic properties (conductivity, transmissivity, and continuity) of the aquifer system. Several parameters are considered to trace out the groundwater flow directions and to identify the recharge and discharge areas. The main parameters and data used are; Slope/gradient and geomorphology, Geological structures, Groundwater level, equipotential contour lines, and Physico-chemical (EC and TDS) parameters. Aquifers in shallow groundwater, the flow is mainly controlled by the local topography of the watershed. In the watershed, topographically controlled shallow springs are good indicators to trace the shallow groundwater flow direction. Recharge, which is water contributing to groundwater passing through the unsaturated zone reaching the static groundwater table, could be direct, indirect, or localized based on the source and mechanism by which water reaches the water table. The amount and type of recharge depend on land use/land cover, topography, climate, drainage, vegetation, structure, soil condition, and other related factors.

Generally, groundwater flows from high elevation to low elevation. Unfortunately, direct observation of water levels is not possible. Thus, groundwater head data were collected and a map that shows points having equal potential was prepared using ArcGIS. Lines perpendicular to these contour lines are constructed. These perpendicular lines show the groundwater flow direction of the aquifer system (Figure-25). The ultimate source of recharge to the regional aquifer is highland rainfall that infiltrates into the fractured and weathered volcanic. Limited indirect recharge from rivers may occur in the highlands and the lowlands of the Upper Mille catchment. As observed below the figure, groundwater flows from the southern and western corridor of the catchment to the central-eastern part of the watershed following faults and lineaments. Based on this it can be confirmed that the western and southern weathered and fractured highlands act as a recharge area whereas, the central-eastern lowlands are the discharge zones of the catchment.

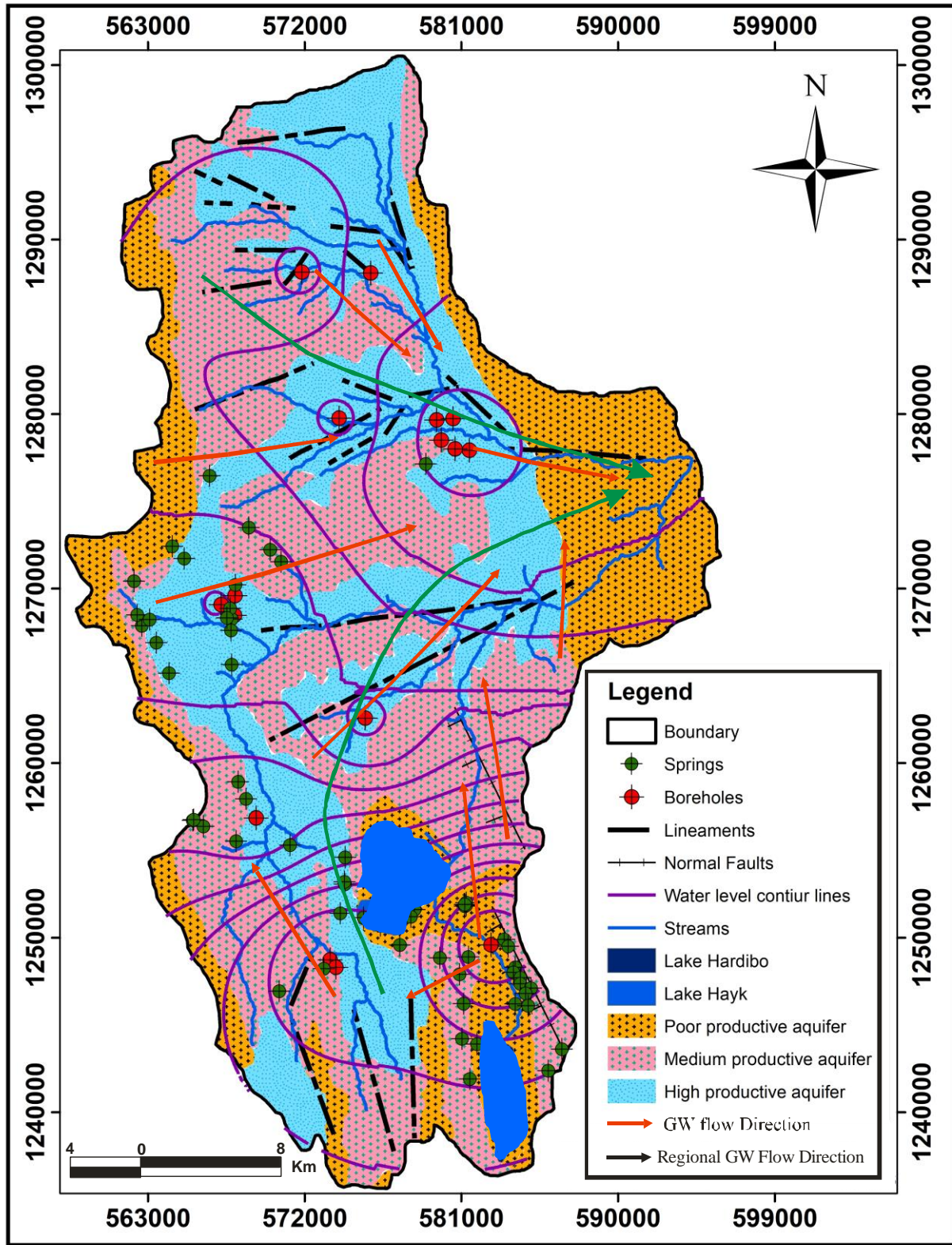


Figure 25: Schematic hydrogeological map which shows the possible groundwater flow direction of Upper Mille watershed.

5.7 Conceptual Hydrogeological Model

A conceptual model is a pictorial representation of the groundwater flow system, commonly in the form of a simplified diagram or hydrogeologic cross-section. The conceptualization of how and where the water originates in the groundwater flow system and how and where it leaves the the system is critical to the development of an accurate numerical model. In developing a conceptual model, the extent of the flow domain to be analyzed is expanded vertically and horizontally to coincide with physical features of the groundwater system that can be represented as boundaries (Anderson and Woessener, 1992). The hydrogeological conceptual model is a result of the combination of static (the rocks and soils: lithology, geological structures, etc.) and dynamic (the water: hydrology) (Anderson and Woessener, 1992). Hence, the construction of groundwater models depends on an understanding of the conceptual hydrostratigraphic model and the development of such a model involves synchronizing data obtained from different approaches such as field investigations (i.e., drilling activities and/or geophysical surveys).

The appropriate conceptual model is the base of any mathematical or numerical modeling. If the conceptual model is incorrect, the model output will be incorrect regardless of data accuracy and modeling approach. A Good mathematical model will not resurrect an incorrect conceptual model (Zheng and Bennet, 2002). Any numerical modeling of aquifers is a mathematical realization of the input parameters described within the hydrogeological conceptual model. Based on converging pieces of evidence from exploratory drilling, litho-stratigraphic relationships, water quality monitoring (pH, EC, and TDS), the groundwater occurrence and flow in the Upper Mille watershed can be conceptualized as shown in the figure below.

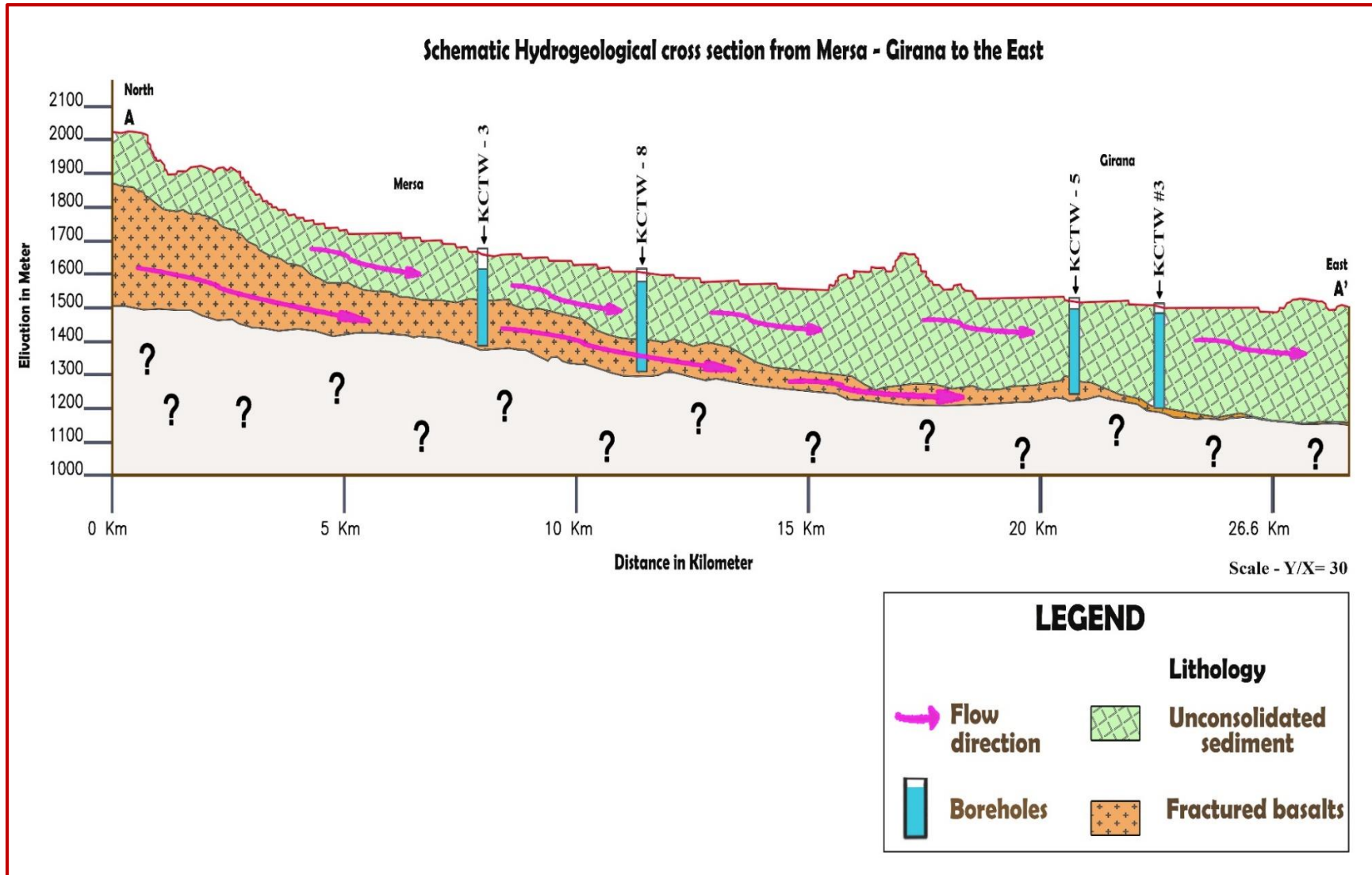


Figure 26: Schematic conceptual model of groundwater level and circulation in the upper Mille watershed (not scaled, deep borehole well log data were used to construct the cross-section).

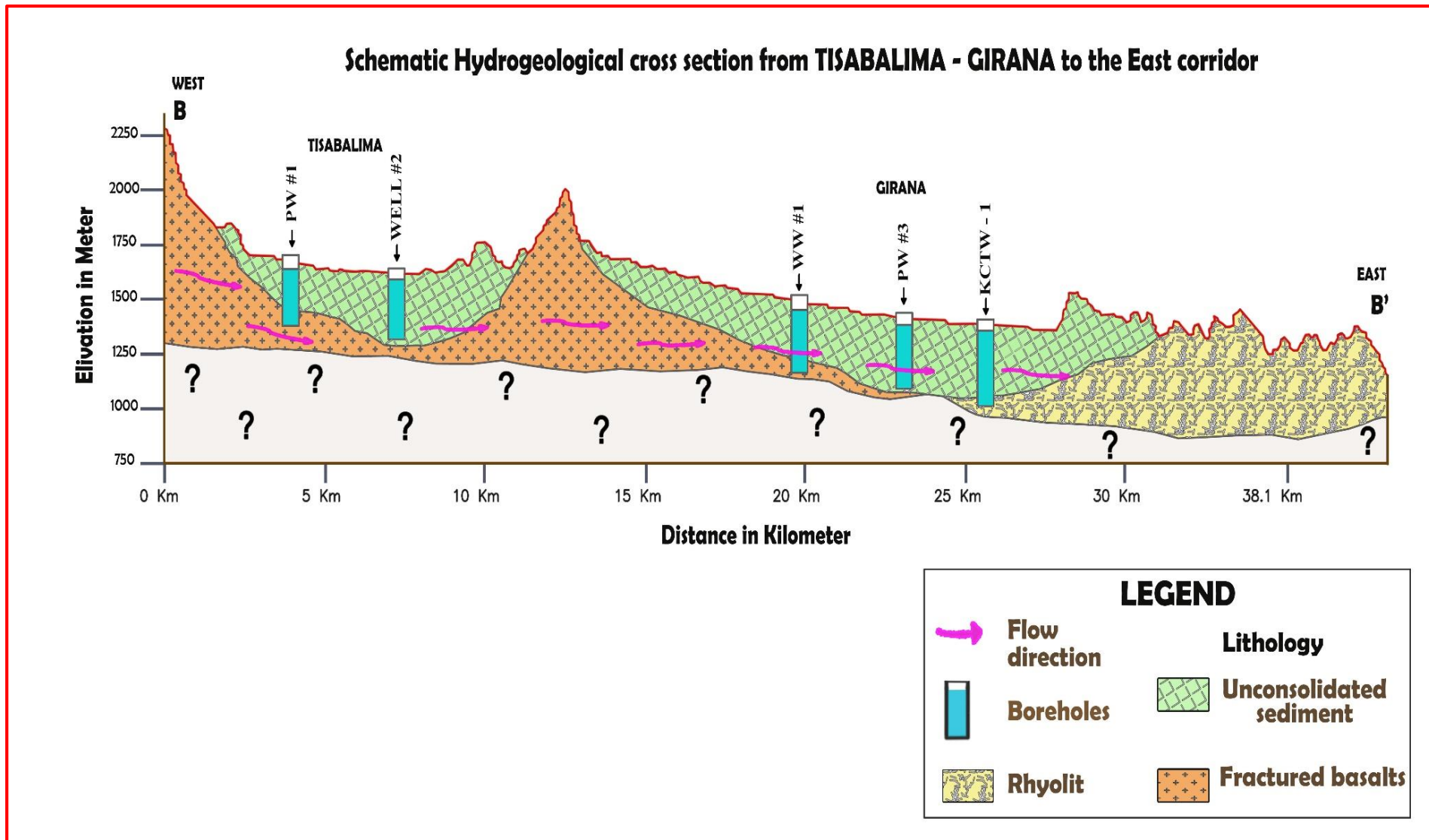


Figure 27: Schematic conceptual model of groundwater occurrence and circulation in the upper Mille watershed (not scaled) exploratory well log data were used to construct the cross-section.

CHAPTER SIX

NUMERICAL GROUNDWATER FLOW MODELING

6.1 Introduction

Groundwater flow models are simplified representations of the groundwater system with mathematical equations solved by a computer program. But the simplification should be on logical assumptions and without compromising reasonable representation of complex hydrogeological dynamics (Anderson and Woessner, 1992). The validity and the usefulness of the groundwater flow model depend on the quality of data, the experience of the model interpreter, and the type of software used to model the hydrogeology of the watershed.

To model the hydrogeology of the watershed, two basic principles are applied; Darcy law and the principle of water balance. The first states that groundwater flows from high to low elevations, or more precisely from high potential energy to low potential (Anderson and Woessner, 1992). Darcy's law says that the discharge rate q is proportional to the gradient (dh/dl), and the hydraulic conductivity (K) ($q = Q/A = -K*dh/dl$). The second principle states that the inflow into any water system is equal to the outflow from the system plus the change in storage during a time interval, and it's used to describe and quantify the flow of water in and out of the system. This law is also known as conservation of mass in which mass is neither created nor destroyed rather conserved. (https://en.wikipedia.org/wiki/Water_balance#:~:text=The%20law%20of%20water%20balance,and%20out%20of%20a%20system.)

6.2 Governing Equation of Groundwater Flow

The governing mathematical equations used in numerical groundwater flow modeling assume that the flow is a single-phase fluid in this case water at a constant density in a continuous porous medium under the applicability of Darcy's law and conservation of mass (McDonald and Harbaugh, 1988). This shows that modeling cannot be the exact indicator of the site's hydrogeological system. This simplification of the real process will limit the accuracy of the model outputs.

The model uses an approximate form of the governing equation to calculate the head at selected locations. The most widely used code for solving groundwater flow problems is the finite difference (FD) code MODFLOW developed by the U.S. Geological Survey (USGS) (Anderson and Wossener, 2002). In this study, Processing MODFLOW-2005 is used to Model the

groundwater system of the upper Mille catchment. The steady-state groundwater flow is simulated based on the following governing differential equation under two- dimensional aerial view (Anderson and Wossener, 2002).

$$\frac{\partial}{\partial x} \left(K_x \frac{\partial h}{\partial x} \right) + \frac{\partial}{\partial y} \left(K_y \frac{\partial h}{\partial y} \right) + R = 0$$

Where: K_x and K_y are hydraulic conductivity components along the x and y-axis respectively [L/T]; R is flux per unit volume representing sources/sinks term [T^{-1}] and H is the hydraulic head [L]

6.3 Model Design

6.3.1 Model geometry

The model is designed for a two-dimensional domain having a horizontal extent of 50kmx30km bounded by UTM zone 37/Adindan- 0557969-0595777 Easting and 1236452-1300230 Northing. The area of the model domain is not regular which decreases the active model domain to an area of 1360km².

6.3.2 Model discretization

Spatial discretization of the model grid

Designing the finite grid or finite element mesh is one of the most important and difficult steps in model design. The number of nodes in the grid/mesh affects the accuracy of the solution, the computational time required to solve the model (Anderson and Woessner, 2002). The nodal network forms the computational framework of the numerical model and the nodal spacing determines the resolution of the output as much as groundwater heads are computed at nodes and must be interpolated between nodes. The area of the conceptual model is transformed into a numerical model by importing the watershed boundary into discrete cells; 438 rows and 254 columns. The model domain is transformed into rows and columns having a constant spacing of 150m by 150m in which each cell covers a 0.0225km². The numerical model of the watershed is simulated by a finite-difference block-centered flow code in which the hydraulic head is computed at the center of the cells.

Time discretization of simulation

The model is designed and simulated for steady-state model simulation. The time unit used for the simulation of this model is in a day.

6.4 Model Input Parameters

6.4.1 Modeling environment

Boundary condition

A boundary condition can be defined as a constraint put on the active model grid to characterize the interaction between the active simulations grid domain and the surrounding environment. In groundwater models, which are used for analyzing groundwater flow analysis, the specification of the boundary conditions usually defines the source of water to the system and its ultimate manner of discharge. For modeling, there are three different types of boundary conditions; specified head including constant head; specified flow including no flow; and head-dependent flow boundary conditions. These boundary conditions define the flow into and out of the model domain (Anderson and Woessener, 2002).

Specified head boundary condition

Specified head boundaries are best used to represent large bodies of water (major rivers, lakes, reservoirs, and oceans) that are not affected by stresses such as pumping and changes in recharge rate. Lake Hayk and Lake Hardibo are treated as constant head boundaries (IBOUND -1)

Specified flow boundary condition

Specified flow can be implemented along the lateral boundaries of a 2D or 3D model to represent horizontal flow across the boundary, such as groundwater entering or leaving the problem domain as underflow. Conceptually, water enters or leaves the cell through one of its faces and then enters the faces of adjacent active cells.

Head-dependent Boundary condition

Head-dependent boundary can represent a wide variety of hydrogeological situations including vertical flow to and from streams, lakes, and other surface water bodies; flow to drains; evapotranspiration from the water table; lateral and bottom boundary flows; and boundaries outside the model domain. When the head-dependent boundary (HDB) is implemented, the code calculates flow across the boundary using the hydraulic gradient between a user-specified external boundary head and the simulated head at the boundary node (Anderson and Woessener, 2002). In this case, areas around the outlet of the river are treated as GHB as shown on the map (Figure-24).

The model has an IBOUND array, which contains a code for each model cell. A positive code value in the IBOUND array defines an active cell in which the hydraulic head is computed, a

negative value defines a constant head or fixed head cell and the value 0 represents an in the active cell, in which the cell is out of the model domain, as a result, the hydraulic head is not computed.

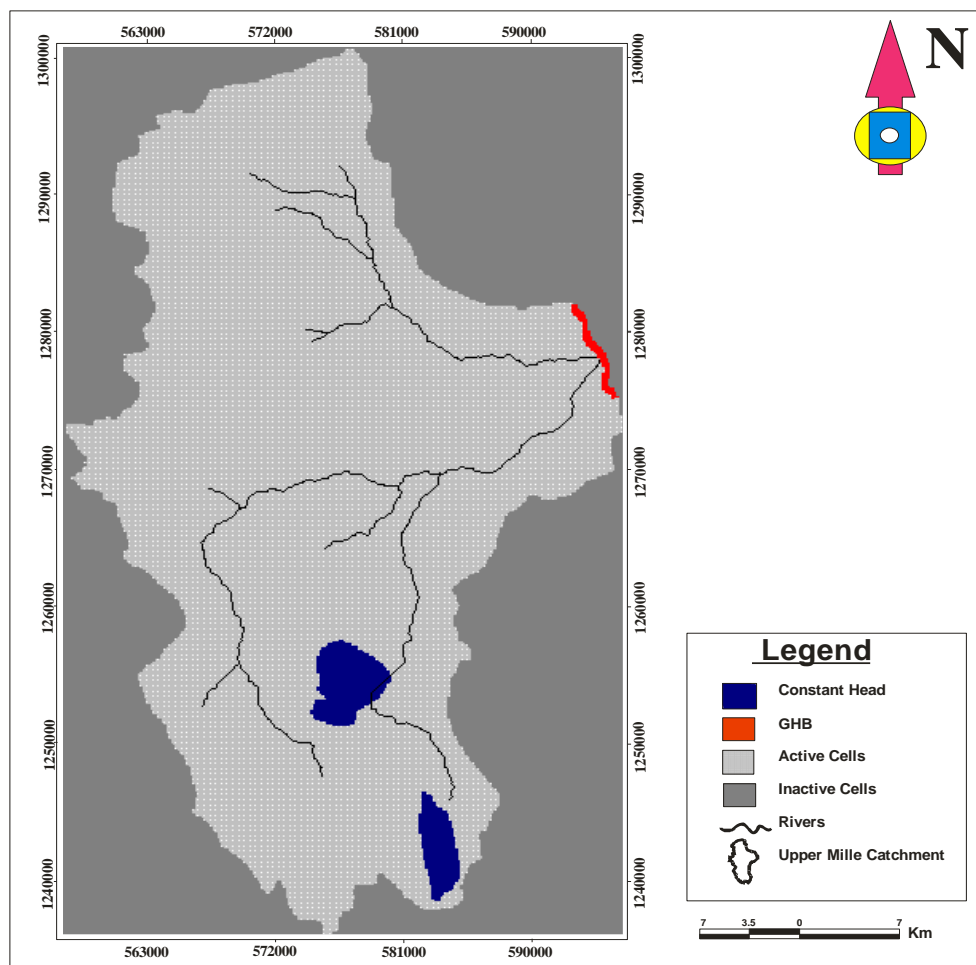


Figure 28: Model domain discretization of Upper Mille river catchment

Top and bottom layer

The aquifer system is assumed to be one layer. The model top elevations of the layer were incorporated into the model using 30m by 30m spatial resolution DEM converted into ASCII matrix format. The model bottom was determined by subtracting the layer thickness from the model top. Then the software computes the values of the elevations from the input ASCII file.

Initial and prescribed head

Processing MODFLOW needs the initial hydraulic head of the groundwater at the beginning of the flow simulation. The initial hydraulic heads at the constant cell can be used as a specific head value of the model domain which remains constant throughout the flow simulation. The heads are measured at each well and the value is interpolated using the ArcGIS software to have a weight head value all over the catchment area which undergoes modeling.

Horizontal hydraulic conductivity

As discussed in the previous section hydraulic conductivity of an aquifer is the most important primary factor that determines and affects the groundwater flow system of the catchments. The flow of the groundwater system is assumed to be horizontal. The hydraulic conductivity of wells in the model domain is estimated from pumping test data of 36 relatively deep drilled boreholes. The hydraulic conductivity map is prepared and incorporated into each active cell within the model domain.

River

For the simulation of the model, the relationship between the aquifer system and the Upper Mille River is modeled using the “River” package menu in the processing MODFLOW interface. To include the river in the simulation of the model, MODFLOW needs the location, bed elevation, stage or river head, and river bed conductance. Hydraulic conductance of the river bed can be calculated using the following mathematical equation

$$CRIV = \frac{K * L * W}{M}$$

Where:

$CRIV$ = Hydraulic conductance of the riverbed (L^2/T), K = Hydraulic conductivity of the riverbed sediment ($[L/T]$), L = Length of the river within a cell (L), W = Width of the river within a cell (L), and M = Thickness of the riverbed sediments (L).

But, because of insufficient data to quantify the conductance of the river bed in every cell river network of the modeled area, it is assumed that the hydraulic conductivity of the riverbed and the river channel sides is the same as the hydraulic conductivity of the surrounding rocks and sediment in which average conductivity values are assigned.

6.5 Stresses

Groundwater recharge

The mean annual groundwater recharge of the area is estimated using WB and SWAT model, which results in 106.5, and 150mm/year respectively. The spatially distributed recharge value obtained from the SWAT model is imported into the model. It is simulated to the groundwater system using recharge packages.

Groundwater pumping rate

It is difficult to know the exact volume of water withdrawal from the ground due to the inconsistent rate of pumping and poor data documentations. The currently estimated groundwater abstraction from the model domain by boreholes and springs is about **19,356.40m³/day**.

6.6 Model Simulation

The model is simulated under steady-state flow model conditions. In steady-state flow model simulation, hydrologic parameters and computed heads and fluxes are constant in time unlike with transient model simulation.

6.6.1 Model calibration

Model calibration is the process whereby model parameter values are adjusted and refined to provide the best match between measured and simulated values of hydraulic heads and flows (Anderson and Woessener, 2002). This requires that field conditions at a site should be properly characterized. The model is calibrated by a trial-and-error process in which model parameters are adjusted within reasonable limits from one simulation to the next to achieve the best model fit. Model fit is commonly evaluated by visual comparison of simulated and measured heads and flows or by listing measured and simulated heads together with their differences and some type of average of the differences, which is then used to quantify the average error in the calibration. The objective of calibration is to minimize this average error which is called calibration criterion (Mandle, 2002).

Fifteen water level measurements wells (Head observation boreholes) were used for estimation of the groundwater level of the aquifer (Figure-29). These boreholes are utilized for the calibration of the steady-state model simulation.

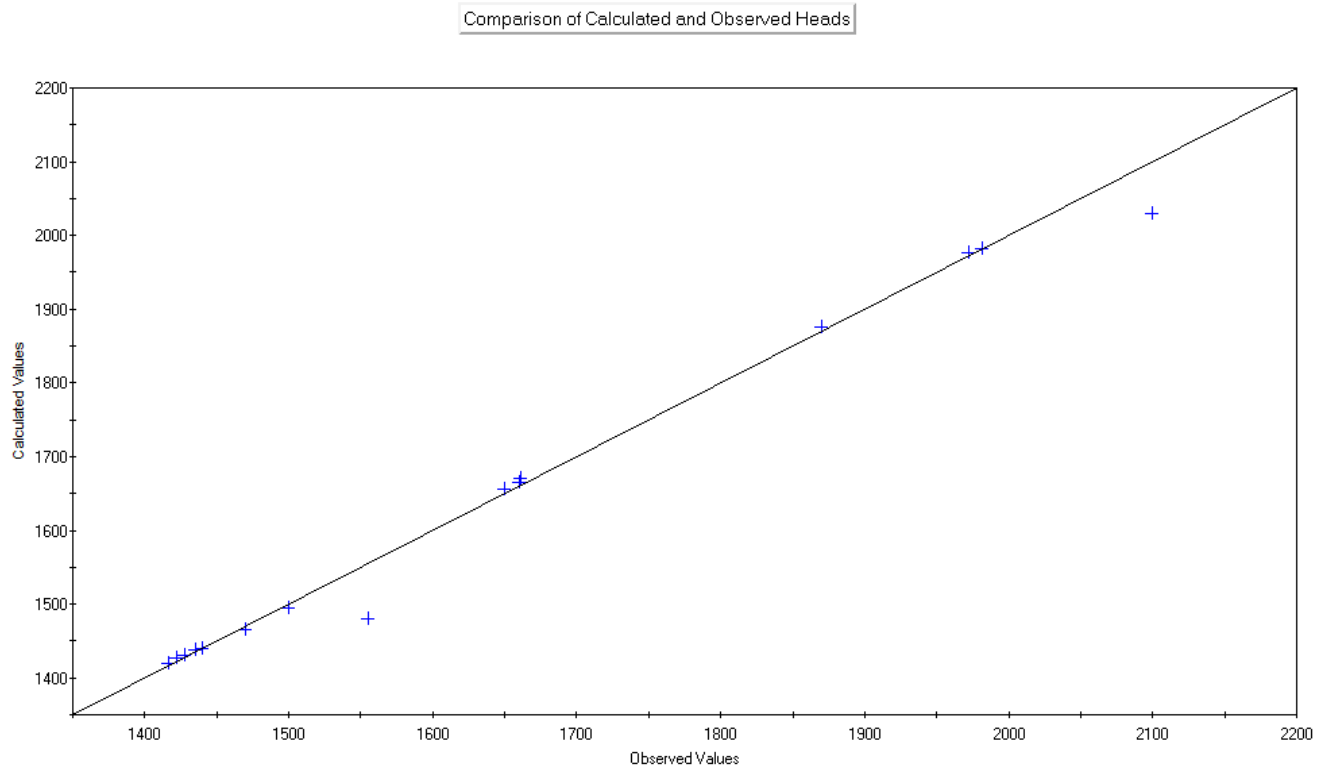


Figure 29: Scatter plot of simulated to the observed fit of water levels

6.6.2 Evaluation of model calibration

Calibration results should be evaluated both qualitatively and quantitatively (Anderson and Woessner, 2002). The average error in the calibration process was calculated by taking the mean of the observed and simulated head differences. The Mean Error (ME), the Mean Absolute Error (MAE), and the Root Mean Square Error (RMSE) are the three ways to express the average difference between simulated (h_s) and measured heads (h_m). The ultimate goal of calibration is to minimize these errors.

1. **Mean Error (ME):** - an average of the difference between measured (h_m) and simulated head (h_s).

$$ME = \frac{1}{n} \sum_{i=1}^n (h_m - h_s)_i$$

2. **Mean Absolute Error (MAE):** - the mean of the absolute value of the difference between measured and simulated heads.

$$MAE = \frac{1}{n} \sum_{i=1}^n |(h_m - h_s)_i|$$

3. **Root Mean Squared Error (RMSE):** - the square root of the mean of the square of all of the errors.

$$RMSE = \left[\frac{1}{n} \sum_{i=1}^n (hm - hs)^2 \right]^{0.5}$$

Table 9: Calibration evaluation of mean errors using observed and simulated heads

Well-ID	Hydraulic Heads		ME (AVG (hm-hs))	MAE AVG((hm-hs))	RMSE (SQRT (AVG (hm-hs) ²))
	Calculated	Observed			
OBS1	1494.483	1500	5.517	5.517	30.43729
OBS2	1420.345	1417	-3.345	3.345	11.18903
OBS3	1431.479	1428	-3.479	3.479	12.10344
OBS4	1479.268	1485	5.732	5.732	32.85582
OBS5	1465.451	1470	4.549	4.549	20.6934
OBS6	1876.468	1870	-6.468	6.468	41.83502
OBS7	1977.228	1972	-5.228	5.228	27.33198
OBS8	1982.776	1982	-0.776	0.776	0.602176
OBS9	1671.443	1661	-10.443	10.443	109.0562
OBS10	1656.279	1650	-6.279	6.279	39.42584
OBS11	1664.675	1660	-4.675	4.675	21.85562
OBS12	1437.93	1435	-2.93	2.93	8.5849
OBS13	1439.156	1440	0.844	0.844	0.712336
OBS14	2029.178	2050	20.822	20.822	433.5557
OBS15	1427.052	1422	-5.052	5.052	25.5227
			0.75	5.74	7.37

CHAPTER SEVEN

RESULT AND DISCUSSION

7.1 Introduction

The results obtained from recharge estimation, aquifer characterization, and steady-state numerical groundwater flow modeling are discussed here below in separate subtopics .

7.2 Estimated Recharge Results

As presented before the long-term mean annual groundwater recharge of the Upper Mille river basin is estimated using water balance and SWAT model techniques and the amount is about 105 and 150mm/year respectively. Averaging the two will give a mean annual groundwater recharge of 127.5mm/year. From the mean annual groundwater recharge, the total volume of water added annually to the groundwater (recharge) in a year is estimated at **173,400,000m³/year**.

The maximum rate at which water can be withdrawn indefinitely from groundwater in a year without violating the natural environment (sustainable yield) is about **40%** of the annual recharge. So, to sustainably use the groundwater resource the maximum volume of groundwater pumping should be less than **69,360,000m³**. Based on this extracting more than **69,360,000m³** volumes of groundwater per year is not recommended and it will harm the natural environment. The current annual volume of water extracted from boreholes and springs is about **7,064,940m³/year**. Which accounts for **4.1%** of the total volume of annual recharge. This indicates that the rate of abstraction is safe and sustainable to support the ecosystem and the groundwater is not depleted with the current rate of abstraction.

7.3 Results of Aquifer Characterization

The aquifers of the area are classified and characterized based on their hydraulic property into three qualitative classes; high productive, medium productive, and low productive aquifers. In the area, volcanic rocks are grouped into low and medium-productive aquifers. Tarmaber and Aiba basalts are categorized under low productive aquifer, whereas, Ashange basalt is a medium productive double porosity aquifer even though they are porous and permeable due to their very steep slope topographic setting. They are good sources of recharge for low land gentle slope volcanic and sediments. This shows having high transmissivity and permeability can't be a

guarantee to have good groundwater potential resources and the topographic setting of an area plays a great role in characterizing and classified the aquifer system of a basin.

7.4 Steady-State Simulated Results

The main outputs of the steady-state groundwater flow simulation in this study are inflow and outflow water budgets and hydraulic heads of the basin. These simulated results were presented and analyzed separately in the next subtopics.

7.4.1 Hydraulic heads

In section 6.5 the hydraulic heads were computed by using the mathematical groundwater flow model. The resulted head analysis was made by comparing the field observed hydraulic heads with the heads simulated by the model (computed heads). The analysis of the results (simulated and measured head) can be shown in **Table 10** below.

Table 10: Simulated and observed hydraulic heads in each observational borehole

Well-ID	Hydraulic Heads	
	Calculated head	Observed head
OBS1	1494.483	1500
OBS2	1420.345	1417
OBS3	1431.479	1428
OBS4	1479.268	1555
OBS5	1465.451	1470
OBS6	1876.468	1870
OBS7	1977.228	1972
OBS8	1982.776	1982
OBS9	1671.443	1661
OBS10	1656.279	1650
OBS11	1664.675	1660
OBS12	1437.93	1435
OBS13	1439.156	1440
OBS14	2029.178	2100
OBS15	1427.052	1422

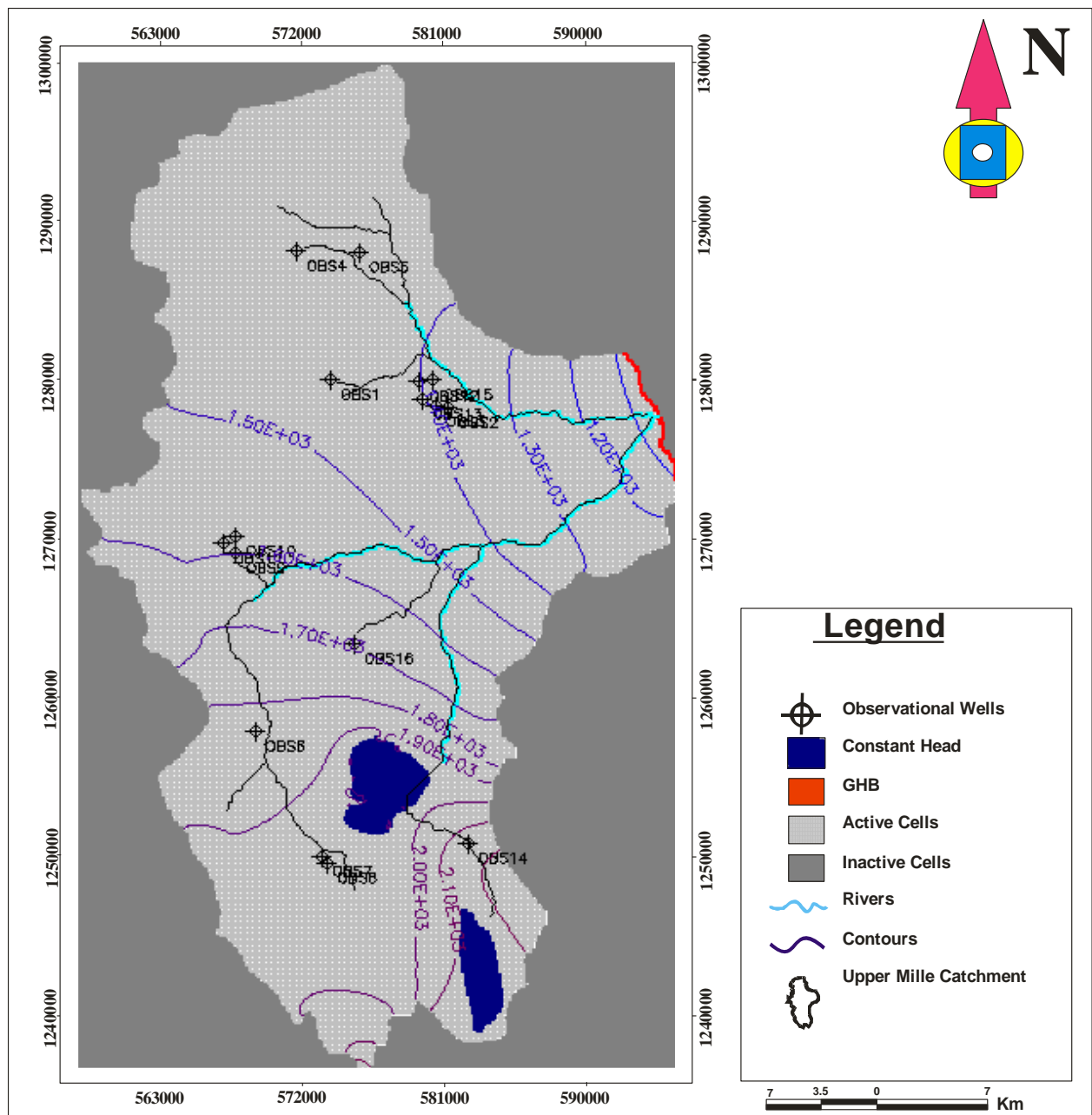






Figure 30: simulated groundwater level contour map of the model domain

7.4.2 Water budgets

Here, are the inflow and outflow components of the water budget simulated by the model domain.

-  Groundwater Inflow from Constant Head Boundary, which is $3.23 \times 10^7 \text{ m}^3/\text{day}$,
-  Groundwater inflow from River Leakage with a value equal to $3.44 \times 10^5 \text{ m}^3/\text{day}$,
-  Groundwater inflow from Head Dependent Boundary, which is about $4.24 \times 10^6 \text{ m}^3/\text{day}$
-  Groundwater recharge ($3.32 \times 10^5 \text{ m}^3/\text{day}$), which is **(89.1mm/year)** less than the calculated recharge by the soil water balance and SWAT model.

The total inflow to the system is about $3.73 \times 10^7 \text{m}^3/\text{day}$.

The simulated groundwater outflow from the system includes

- Groundwater outflow from Constant Head Boundary, which is $2.49 \times 10^7 \text{m}^3/\text{day}$,
- Groundwater Inflow from River Leakage with a value equal to $1.32 \times 10^6 \text{m}^3/\text{day}$,
- Groundwater Outflow from Head Dependent Boundary, which is about $1.10 \times 10^6 \text{m}^3/\text{day}$

The total Outflow to the system is about $3.73 \times 10^7 \text{m}^3/\text{day}$.

Table 11: Model-calculated steady-state hydrologic budget for the whole model (the unit of the flows is $[\text{l}^3/\text{t}]$)

FLOW TERM	IN	OUT	IN-OUT
CONSTANT HEAD	3.23E+07	2.49E+07	7.42E+06
WELLS	0.00E+00	0.00E+00	0.00E+00
RECHARGE	3.32E+05	0.00E+00	3.32E+05
RIVER LEAKAGE	3.44E+05	1.32E+06	-9.81E+05
HEAD DEP BOUNDS	4.24E+06	1.10E+07	-6.73E+06
SUM	3.73E+07	3.73E+07	2.00E+01
DISCREPANCY [%]		0.00	

7.5 Model Sensitivity Analysis

Many assumptions and estimates are used in the design and construction of a groundwater flow model. To test the response of the calibrated model to a range of values for the various input parameter, a sensitivity analysis is done. Sensitivity analysis can help to determine which model parameters have the greatest effect on a model result. Results of the analysis can guide future data collection efforts that will reduce model errors. It is done by varying the values of one input parameter while keeping all others constant.

Separate model simulations were made with varied input properties and the changes in the simulated hydraulic head were recorded. The model is considered sensitive to a parameter when a

change of the parameter value changes the distribution of the simulated hydraulic head. When the model is sensitive to an input parameter, the value of that parameter within the model is more accurately determined during model calibration because small changes to the parameter value cause large changes in the hydraulic head. When the model is insensitive to an input parameter, the value of that parameter within the model is more difficult to accurately determine from model calibration because large changes to the parameter do not cause large changes in the hydraulic head.

Model sensitivity was determined for variations in hydraulic conductivity, and recharge. The results of the sensitivity analysis for this study were evaluated by calculating the sum of square deviation between measured and simulated heads in the modeled area for a decrease or increase in percent, from the calibrated value, of that parameter. The greater the deviations of the water level from its calibrated model value, the greater the sensitivity of the model to an increase (positive percent) or decrease (negative percent) for that parameter. To test the sensitivity of the above parameters, the calibrated values of each parameter were separately decreased and increased by the multiplier factors of 0.5, 0.7, 0.9, 1.1, 1.3, and 1.5 respectively, and then simulated to see the resulting heads.

Table 12: RMSE head changes with different recharge and hydraulic conductivity from the calibrated values

Multiplier factors	Recharge	Hydraulic conductivity
0.5	15	21.5
0.7	12	17
0.9	10.5	11
1	7	7
1.1	11	9
1.3	13	12
1.5	14.5	14.5

In the model, simulated water levels were sensitive and almost similarly reacts to the decrease and increase in the recharge values. Compared to recharge, the model is more or less equally sensitive to the increase in hydraulic conductivity value but highly sensitive to the decrease in hydraulic conductivity, mainly to decrease beyond 0.5 of the calibrated values. Results of the sensitivity analysis show that small errors in estimating values of the aquifer properties to which the model is most sensitive, which in this case is recharge and hydraulic conductivity, can have a significant effect on the model simulation results.

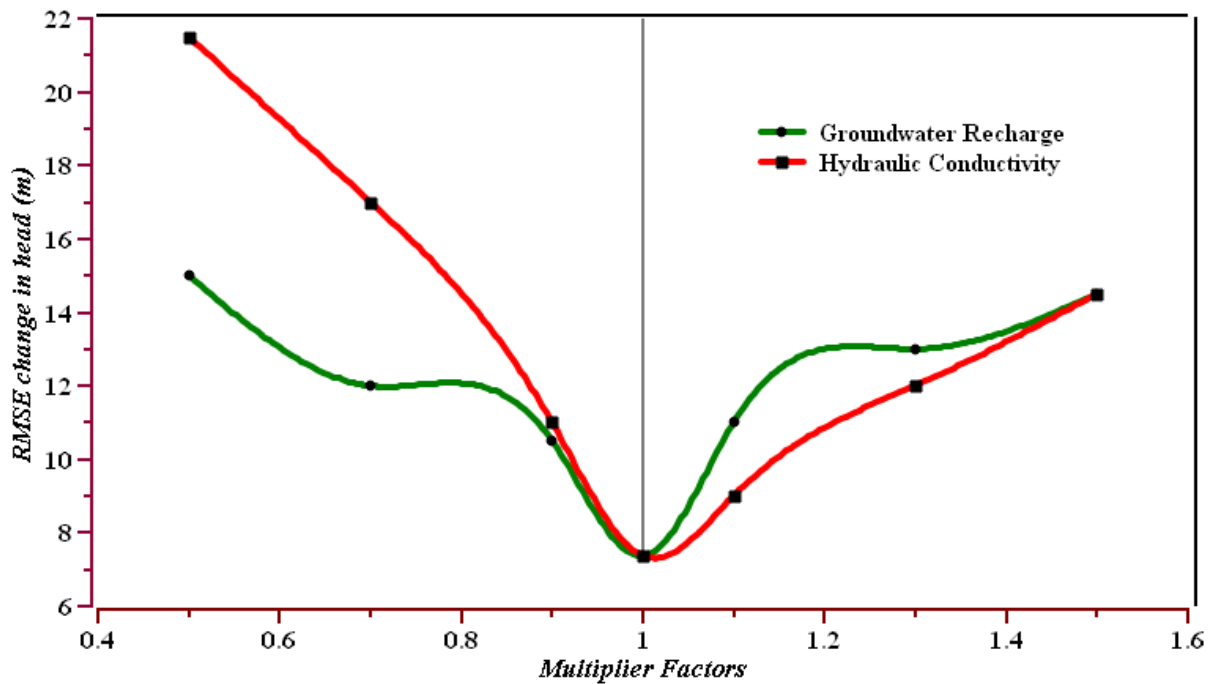


Figure 31 : Sensitivity analysis of the effect of selected parameters on the RMSE Value of Water level

7.6 Scenario Analysis


A calibrated flow model can be used as a tool to evaluate and compare the responses of an aquifer system to potential future stresses. Management actions involving changes in the quantity and distribution of pumpage or altered hydrologic conditions which could be extended dry conditions or conditions of altered recharge that may result, for example, from land-use changes can be simulated. The response of the aquifer system can be compared to evaluate the effectiveness of these probable changes of stresses in such a way that it satisfies management goals. Although water levels simulated for a given scenario may not accurately represent the values in the real system, the relative differences in water levels can be compared to provide useful information for planning and decision making. In this study, the model was used to simulate the aquifer-system response to increased withdrawals and decreased recharge. For the scenarios, all model parameters were unchanged from those specified in the steady-state simulation.


a. Pumping Scenario


As the information obtained from water offices, the amount of groundwater currently extracted through boreholes and developed springs for irrigation and water supply purposes was estimated to be **19,356.39m³/day**. From this, **13,623.75m³/day** is extracted from boreholes and the remaining **5,732.64m³/day** is pumped from developed springs.

The scenarios, which are increment of pumpage by, 50, 100, and 200 percent, were selected to represent possible future changes in water use in the basins or to investigate the effects of water-management practices that could mitigate potentially adverse effects of increased water withdrawals.

The results of the scenario analysis were presented as follows using tables, and graphs.

 **Scenario-one:** - it was simulated by increasing the amount of groundwater abstraction by 50% from the current withdrawn through pumping boreholes and developed springs. Based on this, the rate of extraction will be **29034.6m³/day**. The result of the analysis shows a minimum and a maximum decline of groundwater level by 4 and 10 m respectively.

 **Scenario-two:** - the model was simulated by increasing the amount of groundwater withdrawal by 100% from now. The rate of extraction will be **38712.78m³/day**. A minimum of 6m and a maximum of 20m decline of water level have been observed. The average decline observed is about 14m.

 **Scenario- three:** - the maximum average decline in simulated hydraulic was observed during the increment of pumpage by 200% of the current withdraw. The rate of pumpage will be **58069.17m³/day**. A minimum of 10 and a maximum of 25 m decline were observed. The average estimated decline is about 25m.

⊕ As observed from the results of the scenario analysis, different boreholes respond differently to the increments of pumpage. Generally, the maximum decline in water level has been observed around those boreholes drilled closed together. In the case of the Upper Mille catchment, a greater decline in the head was observed in the Girana and Tisabalima plains in which the wells are relatively closely together than those drilled in the western and southern highlands.

Table 13: Decline in water level simulated by increasing from the current pumping rate

		Current abstraction	Scenario-1	Scenario-2	Scenario-3
Abstraction rate (m ³ /day)		19,356.40	29,034.6	38,712.78	58,069.17
decline	Min.	1	4	5	7
	Max.	14	19	28	33
Head (m)	Average	8.5	12.2	19.1	23

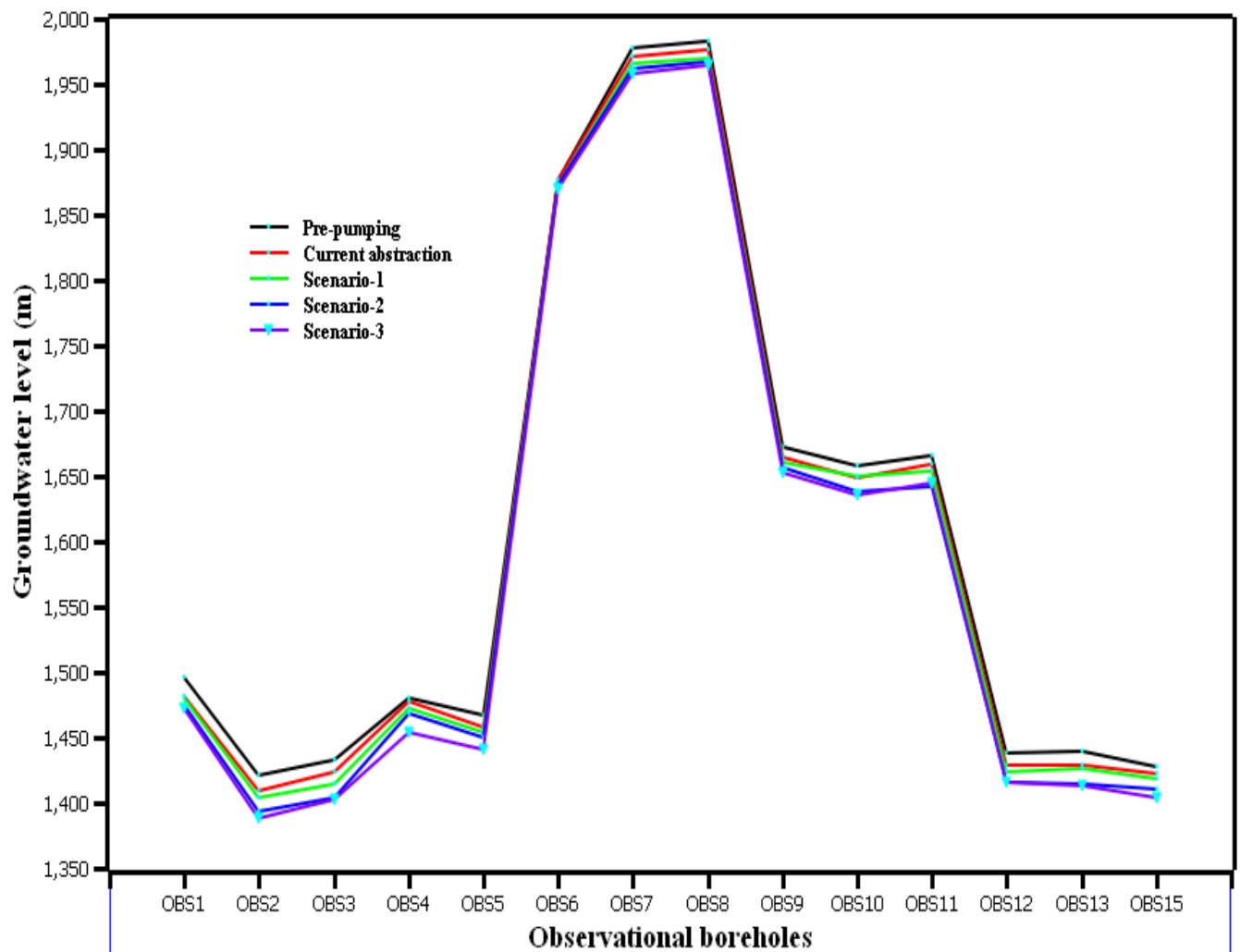


Figure 32: Decline in simulated water level due to possible increase in the pumping rate

b. Recharge Scenario

The second scenario simulated by the model is a decrease in recharge by 50 percent which could be the case if mild drought conditions were imposed on the aquifer system due to climate change since the area is prone to moderate drought.

- In the first simulation, only the recharge is changed (decreased by 50) while water extraction is maintained at the current rate of abstraction. The simulation results in an average of **7m** decline in water level.
- In the second simulation, both the rate of recharge (decreased by 50%) and the rate of groundwater extraction (assumed to be increased by 100%) are changed. The model results in an average decrease in the head by **17.4m** from the current levels due to the common effect of decreased recharge and an increase in groundwater abstraction.

The decrease in recharge and an increase in abstraction caused lower streamflow and groundwater discharge through the general head boundary.

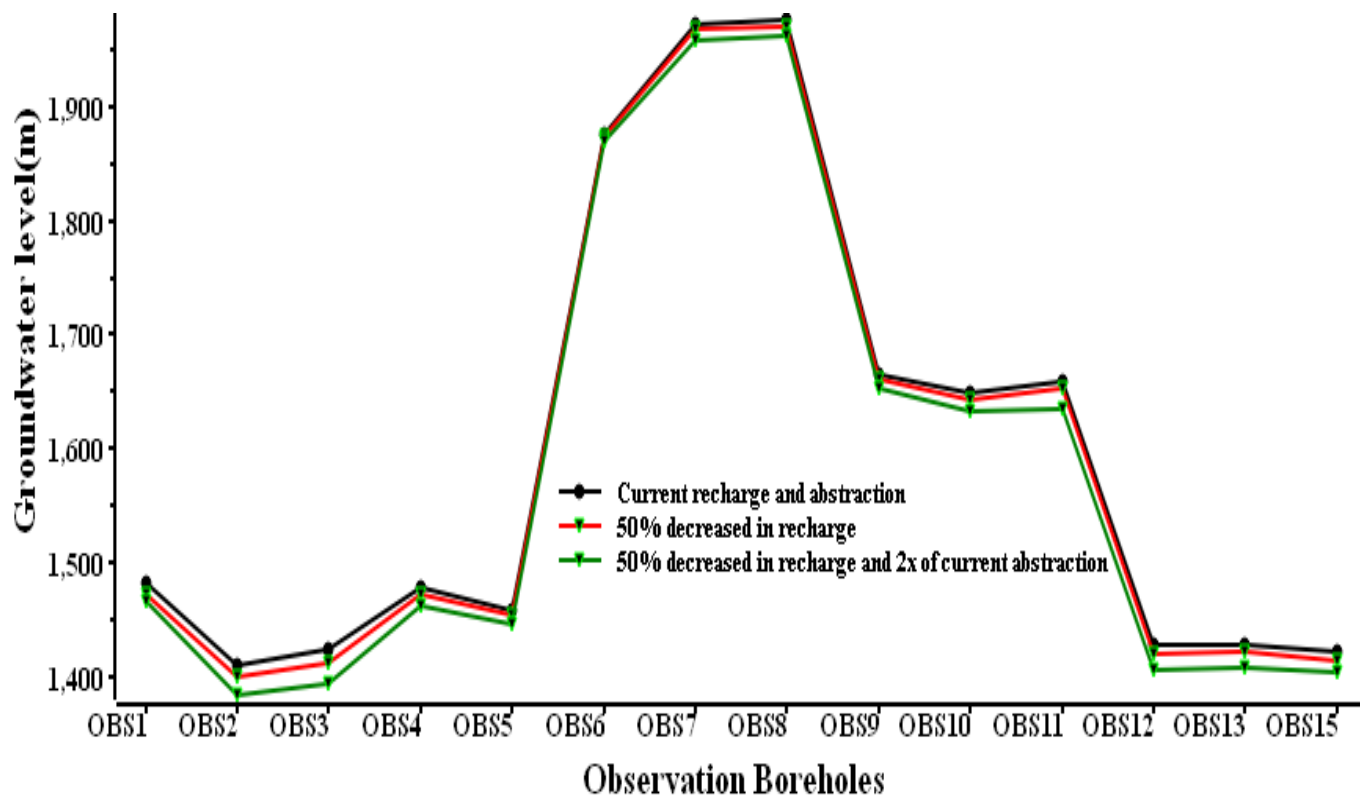


Figure 33: Decline in simulated water level due to possible increase in the pumping and decrease in the recharge rate

7.7 Model Limitations

Numerical models of groundwater flow are limited in their representation of the physical system because they contain simplifications and assumptions during conceptual model development. Errors are introduced during interpretation of the modeling process such as, converting the real world into conceptual model and the conceptual model into numerical model. The degree of uncertainty in the model was raised, due to poor quality and limitation of the existing data such as model geometry are not well documented and the available records of the water level measurements are not continuous and mostly are only single measurements. The uncertainty also occurred during defining the boundary conditions of the model domain.

The boundary conditions were defined based on the surface physical features such as impervious geology, surface water divide and groundwater divide. The locations of the groundwater catchment boundaries are uncertain since they might not coincide with their surface expressions

CHAPTER EIGHT

CONCLUSION AND RECOMMENDATION

8.1 Conclusions

The Upper Mille River catchment is located in the north-eastern part of Ethiopia, in the lower Awash basin within the southwestern margin of the Afar rift. The center of the study area is found 440 Km far in the North –East from Addis Ababa. Using different approaches and methodologies that have been discussed so far in each section of the research the following conclusions have been forwarded on the; description of the study area, quantified recharge, geology, hydrogeology, model result, sensitivity analysis, and scenario analysis.

The total study area is about 1360Km². The topography of the catchment is very variable and complex in which part of the study area are flatlands whereas, ridges, mountains, and escarpments are also common. The elevation ranges from 3640 (western, and southern) to 1123m (eastern, and central parts) A.s.l. The slope is also very variable from nearly horizontal to very steep mountains (0-78⁰). The gentler slope is found mainly on the alluvial and fluvial unconsolidated sediments, while the steeper slope is found on the western and central volcanic ridges and the side hills. The drainage density is relatively high having a dendritic pattern. According to FAO soil classification, the soil type of the catchment is classified into four different soil classes which are; Eutric Cambisols (CMe), Eutric Leptosols (LPe), Eutric Vertisols (VRe), and Lithic Leptosols (LPq). Based on the traditional climate zone the watershed is classified into four different climate regions; Wurch, Dega, Woina Dega, and Kola. The watershed is divided into eight land use landcover classes: Cropland, Shrub cover areas, Grassland, Tree cover areas, Aquatic or regularly flooded vegetation, Built-up areas, Bare areas, and Open water.

Groundwater Recharge was estimated using WB and SWAT Model techniques. Each water balance component of the watershed was properly estimated and quantified. With the WB method the mean annual precipitation, actual ET, and surface runoff of the area is quantified as 1132.5mm, 775mm (69% of the total mean annual precipitation), 251.1mm (22% of the total mean annual precipitation). The groundwater recharge of the watershed is **106.5mm** (9% of the total mean annual precipitation). Based on the SWAT Model output the mean annual precipitation, AET, and groundwater recharge of the watershed are 1083.2mm, 558mm (51.5% of the precipitation), 335.5mm (31% of the precipitation), and **150mm** (13.8% of the precipitation) respectively.

The local lithostratigraphic units in the study area are generally grouped into two rock types; older volcanic (Ashange basalt, Aiba basalt, Kemise rhyolite, and Tarmaber basalt) and younger unconsolidated Quaternary sediments (alluvial, colluvium, aluvio-colluvial, and intermountain sediments).

Hydraulic properties and Physico-chemical parameters were investigated. The transmissivity and hydraulic conductivity of the area range from 2.4 to 1407 m²/day and 0.06 to 17 m/day respectively. EC (310-1200 μs) and TDS (200-669 mg/l) values of the watershed show generally an increasing trend from the recharge area (western part) to the discharge area (eastern part).

The Lithostratigraphic units are transformed into hydrostratigraphic units. To characterize in such a way data from field observation, borehole lithological logs, pumping test results, and measured physicochemical parameters are used. Based on this lithostratigraphic units showing similar hydrogeological characteristics are grouped. Qualitatively, the aquifer types are classified and mapped into three hydrogeologic units; high productive intergranular aquifer, medium productive double porosity aquifer, and low productive aquifer. Unconsolidated quaternary sediments are grouped under high productive aquifers. Ashange basalt is a medium productive aquifer whereas, Aiba basalt, Tarmaber basalts, Kemise rhyolite, and swampy areas are grouped under low productive aquifer. Even if they are classified in such a way, the geological units are hydraulically interconnected. The groundwater source for the Upper Mille catchment is recharged through streams, runoff during the rainy season, groundwater inflow from highlands of western margins, and direct rainfall. The groundwater from the catchment is discharged through base flow (groundwater outflow) and springs and boreholes for irrigation and water supply purposes.

A steady-state numerical groundwater flow model was applied. The conceptual model transformed into the model domain using the processing MODFLOW-8 code package. The model was well-calibrated. The water budget components and hydraulic heads were simulated for the calibrated model.

The simulated groundwater recharge from Precipitation is **89.1 mm/year** which is less than the calculated recharge by the soil water balance and SWAT model. The total inflow to the system is about **3.73 × 10⁷ m³/day**. The total outflow to the system is about **3.73 × 10⁷ m³/day**. The sensitivity analysis result shows that the model is very sensitive to a change in hydraulic conductivity and groundwater recharge. Two types of scenario analysis were done. The first scenario is by increasing the amount of groundwater extraction by 50, 100, and 200% from the current pumping

rate. The simulation results in an average decline of water level by **12.2, 19.1, and 23m** respectively. The second scenario is analyzed firstly by decreasing the recharge by 50% while keeping the current rate of pumping. And then simultaneously decreasing the current recharge by half and increasing the groundwater abstraction by 100%, in these cases the model shows an average declined in the head by **7m** and **17.4m** from the current water levels.

8.3 Recommendations

For the quality of the research as well as for the proper use of the groundwater potential of the Upper Mille watershed the following basic recommendations are forwarded

In the area, meteorological data recording stations are very limited and most of them are not functional, this makes it very difficult to get a complete record of meteorological parameters over many years. Which in turn negatively affects the result of the study. So new meteorological stations should be installed and already existing stations should be regularly monitored to check their functionality. The other thing is that most of the river gauging stations are installed at starting point of streams. This makes the river discharge value non-representative of the watershed. So gauging stations should be installed in the appropriate location.

Most of the shallow and deep boreholes don't have observational wells. Which makes it difficult to know the present groundwater level of the aquifer. So, it would be very important to have observation wells gauged with a Pressure transducer, which monitors the water level fluctuation in instant time and continuous recording of abstraction rate and professional follow up is necessary.

Systematic and planned groundwater pumping would be very important and should be applied to ensure efficient use of groundwater and to at least minimize unnecessary loss of water due to over-pumping of boreholes. Springs should be well developed to increase their discharge which will help to minimize the extraction of water from boreholes.

Further investigations should be made in the study area (Upper Mille catchment), to understand better the groundwater reserves (recharge and abstraction rate), borehole separation distance and groundwater flow movement and thus, to develop a more detailed and realistic groundwater flow model for the whole catchment

REFERENCES

- A. Balasubramanian. (2015). the World ' S Water Crisis. *Research Gate*, 44(0).
- Bekele Abebe, Acocella, V., Tesfaye Korme, & Dereje Ayalew, (2007). Quaternary faulting and volcanism in the Main Ethiopian Rift. *Journal of African Earth Sciences*, 48(2–3), 115–124. <https://doi.org/10.1016/j.jafrearsci.2006.10.005>
- Dereje Ayalew, D., Ebinger, C. J., Bourdon, E., Wolfenden, E., Yirgu, G., & Grassineau, N. (2006). Temporal compositional variation of syn-rift rhyolites along the western margin of the southern Red Sea and northern Main Ethiopian Rift. *Geological Society Special Publication*, 259, 121–130. <https://doi.org/10.1144/GSL.SP.2006.259.01.10>
- Tenalem Ayenew. (2001). Numerical groundwater flows modeling of the central main Ethiopian Rift lakes basin. In *SINET: Ethiopian Journal of Science* (Vol. 24, Issue 2). <https://doi.org/10.4314/sinet.v24i2.18184>
- Tenalem Ayenew & Tilahun, N. (2008). Assessment of lake-groundwater interactions and anthropogenic stresses, using numerical groundwater flow model, for a Rift lake catchment in central Ethiopia. *Lakes and Reservoirs: Research and Management*, 13(4), 325–343. <https://doi.org/10.1111/j.1440-1770.2008.00383.x>
- Tilahun Azagegn, (2014). Groundwater Dynamics in the Left Bank Catchments of the Middle Blue Nile and the Upper Awash River Basins. *Ph.D. Thesis, December*, 119. Addis Ababa university, Addis Ababa, Ethiopia
- Andarge Yitbarek Baye (2009). A hydrogeological and hydrochemical framework of complex volcanic system in the Upper Awash River basin, Central Ethiopia : with special emphasis on inter-basins groundwater transfer between the Blue Nile and Awash. *Ph.D. Thesis, December*, 185.
- Behailu Berehanu, Tilahun Azagegn, Tenalem Ayenew & Masetti, M. (2017). Inter-Basin Groundwater Transfer and Multiple Approach Recharge Estimation of the Upper Awash Aquifer System. *Journal of Geoscience and Environment Protection*, 05(03), 76–98. <https://doi.org/10.4236/gep.2017.53007>
- Behailu Birhanu, Seifu Kebede, Masetti, M., & Tenalem Ayenew, (2018). WEAP-MODFLOW

dynamic modeling approach to evaluate surface water and groundwater supply sources of Addis Ababa city. *Acque Sotterranee - Italian Journal of Groundwater*, 7(2), 15–24. <https://doi.org/10.7343/as-2018-334>

C.W. Fetter-*Applied Hydrogeology (4th Edition)-Prentice Hall (2000).pdf*. (n.d.).

Tadios Chernet, Hart, W. K., Aronson, J. L., & Walter, R. C. (1998). New age constraints on the timing of volcanism and tectonism in the northern Main Ethiopian Rift - southern Afar transition zone (Ethiopia). *Journal of Volcanology and Geothermal Research*, 80(3–4), 267–280. [https://doi.org/10.1016/S0377-0273\(97\)00035-8](https://doi.org/10.1016/S0377-0273(97)00035-8)

Cook, P. G., Walker, G. R., & Jolly, I. D. (1989). Spatial variability of groundwater recharge in a semiarid region. *Journal of Hydrology*, 111(1–4), 195–212. [https://doi.org/10.1016/0022-1694\(89\)90260-6](https://doi.org/10.1016/0022-1694(89)90260-6)

Darrell, I. L. (1999). *Geological Occurrence of Groundwater. The Handbook of Groundwater Engineering*.

Delleur, E. J. W., Rubin, Y., Hubbard, S. S., & Wilson, A. (1999). Rubin, Yoram, et al. “*Aquifer Characterization*.”

Miruts Hagos, M., Konka, B., & Ahmed, J. (n.d.). *A preliminary Geological and Generalized Stratigraphy of Western Margin of*. 8(1), 1–22.

Dereje Ayalew and Gezahegn Yirgu. (2003). Crustal contribution to the genesis of Ethiopian plateau rhyolitic ignimbrites: Basalt and rhyolite geochemical provinciality. *Journal of the Geological Society*, 160(1), 47–56. <https://doi.org/10.1144/0016-764901-169>

Drawdown, L. M. (1996). *Ground Water Issue*. 1–11.

Eden Dessalegn 2020. Groundwater Assesment of Upper Mille Catchment Unpublished Msc thesis, Addis Ababa University, Addis Ababa, Ethiopia

Fetter, C. W. (2001). *Applied Hydrogeology _e7ce669a880a8c4c70b4214641f93a02.pdf* (p. 598).

Feyissa Dejene (2018). *Petrologic and Geochemical Evidence for Diversity of Magma Compositions At the Ethiopian Volcanic Province : Implications for Thermo-Chemical*.

- Girmay, E., Tenalem Ayenew, Seifu Kebede , Mulugeta Alene, Wohnlich, S., & Wisotzky, F. (2015). Modèle conceptuel hydrogéologique d'écoulements des formations sédimentaires Paléozoïque–Mésozoïque de Mekelle et environs (nord de l'Éthiopie) par l'utilisation des isotopes environnementaux et ions dissous. *Hydrogeology Journal*, 23(4), 649–672. <https://doi.org/10.1007/s10040-015-1243-4>
- GSE. (2017). *Hydrogeological and Hydrochemical Maps of Bure NC 37 – 5 Sheet Explanatory Notes*.
- Hunegnaw, A., Sage, L., & Gonnard, R. (1998). Hydrocarbon potential of the intracratonic Ogaden Basin, SE Ethiopia. *Journal of Petroleum Geology*, 21(4), 401–425. <https://doi.org/10.1111/j.1747-5457.1998.tb00793.x>
- Jarvis, J. (2014). System analysis. *Strad*, 125(1495), 8. <https://doi.org/10.7748/ns.18.39.27.s42>
- Seifu Kebede, S., Travi, Y., Asrat, A., Alemayehu, T., Ayenew, T., & Tessema, Z. (2008). Groundwater origin and flow along selected transects in Ethiopian rift volcanic aquifers. *Hydrogeology Journal*, 16(1), 55–73. <https://doi.org/10.1007/s10040-007-0210-0>
- Kieffer, B., Arndt, N., Lapierre, H., Bastien, F., Bosch, D., Pecher, A., Yirgu, G., Ayalew, D., Weis, D., Jerram, D. A., Keller, F., & Meugniot, C. (2004). Flood and shield basalts from Ethiopia: Magmas from the African superswell. *Journal of Petrology*, 45(4), 793–834. <https://doi.org/10.1093/petrology/egg112>
- Kinzelbach, W. (1992). Applied groundwater modeling — Simulation of flow and advective transport. In *Journal of Hydrology* (Vol. 140, Issues 1–4). [https://doi.org/10.1016/0022-1694\(92\)90251-p](https://doi.org/10.1016/0022-1694(92)90251-p)
- Kolka, R. K., & Wolf, A. T. (1998). Estimating Actual Evapotranspiration for Forested Sites: Modifications to the Thornthwaite Model. *United states department of agriculture, Forest Service, Southern Research Station Research Note SRS-6*, 7 pp.
- Tesfaye Korme, Chorowicz, J., Collet, B., & Bonavia, F. (1997). Volcanic vents rooted on extension fractures and their geodynamic implications in the Ethiopian Rift. *Journal of Volcanology and Geothermal Research*, 79(3–4), 205–222. [https://doi.org/10.1016/S0377-0273\(97\)00034-6](https://doi.org/10.1016/S0377-0273(97)00034-6)

- KUMAR, P. A., & GK, D. V. (2017). Estimation of Runoff by using SCS Curve Number Method Integrated with GIS. *Iarjset*, 4(7), 34–38. <https://doi.org/10.17148/iarjset.2017.4706>
- Maliva, R. G. (2004). Aquifer Characterization. In *Aquifer Characterization* (Issue 4). <https://doi.org/10.2110/pec.04.80>
- Mandle, R. J. (n.d.). *Groundwater Modeling Guidance*. 0–54.
- Abreham Mechal, (2015). *Hydrogeology of a Complex Rift System : the Example of Gidabo River Basin, Ethiopian Rift. Unpublished MSc thesis, Addis Ababa University, Addis Ababa, Ethiopia*
- Mohr, P., & Zanettin, B. (1988). The Ethiopian flood basalt province. *Continental Flood Basalts*, 63–110. https://doi.org/10.1007/978-94-015-7805-9_3
- Mohr, Paul. (1987). Structural style of continental rifting in Ethiopia: Reverse decollements. *Eos, Transactions American Geophysical Union*, 68(35), 721–730. <https://doi.org/10.1029/EO068i035p00721>
- Mulatu Tarekegn 2020, Steady-state Numerical Groundwater Flow Modeling of Sunuta Catchment; the effect of Pumping for irrigation. Unpublished Msc thesis, Addis Aababa University, Addis Ababa , Ethiopia
- Pik, R., Deniel, C., Coulon, C., Gezahegn Yirgu., & Marty, B. (1999). Isotopic and trace element signatures of Ethiopian flood basalts: Evidence for plume-lithosphere interactions. *Geochimica et Cosmochimica Acta*, 63(15), 2263–2279. [https://doi.org/10.1016/S0016-7037\(99\)00141-6](https://doi.org/10.1016/S0016-7037(99)00141-6)
- Rogers, N. W. (2006). Basaltic magmatism and the geodynamics of the East African Rift System. *Geological Society Special Publication*, 259, 77–93. <https://doi.org/10.1144/GSL.SP.2006.259.01.08>
- Rooney, T. O. (2020). The Cenozoic magmatism of East Africa: Part IV – The terminal stages of rifting preserved in the Northern East African Rift System. *Lithos*, 360–361, 105381. <https://doi.org/10.1016/j.lithos.2020.105381>
- Mesfin Sahele, (2001). *HYDROGEOLOGICAL INVESTIGATION OF THE UPPER AND MIDDLE BORKENA RIVER CATCHMENT, NORTHERN Ethiopia, WOLLO.*, unpublished

MSc Thesis ,Addis Ababa University, Addis Ababa, Ethiopia

Singhal, B. B. S., & Gupta, R. P. (2010). Fractures and Discontinuities. In *Applied Hydrogeology of Fractured Rocks*. https://doi.org/10.1007/978-90-481-8799-7_2

Varet, J. (2018). Geology of Afar (East Africa). In *Regional Geology Reviews*.

W, Anderson and Woessener, 1992. (1992). Applied groundwater modeling — Simulation of flow and advective transport. In *Journal of Hydrology* (Vol. 140, Issues 1–4). [https://doi.org/10.1016/0022-1694\(92\)90251](https://doi.org/10.1016/0022-1694(92)90251)

Wakgari Furi, K. (2010). *Hydrogeology of complex volcanic systems in the continental rifted zone. Integrated geochemical, geophysical, and hydrodynamic approaches. Middle Awash basin, Main Ethiopian Rift, Ethiopia. Thèse de D, 342p.*

Wang, H. F. (2020). Groundwater Storage in Confined Aquifers. In *The Groundwater Project*.

Williams, F. M. (2016). *Understanding Ethiopia*. <https://doi.org/10.1007/978-3-319-02180-5>

Wolfenden, E., Ebinger, C., Gezahegn Yirgu, Deino, A., & Dereje Ayalew, (2004). *Evolution of the northern Main Ethiopian rift: the birth of a triple junction*. 224, 213–228. <https://doi.org/10.1016/j.epsl.2004.04.022>

Zwaan, F., Corti, G., Sani, F., Keir, D., Muluneh, A. A., Illsley-Kemp, F., & Papini, M. (2020). Structural Analysis of the Western Afar Margin, East Africa: Evidence for Multiphase Rotational Rifting. *Tectonics*, 39(7), 1–25. <https://doi.org/10.1029/2019TC006043>